MINERAL EXPLORATION MODELING AND SINGULARITY ANALYSIS FOR GEOLOGICAL FEATURE RECOGNITION AND MINERAL POTENTIAL MAPPING IN SOUTHEASTERN YUNNAN MINERAL DISTRICT, CHINA

WENLEI WANG

A DISSERTATION SUBMITTED TO
THE FACULTY OF GRADUATE STUDIES
IN PARTIAL FULFILLMENT OF THE REQUIREMENTS
FOR THE DEGREE OF
DOCTOR OF PHILOSOPHY

GRADUATE PROGRAM IN EARTH AND SPACE SCIENCE
YORK UNIVERSITY
TORONTO, ONTARIO

August 2013

Abstract

Nowadays, with the development in construction of geo-exploratory datasets and data processing techniques, mineral exploration modeling for recognition of mineralization associated geological features and mapping of mineral potentials become more dependent on GIS-based analysis and geo-information from multi-source datasets. Geological, geochemical and geophysical data as three main sources of geo-information in support of mineral exploration have long been employed in many researches. Spatial distributions of geological bodies or controlling factors associated with mineralization were frequently interpreted from these datasets. However, former characterizations of the controlling factors were simply focused on their location information; concerns on spatial variations of their geological signatures and controlling effects on mineralization were not sufficiently emphasized. Therefore, through a series of newly developed GIS-based manipulations, current study intends to demonstrate a comprehensive mineral exploration modeling process for more explicit recognition of controlling factors and their interactions on mineralization and delineation of hydrothermal mineral potentials in southeastern Yunnan mineral district, China. The hydrothermal mineralization as a non-linear geo-process is accompanied with anomalous energy release and material accumulation in a narrow spatial-temporal interval. Simultaneously, it is a cascade process associated with various geological activities (e.g., magmatism, tectonism, etc.). Knowledge of these associated geo-activities is consequently beneficial to the exploration of hydrothermal mineralization. As the key point of this study, the singularity index mapping method in the context of fractal/multifractal efficient in separating geo-anomalies from both strong and weak background is applied to characterize variations of geological signatures of three controlling factors (i.e., granitic intrusions, faults and the Gejiu formation). With the guidance of multidisciplinary approaches, these geo-information derived from multi-source datasets is further integrated to produce the potential map. In comparison with traditionally used methods, the newly depicted predictor maps enhance weak geo-anomalies hidden within a strong variance of background. In addition, three geo-information integration methods including RGB composition, the principal component analysis and the weights of evidence method are implemented. By the weights of evidence method, the qualitatively and quantitatively interpretable result possessing advantages of the other two methods, simultaneously, is accepted as the final result of currently proposed mineral exploration modeling. Summarized experiences through this study will not only support future exploration in the study area, but also benefit the work in other areas.

Acknowledgements

My deepest gratitude goes first and foremost to Dr. Cheng, Qiuming, my supervisor, for his constant encouragement and academic guidance. He has walked me through all the stages of my research. Without his consistent and illuminating instruction, my dissertation could not have reached its present form.

Second, I would like to express my heartfelt gratitude to Dr. Jarvis, Gary T. and Dr. Armenakis, Costas members of my supervisory committee at the Department of Earth and Space Science, York University who have instructed and provided constructive comments on my Ph. D. study in the past years. Thirdly, I also owe my sincere gratitude to my colleagues Ji Zhang, Jiangtao Liu, Lei Wang, Linhai Jing, Xitao Xing, Yinhuan Yuan, and Zhijing Wang who gave me their help and time in listening to me and helping me work out my problems.

My greatest thanks go to my wife, Jie Zhao who have never limited my ambitions and have always had absolute confidence in me. Words cannot express how much I love her and how grateful I am to her for loving me continuously. Last but not the least, I would like to thank my mother Fangping Cui and my father Ruijiang Wang for their constant support and continuous encouragements in my life.

Table of Contents

List of Figures

List of Tables

Chapter 1. Introduction

Mineral exploration is a systematic process objective to find mineral deposits with economic values (Haldar, 2012). A general process of mineral exploration includes regional area selection, reconnaissance exploration and a series of follow-up (Hodgson, 1990; Woodall, 1994; Haldar, 2012). Considering the cost-benefit balance and exploration strategies, the regional area selection is critical to mineral exploration, since all of the following stages will be implemented within the selected areas (Fig. 1.1). The selected areas are the delineated spaces with mineral potentials or favorable to the occurrence of mineralization (Bonham-Carter, 1994; Harris and Sanborn-Barrie, 2006). In order to depict the target areas or mineral potentials (i.e., a large area is reduced to a small area with favorability of mineralization), a series manipulations are employed to investigate mineralization associated knowledge (i.e., geo-information), the process of which is so-called mineral exploration modeling (Fig. 1.2) (Hodgson, 1990; Woodall, 1994; Haldar, 2102).

The selection of geological criteria for exploration modeling is mainly dependent on conceptual and empirical models. The conceptual model coincident with metallogenetic models is used to define geological criteria for the exploration. In other words, based on the conceptual model, geological issues significant to mineralization are decided and consequently considered as the main components of the mineral exploration modeling (Bonham-Carter, 1994). For example, the criteria for skarn mineral exploration is

generally associated with three factors consisting of intensive tectonic activities, magmatic intrusions, and carbonate strata (Pirajno, 2009); magmatic mineralization is controlled by magmatic intrusions and associated tectonic activities; sedimentary massive sulphide mineralization (i.e., SEDEX type) may be only related with hydrothermal emanations on or near the sea floor in association with the deposition of sedimentary rocks (Misra, 2000; Edwards and Atkinson, 1986; Guilbert and Park, 1986). In the aspect of empirical models, geological issues regarding the criteria significant to mineral exploration are decided based on statistical analysis and/or experiments rather than the descriptive features of deposit types (Woodall, 1994). In practice, these two models are used jointly. The conceptual models are applied to choose controlling factors of mineralization, while the empirical models are employed to estimate significance of these controlling factors to mineralization (Bonham-Carter, 1994; Harris and Sanborn-Barrie, 2006).

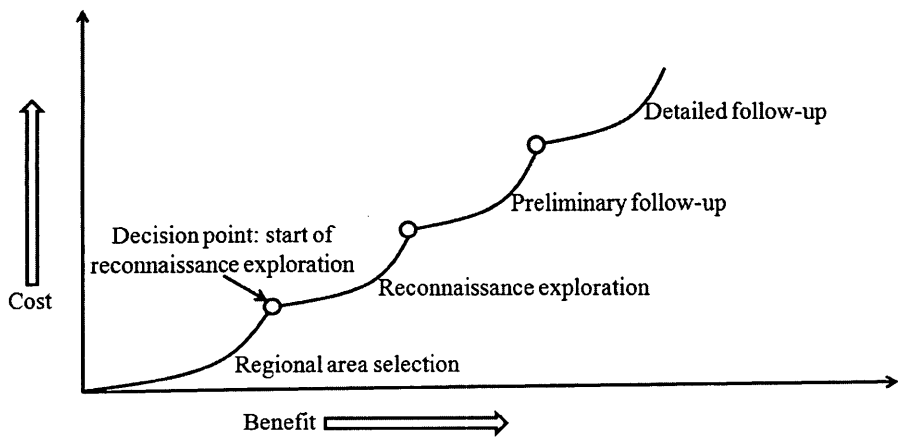

Fig.1. 1. A general process of mineral exploration. All stages of exploration are projected to a cost-benefit system.

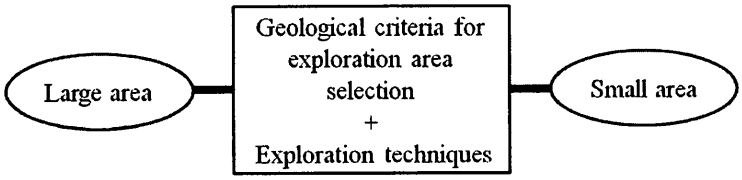

Fig.1. 2. A schematic diagram of mineral exploration modeling. A large area is reduced to a small area based on exploration techniques and geological criteria.

In addition to geological criteria, exploration data and techniques are important to mineral exploration as well. In recent years, commonly used geo-exploratory datasets are geological, geochemical, geophysical and remote sensing data, from which geo-information of mineralization and/or its controlling factors can be identified for mineral potential mapping. With development of observation techniques, more aspects of the Earth's properties can be investigated that greatly improved the efficiency of data collection. For example, some formerly inaccessible locations can be currently observed with the aid of remotely sensed techniques (e.g., remote sensing image, aero-surveys); furthermore, utilization of portable X-ray fluorescence analyzer in field work can greatly improve the efficiency of testing the element content in rock samples.

In recent decades, various advanced observations are mainly recorded in form of geographic information system (GIS) database. With a great numbers of add-on spatial analysis extensions, the GIS-based mineral exploration modeling has become a common practice in support of mineral exploration (Bonham-Carter, 1994; Carranza, 2008; Pan and Harris, 2000). In this dissertation, the GIS-based mineral exploration modeling will be discussed according to a series of applications of geo-information extraction and integration for mapping mineral potentials in southeastern Yunnan mineral district, China.

1.1. Mineral exploration modeling

In order to analyze and delineate geo-anomalies (i.e., geo-information associated with mineralization) for prediction of mineral deposits, a sophisticated exploration model is required to support not only the qualitative description of geo-anomalies according to types, distributions and geneses but also the knowledge of advanced techniques for quantitative mapping of geo-anomalies (Wang et al., 2011, 2012; Zhao et al., 2012). Exploration of hydrothermal ore deposits is one of examples benefitting from the advances of mineral exploration modeling. Hydrothermal mineralization as a cascade process (Cheng, 2008, 2012) is associated with multiple geological activities consisting of transportation of ore-bearing hydrothermal fluids, interaction of fluids with wall rocks, precipitation of minerals and consequent accumulation of ore deposits of certain elements or metals (Cheng, 2007a; Pirajno, 2009). These geological activities can generate diverse geo-anomalies exhibiting significant differences in geological, geochemical and geophysical characteristics from their surroundings (Cheng, 2007a; Cheng and Agterberg, 2009; Zhao, 1999). It has been a common practice that geological interpreters apply analysis techniques in both frequency and spatial domains to recognize geo-anomalies, and identified geo-anomalies are further employed as guidance to mineral exploration (Agterberg, 1989; Bonham-Carter, 1994).

Nowadays, advancements in computer sciences and constructions of geo-databases have led to flourishing developments in spatial analysis of geo-anomalies using GIS (Bonham-Carter, 1994; Darnley, 1995; Pan and Harris, 2000; Carranza, 2008). Characterization and

delineation of geo-anomalies were achieved greatly by advanced spatial analysis methods (Cheng et al., 2010, 2011; Wang et al., 2011, 2012; Zhao et al., 2012). The primary functions of GIS techniques are for extracting and integrating geo-information from uni- or multi-source geo-datasets to characterize occurrences of geological events. Multi-source geo-datasets consist of ground-based and/or remotely-sensed observations. Ground-based geochemical data among the most important sources of geo-information are about the presence and spatial distribution of mineral deposits at or near the Earth's surface, while geophysical data (e.g., ground-based gravity and aeromagnetic data) are efficient to collect geo-information regarding buried geological bodies. In the past decades, two basic methods had been widely used to analyze these geo-exploratory data: frequency analysis and spatial analysis (Grunsky and Smee, 1999; Harris et al., 2000; Xu and Cheng, 2001; Pereira et al., 2003). Statistical approaches including univariate (e.g., Q-Q plot) and multivariate data analyses (e.g., cluster analysis) are, under certain circumstances, effective for solving problems in the statistical frequency domain rather than in the spatial domain. Fractal and multifractal methods consider both frequency distributions and spatial self-similar properties of geochemical variables have been supportive to many case studies (Agterberg, 1994; Cheng et al., 1994; Carranza, 2008, 2011; Carranza et al., 2009; Cheng, 2006; Cheng and Agterberg, 2009; Cheng et al., 2010; Zuo et al., 2009; Zuo and Xia, 2009; Wang et al., 2011).

In the aspect of geo-information integration, identified geo-information representing mineralization associated geo-anomalies are combined to comprehensively characterize geological signatures of mineralization (Harris and Sanborn-Barrie, 2006). Based on

metallogenetic properties of most of the hydrothermal deposits, ore-controlling factors are mainly composed of magmatism, tectonism and wall rocks. Tectonic activities provide spaces for transportation and precipitation of ore materials (Faulkner et al., 2010; Micklethwaite et al., 2010; Yuan et al., 1979; Zhai et al., 1999). Magmatic activities associated with hydrothermal mineralization can be significant sources of both ore-forming elements and heat (Wang et al., 2011). Wall rock is another key factor of hydrothermal mineralization, properties of which are important to the types of mineralization. For instance, skarn-type ore deposits formed in contact zones of felsic intrusions and carbonate rocks (Einaudi and Burt, 1982). Therefore, these three geological features are main concerns in most of hydrothermal mineralization exploration modeling processes.

As previously introduced, a general modeling process is consisted of geo-information extraction and integration (Fig. 1.3). Geo-information extracted from various geo-datasets is so-called geo-anomaly identification which indicates mineralization-favored areas produced by certain geological activities (i.e., controlling factors). According to geo-information integration, identified geo-anomalies are combined by weighted overlay methods. Based on approaches to assign weights to these indicators, data-driven, knowledge-driven and hybrid methods are the three general categories for geo-information integration.

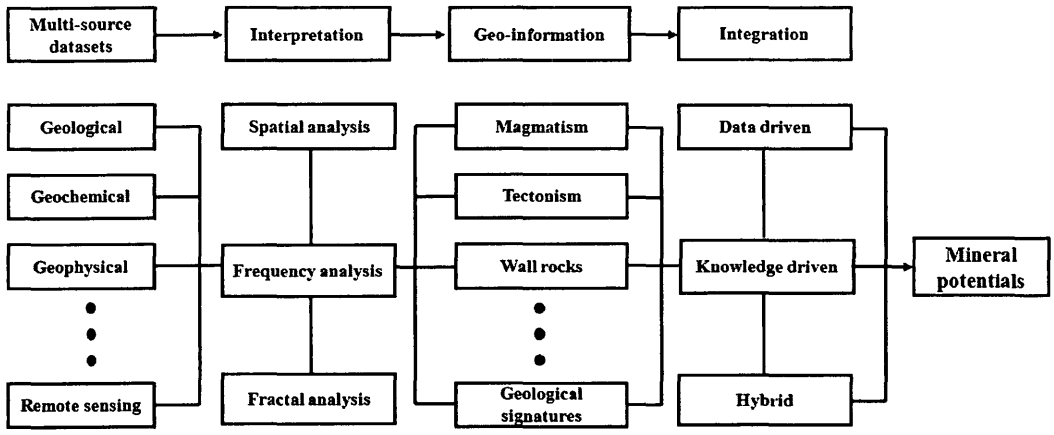

Fig.1. 3. A general mineral exploration modeling process.

Among these three categories of geo-information integration methods, data-driven methods required sufficient samples of mineral occurrences are readily available in many GIS software packages. In these methods, weights of geo-information of individual controlling factors are defined according to their spatial association with mineral occurrences, and consequently used to delineate mineral potentials (Bonham-Carter, 1994). Some frequently used data-driven methods are weights of evidence (WofE) (Bonham-Carter et al., 1989), logistic regression (Chung and Agterberg, 1980), neural networks (Harris et al., 2003), etc. In Bonham-Carter et al. (1989), location information of known gold deposits were used as training data to calculate a series of predictor maps of gold mineralization. The WofE method was further used to integrate these predictor maps for predicting gold mineral potentials in the Meguma terrane of the eastern shore in Nova Scotia, Canada. Knowledge-driven methods require geologic interpreters to define weights for identified geo-information, and used the subjective weights to map target

areas (An et al., 1991). Typical knowledge-driven methods are Boolean overlay (Harris, 1989), index overlay (Renez et al., 1994), fuzzy logic (An et al., 1991), etc. In An et al. (1991), the fuzzy set theory was used to define fuzzy memberships of nine sets of geological and geophysical datasets, integration of which successfully delineate the "base metal deposits" and "iron formation deposits" favored areas in the Farley Lake area, Canada. Besides the methods of data- and knowledge-driven, Cheng and Agterberg (1999) proposed a fuzzy weights of evidence method (Carranza and Hale, 2001; Luo and Dimitrakopoulos, 2003; Porwal et al., 2004). By this hybrid method, patterns of predictor maps in forms of binary or ternary can be reclassified to multi-classes by fuzzy sets according to more expert knowledge,. The definition of membership function is more general where binary or ternary patterns in the ordinary WofE method become two special situations of non-fuzzy sets. In Cheng and Agterberg (1999), this method was applied to predict gold deposits in Meguma Terrane, Nova Scotia, Canada, and the problem of losing useful information by defining non-fuzzy patterns were improved. More detailed reviews on these three categories of methods can be found in Bonham-Carter (1994) and Harris sand Sanborn-Barrie (2006).

In previous researches, geo-information regarding controlling factors of hydrothermal mineralization can be interpreted from geological data which records the location information of geological occurrences consisting of discovered mineral deposits, fault traces and outcrops of igneous or sedimentary rocks. By comparison of spatial correlations between these factors (e.g., outcrops of intrusions, fault traces, carbonate rocks, etc.) and mineral occurrences with statistical analysis (e.g., student's *t*-value),

optimal influencing zones (i.e., buffers) from these locations can be estimated. Areas within the buffers are applied as indicators to mineralization-favored spaces (i.e., geo-information). In Carranza (2004), optimal buffers of granodiorite margins and faults/fractures were defined by using the student's *t*-value, which were further integrated with other geological features by the weights of evidence method for mapping mineral potentials in the administrative province of Abra in the northwestern Philippines. However, regardless of spatial variation of geological signatures or their controlling effects to mineralization within the extent of optimal buffers, indicators supported by the location information are somehow arbitrary in many places. Since the concept of fractal introduced to geology, several nonlinear models have been successfully applied to characterize spatial properties of geological occurrences. For example, fault traces highly associated with hydrothermal mineralization can be analyzed by fractal/multifractal methods. From the fractal/multifractal point of view, active and complex fault systems corresponding with high fractal dimension can benefit ore-bearing fluid flow and provide favorable environment for mineralization (Zhao et al., 2011). There is an increasing interest in applying fractal dimension and multifractal spectra to describe complexity and self-similarity of fault systems in recent decades (Agterberg et al., 1996; McCaffrey, et al., 1999; Wang et al., 2012). Excluding analysis to location information from geological data, there are many options to characterize spatial distributions of ore-controlling factors by employing additional geo-exploratory datasets (e.g., geophysical data and geochemical data).

In geophysical exploration, upward continuation and vertical derivative are commonly employed in gravity and magnetic data processing (Kearey et al., 2002). The upward continuation works as a low-pass filter to attenuate high-frequency anomalies and emphasize low-frequency anomalies by transforming geophysical data as it was measured at a higher altitude. It can be implemented in frequency domain by means of 2-D Fourier transformation for gravity and magnetic data. As the altitude from the causative body increases, wave numbers are influenced exponentially and large wave numbers (i.e., the short wavelength) are filtered. The upward continuation is to determine the form of regional gravity/magnetic variations caused by relatively deep structures stretching over a wide area. In contrast, the first and second-order vertical derivative emphasize local high-frequency anomalies resulting from shallow resources and/or edges of geological bodies and attenuate low-frequency regional anomalies caused by large causative bodies from depth. Based on the fact that the vertical derivative of gravity/magnetic data reaches a zero value at the edge of causative bodies, zero-contour lines of the vertical derivative are frequently used to outline the boundary of causative bodies (Wang et al., 2010). The first order-vertical derivative has become a routine analysis in gravity/magnetic interpretation, while the second-order vertical derivative with more resolving power to high-frequency anomalies can supplement to the first-order vertical derivative. Therefore, a band-pass filter technique composed by upward continuation and the first- or second-order vertical derivative were applied to delineate causative bodies in many cases (Cheng and Xu, 1998). For hydrothermal mineralization associated geological bodies, intrusions as a typical causative body of geophysical anomalies are often detected by gravity and/or

magnetic data, the spatial variations of which can be delineated by the upward-continuation and the vertical derivative (Cheng and Xu, 1998; Kearey et al., 2002); however, identified geophysical anomalies are more dependent on upward distances, interpretations of which are somehow subjective. Furthermore, the application of the band-pass filter technique requires high data quality, because when it emphasizes high frequency anomalies, the undesirable data noise will be greatly enhanced as well.

In geochemical exploration, concentrations of geochemical elements as the end products of various geological processes, spatial distributions of which are consequently heterogeneous. Geochemical samples collected from rocks or other secondary media (e.g., stream sediments, lake sediments, soils, etc.) as good carrier of geo-information are necessary to be analyzed for further interpretation (Ali, 2005; Cheng et al., 1994; Xu and Cheng, 2001). For identifying geochemical signatures of mineralization, the separation of anomalies from background is one of the top issues in exploration geochemistry. Ali et al. (2006) applied principal component analysis (PCA) to map the spatial distribution of mineralization associated element associations in Yunnan, China. Cheng (1999) introduced a multifractal-based singularity index mapping techniques to characterize spatial variations of ore-forming elements. Some other commonly used approaches to separate geochemical anomalies from background include mean $\pm 2\sigma$ (σ is the standard deviation) statistical methods (Hawkes and Webb, 1962), probability graphs, and fractal models such as Concentration-Area (C-A) model (Cheng et al., 1994). However, other than focusing on the geochemical signatures of ore-forming elements in previous works, attentions to delineate spatial distributions of other mineralization associated geological

features (i.e., geological bodies produced by diverse geological activities) have not been paid sufficiently.

In recent decades, acquisition of geo-information resources is more dependent on multiple investigations (e.g., geological, geochemical, and geophysical surveys). With the development of multidisciplinary approaches, mineral exploration as one of beneficiaries possesses enormous application prospects. Interactions of geological activities associated with hydrothermal mineralization, which are significant to mineral exploration can be analyzed by quantitative collaborations of geography, geochemistry, geophysics, etc. Several common attempts of interdisciplinary collaborations are the integration of aeromagnetic data and remotely sensed images for structural interpretation (Kowalik and Glenn, 1987), fusion of remote sensing and geochemical data to identify mineral exploration target areas (Harris et al., 1998), and fusion of remote sensing, geophysical and geochemical data to identify geological features (Harris et al., 1994; Rivard et al., 1994; Teruiya et al., 2008). Although interdisciplinary collaborations of multi-geosciences have been strongly supported by theories and applications (Zhai et al., 1999), due to some uncontrollable limitations (e.g., algorithms, software, exploration models, etc.), they have not been thoroughly investigated. For example, there are still no significant collaborations to enhance knowledge of spatial distributions of geochemical features of faults or the spatial association between the tectonism and the heterogeneously distributed elemental concentration. The latest achievement on this topic is to identify faults along the axis of anomalous geochemical patterns in some case studies (Zhai et al., 1999).

Analyzed by advanced geo-information extraction and integration methods, characterization of properties of controlling factors (i.e., geological activities or geological bodies) have been improved significantly; however, there still are some shortages and/or limitations of formerly introduced hydrothermal mineralization modeling processes. First of all, a majority of identified geochemical anomalies are focused on ore-forming elements, while the geochemical anomalies associated with other ore-controlling factors are frequently ignored. Concerns to spatial distributions of geochemical signatures of intrusions, faults and wall rocks are insufficient to support a comprehensive mineral exploration model. Secondly, interactions of ore-controlling factors significant to hydrothermal mineralization were only indicated by means of weighted overlay (i.e., geo-information integration) that cannot quantitatively describe spatial variations of the interactions. Thirdly, mineral exploration modeling simply delineates spatial distributions of mineral potentials without any suggestion for the spatial variations of controlling effects of geological bodies in many cases. As a result, the same weight will be assigned to all locations of identified controlling factors, which is somehow subjective. To overcome the shortage, multidisciplinary approaches can be attempt.

1.2. Objectives

Hydrothermal mineralization being a cascade geo-process associated with various geological activities is often accompanied with energy release and material accumulation. Appropriate interpretation to the singular properties and its associated non-linear geo-

processes will greatly improved the efficiency of the hydrothermal mineral exploration. In most of the previous work in southeastern Yunnan mineral district, China, there are two main components of the mineral exploration modeling: (1) location information of controlling factors (i.e., geological bodies); (2) spatial distributions of geochemical and geophysical signatures of mineralization. These geological features with location information are valuable for potential mapping; however, variation of the influence of individual controlling factors (e.g., magmatism, tectonism, etc.) on mineralization may not be sufficiently illustrated. Furthermore, as introduced in previous sections, advanced spatial analysis techniques are necessary to be used to characterize these geological features. Therefore, current study will demonstrate an improved mineral exploration modeling process to recognize mineralization associated controlling factors and delineate spatial distributions of mineral potentials in southeastern Yunnan mineral district, China, summarized experiences of which will not only support future exploration in the study area, but also benefit the future work in other areas.

Primary objectives of current mineral exploration modeling are to: (1) characterize hydrothermal mineralization associated geological signatures by considering the non-linear properties of corresponding singular geo-processes; (2) delineate spatial distributions of ore-controlling factors and their influences on hydrothermal mineralization in Southeastern Yunnan Sn-Cu polymetallic mineral district, China; (3) map mineral potentials in the study areas.

In order to achieve these primary objectives, the singularity index mapping method, the principal component analysis (PCA), and the weights of evidence (WofE) method are employed in this dissertation. Among these methods, the singularity index mapping technique efficient in characterizing spatial variations of physical quantities is applied to derive geophysical and geochemical behaviors of the controlling factors; the PCA advanced in reducing the multi-dimensional geo-datasets to less variables with interpretable geo-information is employed to integrate singularity indices of geophysical/geochemical signatures; and the WofE as a classic geo-information integration method is utilized to produce comprehensive spatial distributions of mineral potentials. During mineral exploration modeling, there are several issues are taken into consideration to facilitate future geological exploration.

1. In previous geochemical exploration of hydrothermal mineralization, only ore-forming elements were characterized by their spatial distribution of geochemical signatures; whereas geo-information of geological bodies (i.e., controlling factors) which might be more significant to locate occurrences of mineralization was only analyzed by limited sources of geo-exploratory datasets. To improve the characterization of mineralization, current study will apply a series of advanced spatial analysis techniques (e.g., singularity index mapping, PCA, etc.) to delineate spatial variations of geochemical signatures of geological bodies in the study area.
2. The band-pass filter technique is commonly used to extract anomalies from geophysical datasets; however, results derived from this process are more dependent on scales of measurements (i.e., scale dependence). By applying multifractal-based

singularity index mapping technique to geophysical data, current study intends to achieve scale independent results for depicting spatial variations of geophysical properties of granitic intrusions in the study area.

3. In order to extract mineralization associated geo-information from faults and characterize controlling effects of fault activities to the mineralization, several manipulations were implemented. Although numerous efforts (e.g., fault density) were attempted to characterize faults, spatial variations of physical properties of which associated with mineralization have not been described in a spatial scenario. In this dissertation, spatial variations of fault density will be characterized. The areas with the accumulation of fault density which transmit magma and/or ore-forming fluids will be indicated to delineate mineralization favored spaces produced by fault activities.
4. Anisotropy of geochemical, geophysical and geological signatures has been noticed in a long time. In mineral exploration, the anisotropic mineralization is caused by interactions of various geo-processes. The influence of controlling factors (e.g., faults, geochemical signatures) which are significant to locate favorable areas of mineralization can be interpreted by characterizing the anisotropy of their associated geo-exploratory datasets. In this dissertation, location information of fault traces and spatial distributions of geochemical signatures will be characterized jointly to describe the anisotropic properties of geochemical signatures of mineralization. Furthermore, the newly identified anisotropy of interactions of fault activities on ore-

forming fluids can further describe the controlling effects of faults to the mineralization.

1.3. Outlines

In chapter 2, details regarding geological background and geo-exploratory datasets of the study area located in southeastern Yunnan mineral district, China are introduced.

In chapter 3, methods involved in current mineral exploration modeling process are introduced. As the key method of this dissertation to characterize hydrothermal mineralization associated geological activities, the singularity index mapping technique frequently applied to extract geo-anomalies from geo-exploratory datasets is reviewed. Furthermore, a newly developed fault trace-oriented singularity index mapping technique is firstly introduced to identify anisotropy of geochemical signatures. Principal component analysis (PCA) and weights of evidence (WofE) methods for integrating identified geo-information are reviewed as well.

In chapter 4, the fractal/multifractal based singularity index mapping technique efficient in characterizing singular physical or chemical properties is applied in the analysis of gravity and aeromagnetic data in the southeastern Yunnan mineral district, China. As follow-up after the introduction of singularity theory to geochemical mapping scenarios, this study extends its application to delineate geophysical potential fields. Based on low gravity and low magnetic properties of granitic intrusions in the study area, singularity mapping technique is used as a high-pass filter to emphasize the geophysical anomalies

caused by granitic intrusions in support of future mineral exploration. Comparing with traditionally used band-pass filtering methods, it is shown that the new technique provides an improved and simplified approach in geophysical data analysis with the advantage of scale independence. Two journal papers associated with this chapter had been published in Journal of Computer & Geosciences (Wang et al., 2011) and Journal of Applied Geophysics (Wang et al., 2013a).

In chapter 5, a tectonic-geochemical exploration model is constructed to support mineral exploration in the southeastern Yunnan mineral district, China. Fault systems are significant to mineralization in this district because faulting activities have confined magmatic activities into certain spatial scales and temporal stages, which provide both hydrothermal fluids and heat for mineralization within fracture zones. Analysis of fault density using the singularity theory to characterize development of fault systems suggests that spaces produced by faulting activities favored the migration of hydrothermal fluids and mineralization. In addition, the singularity theory is applied to examine singular distributed ore-forming elements. Principal component analysis (PCA) was used to model the spatial distribution of enrichment of the association of ore-forming elements, which suggests that geochemical haloes are linked with characteristic hydrothermal mineralization in the study area. In addition, PCA is further employed to integrate these identified anomalies of faults and ore-forming elements. By the integrated patterns, distributions of enrichments of ore-forming elements and faulted spaces favorable to mineralization can be delineated. The consistency of the results with information from published documents demonstrates that the exploration model discussed in this study is

useful and effective for investigating geological issues related with faulting activities. This part of work had been published in Journal of Geochemical Exploration (Wang et al., 2012).

In chapter 6, as an example of interdisciplinary collaboration, this chapter using a newly developed fault trace-oriented singularity index mapping technique intends to characterize hydrothermal mineralization associated anisotropic geochemical signatures. Fault traces located in a sub-district of southeastern Yunnan mineral district, China are divided into segments with equal length. Centered by fault segments, a set of rectangular windows are defined to estimate singularity index. Variations of geochemical signatures along the vertical direction of fault traces are characterized. The fault trace-oriented singularity indices assigned to their corresponding fault segments term faults as positive, negative and regular fault segments to qualitatively and quantitatively describe interrelations between fault structures and hydrothermal fluids or mineralization. In comparison with frequently employed fault properties (e.g., length, density, types, etc.), the new fault attributes (i.e., positive, negative, and regular fault segment) are applicable to describe variations of physical-chemical reactions between ore-forming fluids and wall rocks along fault traces that benefit the interpretation to metallogenic mechanism. The newly developed method can considered as a supplement to the formerly introduced square window-based isotropic singularity index mapping technique. This part of work had been published in Journal of Geochemical Exploration and under reviewed (Wang et al., 2013b).

In chapter 7, the Gejiu formation as another important geological body with controlling effects to hydrothermal mineralization in the study area is analyzed. The geochemical signatures of elements associated with the Gejiu formation are integrated by PCA. Obtained principal components (PCs) are evaluated, and the approximate one is selected to represent spatial distributions of geochemical signature of the Gejiu formation. In addition, singularity indices of these selected elements/oxides are integrated by PCA. The integration result well indicates the spatial variations in geochemical signatures of the Gejiu formation which is coincident with the mineralization-favored positions within the Gejiu formation. The general idea of this chapter applied to another district had been published in Journal of Geochemical Exploration (Zhao et al., 2012).

In chapter 8, based on the identified geo-information of geological bodies (i.e., controlling factors), three selected geo-information integration methods are employed to depict mineral potentials in southeastern Yunnan mineral district, China. First of all, the RGB composite image is produced to illustrate spatial variations of interactions of these three controlling factors. Secondly, PCA is applied to integrate these three sets of geo-information for quantitatively delineate spatial distributions of mineral potentials. Thirdly, other than PCA method, the student's *t*-value is applied in the three sets of geo-information to define three binary patterns. By each of binary patterns, one part corresponds to mineralization while the other corresponds to background. By using the WofE method, spatial distributions of both mineral potentials and interactions of the three controlling factors are depicted, simultaneously. Comparison on these three integration methods is made at the end of this chapter.

In chapter 9, summaries and discussions of current study are provided which can be useful experiences to the future studies regarding GIS-based geological exploration modeling not only in southeastern Yunnan mineral district, China, but also in other areas with hydrothermal mineralization.

Chapter 2. Study area and geo-exploratory datasets

2.1. Study area

Southeastern Yunnan district, China is chosen as the study area because of its world-class reserves of Sn-Cu polymetallic resources. It covers an area of about 300 km by 150 km at a longitude of 102°25′ ~ 104°43′E and a latitude of 23°50′ ~ 24°50′N and bounded to the north by the Wenshan fault, to the south by the Red River fault, to the east by the Malipo area, and to the west by the Jianshui-Yuanyang area (Fig. 2.1). The long history of mining activities in this area can be dated back to 2000 years ago (i.e., Han dynasty of China). After the founding of P.R. China, systematical exploration and investigations were significantly developed. In past two decades, knowledge on types, origins and distributions of the Sn-Cu polymetallic deposits had been greatly improved by profound and detailed researches.

From a geological point of view, southeastern Yunnan mineral district, China is located in a mineralization-favored environment which is advantage to ore-forming element accumulation and metal mineralization. In Zhuang et al. (1996), the specific geological environment was summarized in three factors. First of all, well developed fault/fold systems by intensive tectonic activities provide favorable spaces for mineralization (Li, 1998; Tan et al., 2004; Zhuang et al., 1996). The study area is located in the junction zone between Tethyan tectonic domain and the Pacific tectonic domain. Secondly, structural layers of the Yangtze craton where the study area locates in is believed as a source of

minerals from depth that is significant to mineralization. Thirdly, the tension of Youjiang basin during the Hercynian (386-257 Ma) to the Indo-China (257-205 Ma) epoch caused widespread volcanic eruption which triggered the earliest metallic mineralization in this area. The subsequent plate subduction and collision in the Late Indo-China epoch led to the formation and emplacement of the remelted granite in the Yanshanian epoch (205-135 Ma) which facilitated the enrichment of ore materials. A simplified regional geological map of southeastern Yunnan Sn-Cu polymetallic metallogenic belt can be found in Fig. 2.1.

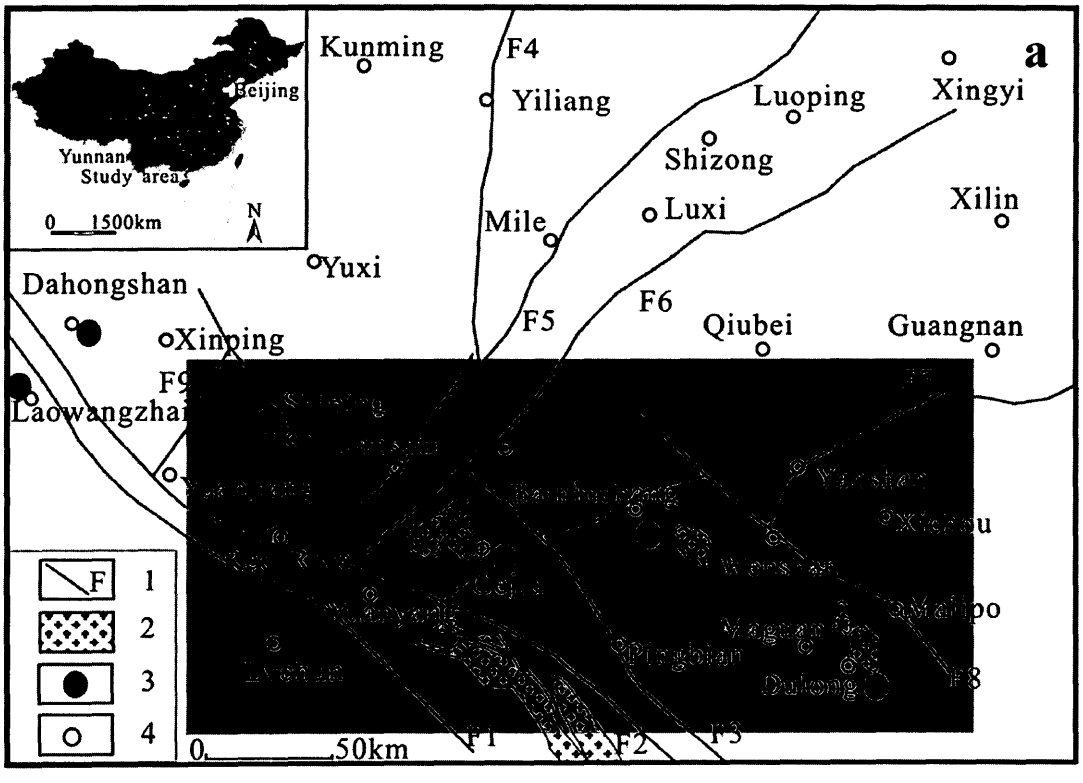

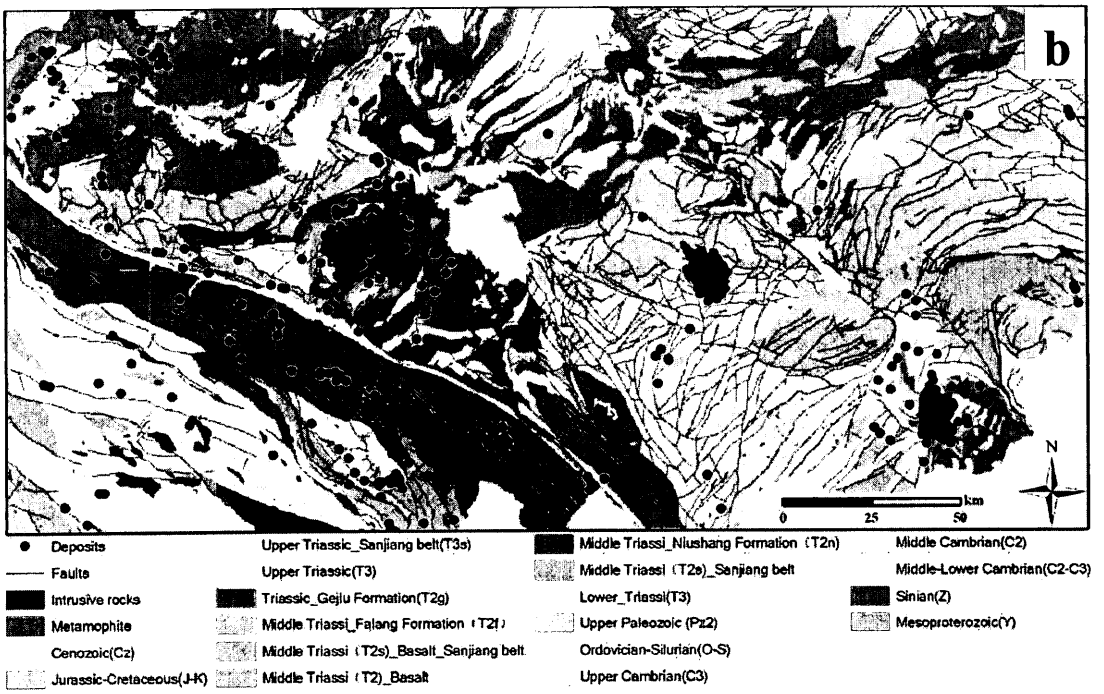

Fig.2. 1. **a:** Simplified map of regional tectonics, magmatic rocks and main metal mineralization district in southeastern Yunnan Province (after Wang et al., 2012). 1 = faults. 2 = Yanshanian granite. 3 = main metal deposits. 4 = cities and towns. F1 = Ailaoshan deep fault. F2 = Red River fault. F3 = Ping-Jian-Shi fault. F4 = Xiaojiang fault. F5 = Shizong–Mile fault. F6 = Nanpanjiang fault. F7 = Mengzi–Yanshan fault. F8 = Wenshan–Malipo fault. F9 = Lvzhijiang fault. The study area is shaded in gray. **b**: Geological map of southeastern Yunnan mineral district, China from 1:500,000 geological map database produced by China geological survey. The NS trending blue straight line on the southeast of the Gejiu batholith is shown to indicate location of the profile in Fig. 2.2.

In general, there are three main opinions of the metallogeny of southeastern Yunnan mineral district, China. Before the 1990s, it was believed that the source of the deposits was magmatic hydrothermal deposits associated with the Yanshanian granitic intrusions (Yang, 1990). Some researchers argued that the mineralization is part of "massive sulfide deposits from submarine exhalative sediment" (Zhou et al., 1997). The third model which has been widely accepted to support mineral exploration and exploitation

holds that the mineralization is a superimposed process involving submarine exhalative sedimentation and magmatic hydrothermal alteration (Chen et al., 1998).

Magmatic-hydrothermal ore deposit as a major type of Sn-Cu polymetallic mineralization in the study area is the main target of interest in this dissertation. The magmatic-hydrothermal mineralization is therefore accepted as a guideline to current mineral exploration modeling process. Gejiu, Wenshan and Dulong are three most productive ore districts distributed from the west to the east in the study area. The magmatic-hydrothermal ore deposits in the study area are genetically and spatially associated with granite batholiths including the Gejiu granite (107-85 Ma) (Guan, 1991), Bozhushan granite (114-97 Ma) (Gao, 1996) and Laojunshan granite (102-93 Ma) (Guan, 1991). These granite batholiths are spatially and genetically confined by fault systems. Most of the magmatic-hydrothermal ore bodies in the three ore districts are hosted in carbonate rocks. In Gejiu, wall rocks are the Middle Triassic dolomite and limestone. In Wenshan, wall rocks are the low-grade metamorphic Middle to Late Cambrian pelitic-arenaceous carbonatite formation. The ore-hosting strata in Dulong consist of the Early-Middle Cambrian alternating layers of medium to high-grade metamorphic mica-quartz schist, plagioclase gneiss and marble (Luo, 1995). Therefore, three main controlling factors of magmatic-hydrothermal mineralization in southeastern Yunnan mineral district are tectonic systems, granitic intrusions and the sedimentary layers (Zhuang et al., 1996).

2.1.1. Regional tectonics

In southeastern Yunnan mineral district, well-developed fault systems are mainly crustal fractures which dominate tectonic frameworks, basin structures, sedimentary evolution, magmatic activities and mineralization (Cui, 2000; Zhuang et al., 1996) (Fig. 2.1). Depending on characteristics, activities and influences, fault systems in the study area can be grouped in two types. The first one is the long-term active and large-scale deep crustal fracture. The second is the contemporaneous faults exhibiting both long-term and intermittent activities (Zhuang et al., 1996). Former researches (Qin and Li, 2008; Wang, 2004; Zhuang et al., 1996) suggest that regional fault systems are significant to mineralization-associated granites in the study area. According to geochemical analysis, most of mineralization-associated anomalies are centered on the fault systems (Tao et al., 2002). For some sub-districts, ore bodies can even be found in the faults (Gao et al., 2004a). In addition, applications of remotely sensed techniques can support the point of view that fault systems dominate the distribution of Sn deposits (Tang et al., 2004).

Major faults (Fig. 2.1) in the study area include the following. The Red River fault is a NW-SE trending deep crustal fault accompanied by ultramafic intrusion, mafic extrusion and sedimentation of siliceous rocks (Qin and Li, 2008). The N-S trending Xiaojiang fault divides the Gejiu ore district into two parts, the eastern and the western. The earliest activities of the Xiaojiang fault occurred in the Late Neoproterozoic. It developed into a tensile fault in the Permian and was the migration channel of massive mafic extrusion and intrusion. The Ailaoshan fault parallel to and situated in the south of the Red River fault

is another deep crustal fault in the study area. Frequent and intensive magmatic activities during the Lvliang (2500-1800 Ma) to the Himalayan (23.5-0.78 Ma) epoch caused the pinch and swell structure of igneous rocks along the Ailaoshan fault. Siliceous sedimentation can be found in the fault zone as well. The NE-SW trending Zongshi-Mile fault is the boundary of the Yangtze craton (in the west) and the Youjiang basin (in the east). Permian basalt is distributed along the Zongshi-Mile fault. Parallel to the Zongshi-Mile fault, the Nanpanjiang fault was formed in the Neoproterozoic and became a reverse fault in the Triassic. Basalt is extensively distributed along the Nanpanjiang fault zone ($\approx$ 688 ~ 1,603 m thick). In the study area, the ore belt along the Nanpanjiang fault is characterized by mineralization of Sb, Hg and Au. The faults described above constitute the tectonic framework of the study area, and control the scale and the spatial distribution of intrusive rocks.

Four groups of faults spread along different orientations (i.e., NE, EW, NS and NW trending faults) throughout the study area. Over the history of the basin evolution, their activities occurred in different directions and durations (Zhuang et al., 1996). NE trending faults (e.g., the Shizong-Mile fault and the Nanpanjiang fault) in the study area were caused by tectonic activities in the Middle Hercynian, Indo-China, and Yanshanian epoch. Most of the faults in this group are deep-rooted and extend for long distances. EW trending faults (e.g., the Mengzi-Wenshan-Geduo fault and the Qiubei-Guangnan fault) are well-developed in the eastern of the Gejiu mineral district and often play as primary spatially controlling factors of mineralization. EW trending faults are not widespread in the western of the Gejiu mineral district and their controlling effects on mineralization

are not as important as in the eastern district (Zhuang et al., 1996). The Xiaojiang fault as the most important and the largest NS trending faults separate the Gejiu sub-district into two parts. Similar to NE trending faults, it is large-scale and deep-seated. Performing as main regional division faults, Xiaojiang fault does not support mineralization itself. However, the intersections with other geological or tectonic features (e.g., fold and feather fractures) may have ore-controlling effects on the tin-polymetallic mineralization (Qin et al., 2006a; Zhuang et al., 1996). The activities of NW trending faults (e.g., the Ailaoshan fault and the Red River fault) highly influenced magmatic activities and mineralization in southeastern Yunnan mineral district. They confine the spatial distribution of both igneous rocks and sediment rocks in the study area. In general, NE, NS and EW trending faults are large in scale but less active during the geological evolution; whereas NW faults are small in spatial distribution but more active. They all contributed in controlling the main basin structure and stratigraphic distribution (Zhuang et al., 1996).

Besides these fault groups, there are three fold systems spreading in the EW, NE and NW directions. They constrained the spatial distribution of magmatic emplacement and ore bodies. Two large-scale folds (i.e., the Wuzishan duplex anticline and the Jiasha duplex syncline) dominate extents of the east and the west of mining areas in the Gejiu sub-district, respectively (Zhuang et al., 1996).

2.1.2. Regional stratigraphy

The sedimentation history of strata in southeastern Yunnan mineral district can be summarized as follows (Yang, 1990; Zhang et al., 2006; Zhou et al., 1997). A series of flyschoid facies formed in the Sinian (Late Proterozoic) period (800-570 Ma). Then, a series of marine carbonate rocks formed during the Cambrian and Middle Ordovician. An uplift-erosion stage occurred during the Late Ordovician to the Silurian. Continental clastics and carbonate rocks then formed during the Devonian to the Early Permian. Mafic volcanic rocks and volcaniclastic rocks were precipitated during the Late Permian to the Late Triassic. The Indo-China orogeny (230-200 Ma) in the Middle to Late Triassic changed the study area into a denudation environment. The emplacement of three main granite batholiths occurred during the Late Yanshanian.

Sedimentary rocks are well developed and widespread in the study area. Besides the Cretaceous, strata formed during the Precambrian to Quaternary are outcropped in the study area (Fig. 2.1). The strata formed before the Upper Triassic is dominated by marine materials, while after that is by continental sediments (Li, 1998; Lue, 2005; Zhuang et al., 1996).

The Proterozoic strata are mainly distributed in the Jinpin-Jianshui and Shiping-Jianshui areas, some of which are exposed in the Pingbian area as well. As the oldest outcropped rock series of folded basement, the Kunyang group (i.e., formed in the Mesoproterozoic spreading over the areas of Kunyang, Dongchuan and Huize) is a set of quasi-flysch and

shallow marine carbonate sediment with a thickness of more than 11,550 meters. It can be found in the Shiping and Jianshui areas. Besides, The Pingbian group (i.e., formed in the Precambrian spreading over Pingbian area) is composed of a set of low metamorphic sand-shale rocks with a thickness of more than 4,292 meters. The Ailaoshan group (i.e., formed between the Proterozoic and the Early Cambrian lies between the Red River and the Ailaoshan fault) is shown as a strip of metamorphic rock extending in the NW orientation. It consists of a series of deeply metamorphic complex rocks with a thickness of more than 9,226 meters. The Sinian strata (i.e., formed between the Proterozoic and the Early Cambrian) consisting of sandstone, dolomite, conglomerate, shale and slate are mainly located in Shiping and Jianshui areas, (Zhuang et al., 1996).

The Paleozoic strata are well developed in the study area. The Cambrian strata are located in Shiping, Jianshui, and Mengzi and Malipo areas. The Lower Ordovician strata are widespread, whereas Middle-Upper Ordovician strata have been generally eroded except the Yuanyang area. The Silurian strata are scattered. Except in Shiping and Jianshui areas, the Lower Devonian strata are generally missing, while the Upper and Middle Devonian strata are extensively developed. The Carboniferous strata are also well distributed. For the Permian strata, both carbonate sediments in the Lower Permian and basalt in the Upper Permian are prevalent (Zhuang et al., 1996).

Mesozoic strata are not well developed in the study area. Only the Triassic has a relatively complete stratigraphic distribution. The Middle-Lower Jurassic strata can be

found in the Lvchun and Shiping areas. The Cretaceous strata are generally missing in the area (Zhuang et al., 1996).

The Tertiary strata are scattered throughout Jinping, Gejiu, Jianshui, Kaiyuan, Mengzi, Maguan, Wenshan areas and the strip district along Yuanjiang to the Red River. Quaternary strata composed of lacustrine, deluvium, saprolite and cave deposits are distributed in the lakes, rivers, mountains, and the Cenozoic basin (Zhuang et al., 1996).

2.1.3. Regional magmatic rocks

Caused by tectonic activities occurred from the Proterozoic to the Cenozoic, magmatism in the study area presents multiphase and multistage characteristics. Magmatic activities during the Jinning (1000-800 Ma) to the Hercynian epoch (386-257 Ma) were dominated by medium- to small-scale ultramafic-felsic extrusions. Drastic activities of the Red River fault during the Indo-China epoch (257-205 Ma) caused the massive emplacement of mafic magma along the fault (Guan, 1991; Wang, 2004). Magmatic activities during the Yanshanian epoch (205-135 Ma) are important, which are highly related with the Sn-Cu polymetallic mineralization in the three main ore districts (Guan, 1991; Luo, 1995). The main ore-forming elements in the study area consist of Au, Ag, Cu, Pb, Zn, Sn and W (Dai, 1990). In the Himalayan epoch (23.5-0.78 Ma), magmatic activities were moderate resulting only mafic-ultramafic rocks scattered in the Maguan area (Guan, 1993).

According to Zhuang et al. (1996), primary types of magmatic rocks produced during the Proterozoic era are granite, diorite and other mafic/ultramafic rocks. The biotite granite

distributed in Shiping-Longwu-Takeju is considered as a part of Eshan-Chahe complex rocks, outcrop of which is about 4 km^2. Alteration in the contact zones of granitic rocks and country rocks are weak. Besides, metamorphosed granite can be found in the areas along the Ailaoshan fault as well. Diorite mainly appears in northwest of Shiping area in forms of dikse, veins, and stocks, etc. Mafic/ultramafic intrusive rocks are scattered in Ailaoshan fault belt (Liu, 2007).

The main magmatic rocks produced in the Hercynian epoch are mafic/ultramafic extrusive and intrusive rocks (Tan et al., 2004; Xiong and Shi, 1994; Zheng and Yang, 1997). Basalts by fissure eruptions are broadly spread over Jianshui, Kaiyuan, Jinping, Lvchun, Mengzi, and Wenshan areas. Lithologically, the lower part is consisted of huge thickness of basaltic volcanic breccia and/or compact or amygdaloidal basalts. A small amount of basaltic phosphate rocks, intermediate-felsic lava and marine sediment layers are presented; the content of phosphatic materials are increased from lower to higher parts. Intrusions in Hercynian epoch are mainly mafic, which intruded into the Ailaoshan group and are mainly located in Mianhuadi to Maandi areas. Mineralization of Cu, Ni, V, Ti and Fe can be found in the Ailaoshan group (Liu, 2007; Zhuang et al., 1996).

Magmatic activities are intensive in the Indo-China epoch. Both felsic intrusions and mafic extrusions/intrusions were witnessed in the study area (Gao et al., 2004b; Qin et al., 2006b; Zhuang et al., 1996). Most of them are distributed mainly in Jinping, Wenshan, Pingbian, Yuanyang, and Lvchun areas and a few scattered in other areas. The felsic intrusive rocks with gneissic structure are primarily composed of biotite granite, biotite

monzogranite and biotite plagiogranite. These felsic intrusive rocks present as aluminum-supersaturated series. The mafic/ultramafic intrusive rocks in this epoch are mainly composed of olivine gabbro and gabbro dolerite (in Jinping-Jiangjiaping to Niulanchong areas), diabase gabbro (in Chonggang area), quartz-gabbro dolerite (in Gulinqing area), and peridotite and diabase gabbro (in Malipo area). All these magmatic rocks which intruded into the Paleozoic to the Middle-Upper Triassic strata are considered as productions of the Indo-China tectonism. Moreover, outcrops of the extrusive rocks are mainly distributed in Yuanyang and Lvchun areas while scattered in Jinping, Gejiu and Kaiyuan areas (Liu, 2007; Zhuang et al., 1996). Some scholars suggested that the mafic magma in the Late Indo-China epoch and the felsic igneous rocks in the following Early Yanshanian epoch originated from the Earth's mantle provided parts of ore-forming materials. The abundance of Sn is, therefore, much higher than the average in the Earth's crust (Li et al., 2005, 2006; Qin et al., 2006a).

Magmatic activities in the Yanshanian epoch are characterized by hypabyssal emplacement of magma. Lithologically, the magmatic rocks show a complete evolution series from mafic/ultramafic, intermediate, felsic to alkalic members. Meanwhile, noticeable concentrated skarn type mineralization was accompanied as intruding of these rocks. Therefore, magmatic activities in the Yanshanian epoch played an important role in the mineralization of this area (Li et al., 2005; Qin et al, 2006a; Xiong and Shi, 1994). The lithology and spatial distribution of various types of the igneous rocks are described as following.

Mafic/ultramafic rocks are extensively spread over Gejiu, Jianshui, Red River, Jinping and Yuanyang areas. The intrusive rocks are consisted of gabbro, pyroxenite, peridotite and dolerite. Intermediate rocks are primarily distributed in Shiping area as stocks, dikes, and veins along faults. Most of them have been intensively weathered off. The main types of these rocks are biotite quartz diorite and diorite in fine to medium-grained semi-automorphic granular texture. Plagioclase, hornblende, biotite and quartz are primary minerals. Accessory minerals include leucoxene and apatite. Granite is the most important felsic rocks which is wildly distributed in Gejiu, Wenshan, Eshan, Yuanjiang, Jinping, and Lvchun areas. Main felsic rocks include Eshan granite (not discussed in this dissertation), Gejiu granite, Bozhushan granite, and Laojunshan granite. The felsic rocks, especially the well-differentiated remelting granitic intrusions are greatly associated with the formation of Sn, Cu, Pb, Zn and W deposits in the study area (Zhuang et al., 1996). Alkalic rocks in the study area are less outcropped, which are mainly found in Baiyunshan area.

The magmatic activities in the Himalayan epoch were inactive. The magmatic rocks are mainly composed of mafic extrusive rocks and alkalic rocks, and only scattered in the Ailaoshan area (Liu, 2007).

Table 2. 1. Average concentrations (in ppm) of trace elements in granites, southeastern Yunnan (Zhang et al., 2006).

Area	Intrusion	Li	Rb	Cs	Sr	Ba	Be	Nb	Ta	Sn	W	Mo	Pb	Cr	Ni	Co	V
Gejiu	Longchahe	72.59	345	15.29	508	1079	2.19	23.14	2.93	13.97	2.50	1.03	62.4	12.72	13.89	11.55	31.36
	Masong	79.71	467	33.40	162	302	5.47	41.09	5.59	28.40	16.00	1.51	61.3	5.19	6.60	3.98	1.70
	Shenxianshui	57.20	517	28.00	201	308	4.79	28.00	9.00	1.15	5.89	0.65	48.7	2.84	5.80	6.00	5.86
	Baishachong	127	584	79.30	199	335	5.35	54.00	8.12	29.80	9.00	1.15	64.3	14.40	1.60	3.89	15.00
	Laoka	153	861	53.40	38.2	107	4.50	45.9	11.50	22.00	10.50	1.05	43.4	3.29	1.93	0.75	3.4
Bozhushan	Bozhushan	100	287	24.10	350	1025	0.85	24.4	1.62	11.80	1.00	0.95	16.9	20.00	7.60	7.70	43.60
	Bainiuchang	35.30	n/a	n/a	259	846	5.08	18.45	>10	11.40	4.05	<4	31.98	18.35	5.27	8.0	50.28
Laojunshan	Stage I	87.2	399	33.40	48.1	175	10.50	30.4	4.00	71.00	30.00	0.75	57.0	5.18	15.80	2.86	10.05
	Stage II	146.8	519	68.30	26.3	128	16.90	29.00	14.90	103	26.50	0.55	96.7	3.9	2.7	19.1	8.7
Average in granite intrusions (Vinogradov value)		40	200	100	300	830	5.5	1.0	3.5	3	1.5	1.0	20	25	8	5	40

2.1.4. Metallogenetic model

Former researches suggested that the Sn-Cu polymetallic mineralization in southeastern Yunnan district is a complex process controlled by various geo-processes including the Middle Triassic Gejiu carbonate formation, fault systems and the Yashanian granitic intrusions (Gao, 1996; Guan, 1991; Zhuang et al., 1996). Among the three factors, the Gejiu formation is the main ore-bearing strata; interactions of tectonic-magmatic activities dominate the intensity and scales of mineralization; the Yanshanian granitic intrusions provide not only ore-forming elements but also fluids for hydrothermal alteration.

There are three reasons in support of the granitic intrusions to be main controlling factors of the mineralization in the study area. Firstly, most of the known Sn-polymetallic deposits in southeastern Yunnan ore district are distributed around the intrusions. Many large scale Sn-polymetallic deposits in the study area sit on the protuberances of the granite intrusions. The primary sulfide ores in the Sn-polymetallic deposits are mainly found in the Middle Triassic Gejiu carbonate formation and in contact zones of these strata and surrounding granitic intrusions. Although most of the orebodies are hosted by sedimentary strata overlying the granites, they are skarn deposits and, thus, were likely associated genetically to certain igneous intrusions. Secondly, in the study area, the trace element associations characterizing the Sn-polymetallic deposits are coherent with the trace element associations characterizing the granites (Table 2.1). The concentrations of

Sn, W, Pb, Nb, Ta, etc. in the granite intrusions are comparable to the enrichment of each of these elements in the Sn-polymetallic deposits. Thirdly, the protuberances of the granite intrusions and their surroundings and the fracture zones in the overlying sedimentary strata are the main controls on ore formation and localization.

Tectonism is another important factor in controlling the mineralization in the study area. First of all, large-scale faults control the spatial distribution of regional geochemical fields by dominating the emplacement of granites. Secondly, small-scale faults and fractures within the carbonate rocks supported the migration and differentiation of hydrothermal fluids. During the emplacement of granites, interchanging of ore materials occurred within the fracture zones between magma and wall rocks, which benefitted the enrichment of metal elements. Therefore, these small faults, especially the intersections of faults provided favorable places for mineralization.

In general, granitic intrusions, the Gejiu formation and fault systems as the main controlling factors to the formation of Sn-Cu polymetallic deposits in the study area mean significantly to mineral exploration (Fig. 2.2). More details can be found in Zhang et al. (2006).

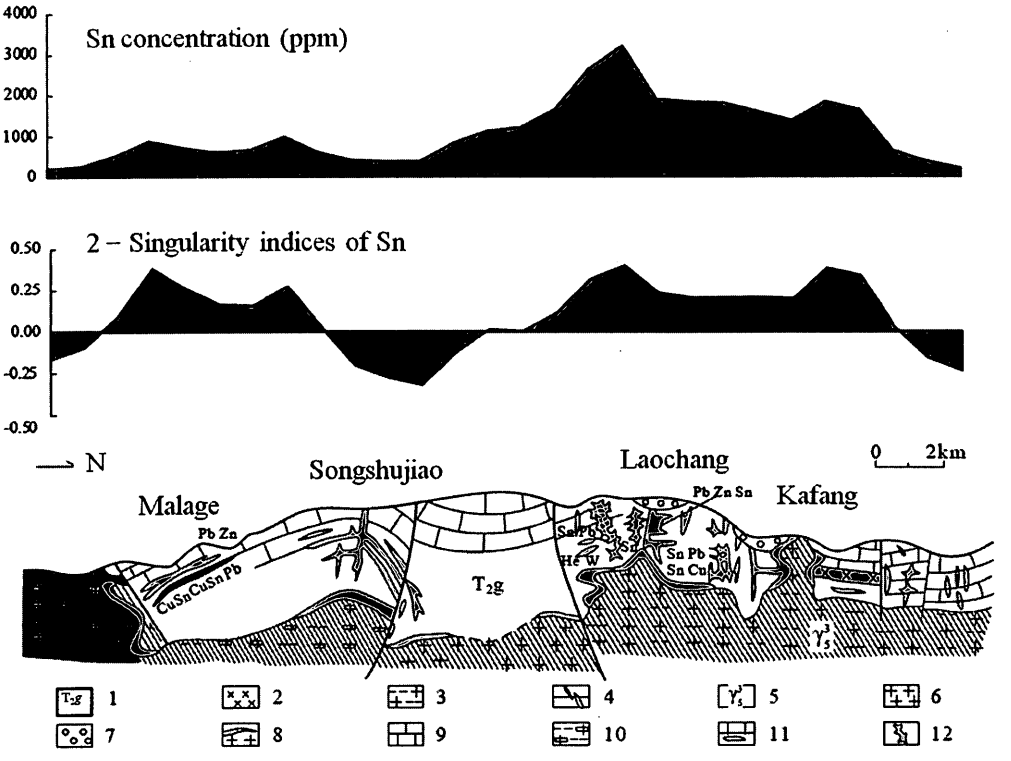

Fig.2. 2. A schematic diagram of profile of Sn ore, granites and surface geochemical anomalies demonstrate the metallogenetic model of the study area (after Cheng, 2011). The singularity indices describing spatial variations of geochemical anomalies will be introduced in following chapters. Occurrence of the mineralization is coincident with the accumulation of ore elements. 1: the Middle Triassic Gejiu formation; 2: Dolerite; 3: Altered biotite granite; 4: Vein orebody; 5: the Late Yanshanian granitic intrusions; 6: Granitic rocks; 7: Placer deposits (Cu); 8: Skarns; 9: Carbonate rocks; 10: Porphyritic biotite granite; 11: Stratabound orebodies; 12: Reticular orebodies.

2.2. Geo-exploratory datasets

According usages of exploratory datasets associated with geological exploration, geological data including location information of geological features, geophysical data investigating the spatial distribution of subsurface objects, and geochemical data of the concentration of different elements can be considered as spatial indicators of geological bodies. The GIS datasets including geological data, stream sediment geochemical data, ground-based gravity data and aeromagnetic data used in this dissertation were produced by China Geological Survey.

2.2.1. Geological data

The geological data are from the database of 1:500,000 scale geological maps of China, and stored in vector type format. It includes locations of mineral deposits and occurrences (i.e., points), fault traces (i.e., polylines) and outcrops of lithological units (i.e., polygons) (Fig. 2.1b). Descriptions of the properties of these datasets (e.g., name, age, length or lithology) are recorded in the tabular database associated with the vector data.

2.2.2. Geochemical data

Since the initiation of the Chinese National Geochemical Mapping Project in 1979, a great amount of geochemical data covering 5.17 million km^2 of P. R. China were collected and associated geochemical database had been constructed (Xie et al., 1997). Geochemical data used in this dissertation includes stream sediment sampling data. Each

sample recording concentration values of 39 elements/compounds was mainly analyzed by means of X-ray Fluorescence. The data points are distributed evenly at an interval of 2 km throughout the whole study area. Further details with respect to the characteristics of geochemical data can be found in Xie et al. (1997). As an extension provided by GeoDAS (Cheng, 2000), the Inverse Distance Weighted (IDW) method is currently applied to interpolate and convert the vector data (i.e., point) to grid surface (i.e., image) at a 2 km spatial resolution. 39 images are available to represent the geochemical distributions of these elements and compounds.

2.2.3. Geophysical data

Geophysical datasets used in this dissertation are composed of ground-based gravity data and aeromagnetic data. The gravity and aeromagnetic data were acquired from 1:200,000 and 1:100,000 scale geophysical databases, respectively, produced by Chinese national geological exploration project. Sample points at an interval of 2 km are currently interpolated by the IDW technique. Similar as the geochemical data, the spatial resolution of gravity and aeromagnetic grid maps are 2 km as well.

Chapter 3. Methodologies

Mineralization-associated geo-anomalies play an important role to guide mineral exploration, recognization of which often depends on geo-information extraction and integration (Cheng, 2012; Wang et al., 2011, 2012, 2013; Zhao et al., 2012). In this chapter, some recently developed and advanced GIS-based geo-anomaly analysis methods (i.e., key methodologies of this dissertation) are introduced before mineral exploration modeling in following chapters. In the aspect of geo-anomaly extraction, a square window-based singularity index mapping technique initiated by Cheng (1999) is reviewed, and an improved fault trace-oriented singularity index mapping method is introduced. In the aspect of geo-anomaly integration, principal component analysis (PCA) and weights of evidence (WofE) are reviewed as well.

3.1. Singularity index mapping techniques

Geo-information extraction so-called geo-anomaly identification or separation from background is a primary task in geological exploration (Cheng et al., 1994). After the introduction of multifractals by Mandelbrot (1972), various fractal/multifractal models were developed and commonly used to investigate geological issues (Agterberg, 1995; Turcotte, 1997; Cheng, 2007a; Carranza, 2008; Carranza et al., 2009; Carranza and Sadeghi, 2010). Singular geo-processes like earthquakes, volcanoes, floods, cloud formation, rainfall, hurricanes, landslides and mineralization have been discussed in

many published literatures (Malamud et al., 1996; Schertzer and Lovejoy, 1987; Turcotte, 1997; Veneziano, 2002). "Singularity", a multifractal concept proposed by Cheng (1999), is a quantitative and qualitative characteristic of particular natural phenomena accompanied by energy release or material accumulation within narrow spatial-temporal intervals. In Cheng (2007a), anomalous concentrations of ore-forming elements caused by hydrothermal mineralization were delineated by the singularity index mapping technique. It has been demonstrated that the results may provide new geo-information as complements of original concentration values. In Cheng et al. (2009), peak flow events considered as special phenomena of environmental issues were analyzed by singularity analysis to characterize their frequency distribution. In Wang et al. (2011), the singularity theory was applied to characterize singular physical properties caused by magmatic activities. Zuo et al. (2009) stated that the singularity index mapping technique is efficient in indicating weak geo-anomalies usually hidden within a strong variance of background. More sophisticated association between singularity and other subjects of geostatistics can be found in Cheng (2006) and Agterberg (2012a).

3.1.1. A window-based singularity index mapping technique

Within a system of hydrothermal mineralization, the amount of metal in a small area A can be denoted as $\mu(A)$ and the average concentration of metals in A can be denoted as $C(A)$ (Cheng, 2007a). Within a heterogeneous medium, both $\mu(A)$ and $C(A)$ change as A changes. From a multifractal point of view, $\mu(A)$ and $C(A)$ follow power-law relationships with A:

$$\langle \mu(A) \rangle = cA^{\alpha(x)} \qquad (3.1)$$

$$\langle C(A) \rangle = cA^{\alpha(x)-1} \qquad (3.2)$$

where c is a constant and $\alpha(x) = \alpha/E$ is the exponent of the power-law relationships. E is the Euclidian dimension of area A. The power-law relationship is generally represented in a statistical sense as $\langle\ \rangle$ or "expectation". Regarding other singular geo-processes and without loss of generality, the $C(A)$ can denote the amount of certain physical quantities (e.g., energy, rainfall, etc.) in a spatial or temporal interval (e.g., volume, day, etc.). The power-law relationship in either Eq. (3.1) or Eq. (3.2) is determined by c and α. The constant c determines the magnitude function. The α, so-called singularity index, is a scaling exponent and preserves the shape of the magnitude function and the changes in certain physical quantities across various scales of spatial-temporal intervals.

If α remains constant throughout an area, then the physical quantities of singular geo-processes do not have fractality. Otherwise, if α has multiple values, the physical quantities of singular geo-processes may follow a multifractal distribution. In general, the parameter α can be divided into three categories: (1) $\alpha = E$ corresponds to a linear distribution when $C(A)$ (i.e., a given physical quantity) is independent of A (i.e., the interval); (2) $\alpha < E$, considered to be positive singularity, implies a "convex" property of $C(A)$ within A and indicates enrichment of the physical quantity; (3) $\alpha > E$, considered to be negative singularity, implies a "concave" property of $C(A)$ within A and indicates depletion of the physical quantity.

In addition, the singularity index in Eqs. (3.1) and (3.2) can be expressed as:

$$\alpha = \frac{d\mu(A)}{dA} \cdot \frac{2}{C(A)} \tag{3.3}$$

where the singularity index α is related to a high-pass filter transformation of the amount of a certain physical quantity $\mu(A)$. It implies that α is the result of the first derivative transformation of the $\mu(A)$ with a characteristic of scale independence in comparison with other types of high-pass filters (Cheng, 2007b, 2008). Although there is an A in the Eq (3.3), the estimation of α is independent of scales of A if the scale independence in Eqs. (3.1) and (3.2) are existing (Cheng, 2007b).

The value of α in 2D is estimated by means of a windows-based method (Cheng, 1999). Preparations for the estimation of α include delineation of study area, definition of a set of windows with an area $A(\varepsilon_i)$ and sizes ε_i ($\varepsilon_i = \varepsilon_1 < \varepsilon_2 < \varepsilon_3 \ldots < \varepsilon_n$), and calculation of average values $C[A(\varepsilon_i)]$ (Fig. 3.1). If values of $C[A(\varepsilon_i)]$ and ε_i are plotted in a log-log graph, a linear relationship between them can be described by the least-squares method (Fig. 3.1). The value of α is given by the slope of Eq. (3.4). By sliding the windows, singularity indices for all locations are estimated. More details can be found in Cheng (2000).

$$\log C\left[A(\varepsilon_i)\right] = \log(c) + (\alpha - 2)\log(\varepsilon_i) \tag{3.4}$$

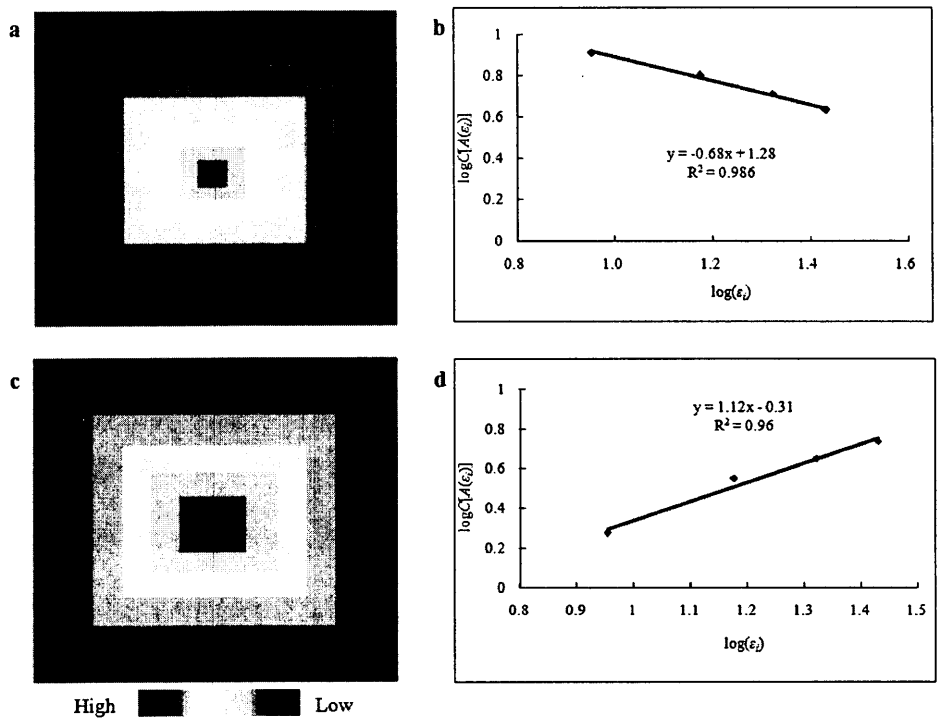

Fig.3. 1. A schematic diagram to demonstrate singularity index estimated by a square window-based method. (**a**) and (**b**) represent a calculation process for positive singularity index (i.e., $\alpha < 2$). (**c**) and (**d**) represent a calculation process for negative singularity index (i.e., $\alpha > 2$).

3.1.2. A fault-orientated singularity index mapping technique

Being non-linear and complex, the occurrence of mineralization is usually dominated by a cascade process involving various controlling factors (Cheng, 2012). Geochemical distributions indicating mineral deposits are anisotropic in many cases. Therefore, in addition to characterize the heterogeneity by the isotropic square window-based method, a fault trace-oriented singularity index mapping method is introduced here.

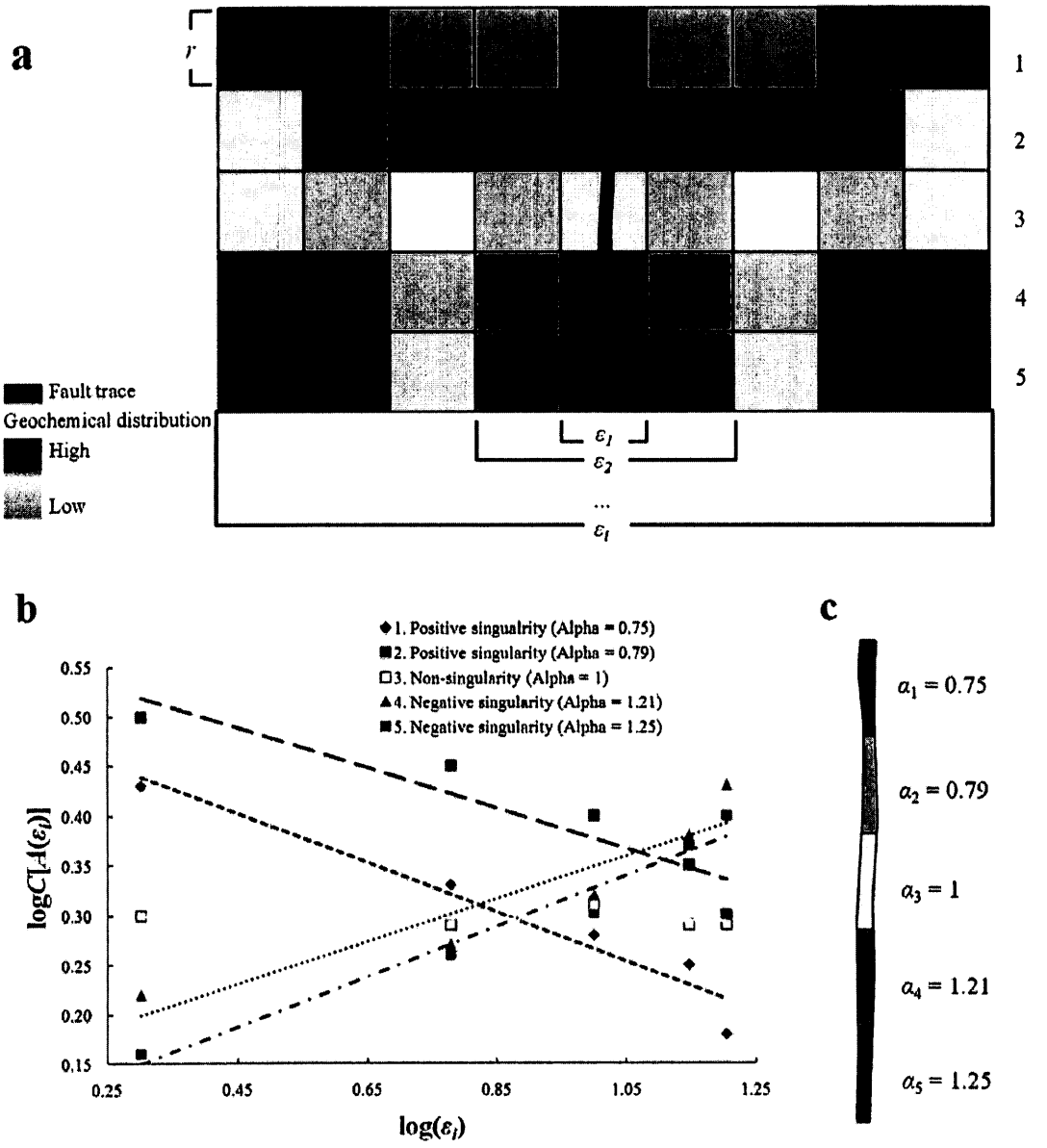

Fig.3. 2. A schematic diagram to demonstrate an estimation process to characterize anisotropic properties of geochemical signatures based on a fault trace-oriented singularity index mapping technique. (a) represents definition process of a set of fault trace-oriented windows with a predefined height r and a set of width ε_i for a certain physical quantity, and the fault trace are divided into segments at a length r. (b) and (c) illustrate the calculation process of singularity indices for different segments of the fault trace.

By the fault trace-oriented method, each individual fault trace is divided into segments with a pre-defined constant length r. Centered by an individual fault segment, a set of rectangular windows are defined with sizes of $r \times \varepsilon_i$ (Fig. 3.2). The width values of ε_i are same as the definition in the square window-based method. Therefore, rather than the isotropy described by a square window-based method, only variations of geochemical distributions along the vertical direction of the fault trace are considered to characterize anisotropy of geochemical signatures. The new $C(A_i)$ will be the average concentration of metals within different rectangular areas A ($r \times \varepsilon_i$). Since the ε_i^2 used in square window-based mapping method (i.e. 2-D) is changed to $r \times \varepsilon_i$, an updated Eq. (3.2) will be in a 1-dimensional scenario:

$$\langle C(r \times \varepsilon_i) \rangle = c\varepsilon_i^{\alpha_r - 1} \qquad (3.5)$$

where, $\alpha_r = \alpha/2$ and α is the singularity index in the 2-dimensional scenario. Similarly, if a log-transformation is applied to both sides of Eq. (3.5), a linear relationship between $\log(\varepsilon_i)$ and $\log C(r \times \varepsilon_i)$ (Fig. 3.2) can be expressed as:

$$\log C(A_i) = \log(c) + (\alpha_r - 1)\log(\varepsilon_i) \qquad (3.6)$$

where, c is the constant and α_r is the singularity index estimated by the rectangular window-based mapping method. Compared with isotropic singularity index, newly proposed anisotropic singularity index is sorted into comparable categories. $\alpha_r = 1$ indicates monofractal geochemical distributions along the direction perpendicular to a fault segment. $\alpha_r \neq 1$ depicts variations of a certain geochemical element concentration

along the vertical direction to a fault segment. Specifically, $\alpha_r < 1$ is termed as positive singularity corresponding with continuous enrichment of metals during approaching to the fault space, while $\alpha_r > 1$ is termed as negative singularity corresponding with gradual depletion of metals during approaching to the fault space. Since the definition of rectangular windows is based on the spatial distribution of fault traces, the updated singularity indices of different fault segments along the fault traces are meaningful to characterize geochemical behaviors of metallic concentration within the fault spaces.

When ore-bearing fluids transport through a fault trace, interactive geochemical reactions facilitating hydrothermal mineralization might occur between fluids and the wall rocks along the fault trace. These reactions can be characterized by fault trace-oriented singularity index α_r. In segments with $\alpha_r = 1$, homogenous metal concentration within rectangular windows implies that no and/or equivalent interactions between hydrothermal fluids and wall rocks occurred. Segments with $\alpha_r > 1$ imply that fluids may extract ore-forming materials from wall rocks and cause metal depletion in wall rocks. In segments with $\alpha_r < 1$, metal enrichment implies that ore-forming materials migrated by fluids may increase contents of them in wall rocks. Extremely, the fluids might be ore-forming ones, and variations of the circumstance within fault segments facilitate deposition and mineralization of the fluids. As a result, the vein-type hydrothermal deposits might be presented within the fault spaces. Therefore, based on these influences on hydrothermal mineralization, a fault trace can be subdivided into positive segments ($\alpha_r < 1$), negative segments ($\alpha_r > 1$) and regular segments ($\alpha_r = 1$).

3.2. Principal component analysis (PCA)

Principal component analysis (PCA) is one of the best-known techniques for multivariate analysis. It is a useful statistical technique frequently employed in various fields such as face recognition (Zhao et al., 2003) and image compression (Smith, 2002). A main purpose to use PCA is to reduce the dimensionality of datasets by transforming interrelated variables of datasets into new sets of datasets consisting of uncorrelated variables. These uncorrelated variables are the so-called principal components (PCs) (Joliffe, 2002).

The foundation of principal component analysis is the covariance or correlation coefficient matrix, which represents interrelationships among multidimensional variables. By orthogonal transformation, a set of interrelated variables are converted into a new coordinate system, in which the eigenvectors acting as the axes are linear combinations of the original variables (Fig. 3.3). Eigenvalues (i.e., variances of PCs) and eigenvectors can be used to characterize PCs (i.e., vectors). In the vector space, these directions of these vectors are orthogonal, meaning that these PCs are independent. Stretching degrees are associated with their corresponding eigenvalues. The definition of the covariance and correlation coefficient between two sets of variables X and Y can be expressed as (Cheng, 2006b):

$$\mathrm{cov}(X,Y) = \frac{\sum_{i=1}^{m}\sum_{j=1}^{n}(X_i - \overline{X})(Y_j - \overline{Y})}{mn} \tag{3.9}$$

$$\rho_{X,Y} = \frac{\frac{1}{mn}\sum_{i=1}^{m}\sum_{j=1}^{n}(X_i - \overline{X})(Y_j - \overline{Y})}{\sqrt{\frac{1}{mn}\sum_{i=1}^{m}(X_i - \overline{X})^2}\sqrt{\frac{1}{mn}\sum_{j=1}^{n}(Y_j - \overline{Y})^2}} \tag{3.10}$$

where i and j represent the indices in X and Y, X_i and Y_j represent the variables, and $\overline{X}$ and $\overline{Y}$ are the mean values of X and Y, respectively. The values of m and n represent the column and row of X and Y, respectively. When it is supposed that the correlation coefficient matrix of X and Y is A, If there is a vector x that satisfies the function:

$$Ax = \lambda x \tag{3.11}$$

then the x and λ are termed as the eigenvector and the eigenvalue, respectively. The newly achieved PCs represent most variability (i.e., information) of original multidimensional variables. For the case of two variables X and Y, the first PC (i.e., PC1) contains more information, while PC2 carries residual information independent of PC1. The two PCs can be expressed as follow:

$$PC_i = a_i X + b_i Y \tag{3.12}$$

where i is the order of PCs, while a_i and b_i are contributions of X and Y. As linear combinations of original variables, individual PCs are often interpreted to achieve geo-information.

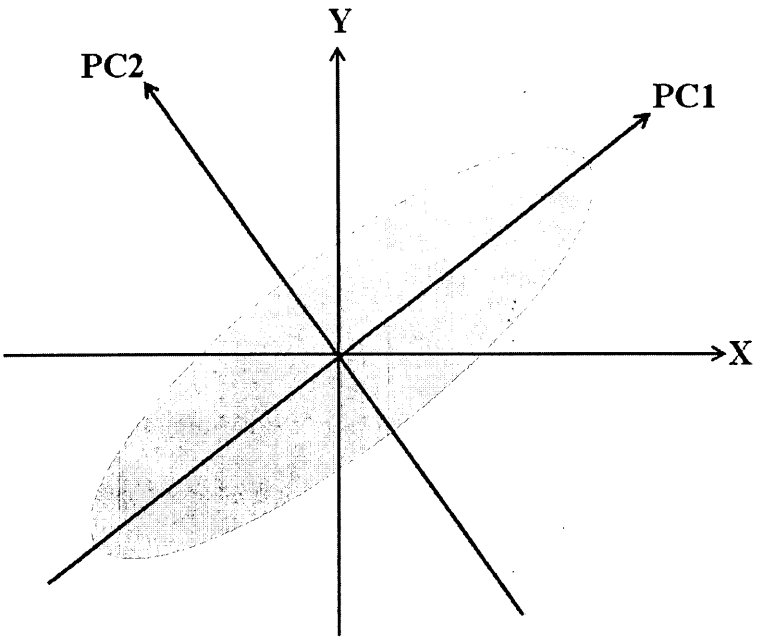

Fig.3. 3. A schematic diagram of applying principal component analysis to two input variables.

3.3. Weights of evidence (WofE)

One of the most well-known approaches to mapping mineral potential is weights of evidence (WofE) method based on Bayesian probability theory (Agterberg et al., 1990; Agterberg 1992; Bonham-Carter et al., 1989). By WofE (i.e., a geo-information integration method), binary patterns can be defined for each of identified geo-information according to their associations with mineral deposits, and posterior probabilities of all combinations of these patterns can be estimated to indicate presence and absence of mineralization in a study area.

In the aspect of binary pattern definition, weights of Evidence method (WofE) commonly

used for mineral potential mapping can quantitatively describe spatial associations of identified geo-information and objective geological features (Bonham-Carter 1994). This method had been successfully used to reclassify multi-category patterns to binary patterns in many cases (Cheng et al., 1994; 2007a; Wang et al., 2012; Zhao et al., 2012; Zuo et al., 2009). If we assume that a study area is divided into N cells with n cells corresponding with mineral deposits (i.e., events D), then the prior probability of mineral occurrences $P(D)$ can be:

$$P(D) = \frac{n}{N} \tag{3.13}$$

Suppose that there are a set of binary pattern of identified geo-information, A for presence of mineral occurrences and $\overline{A}$ for absence of mineral occurrences, the conditional probability of mineral deposits located in these patterns can be:

$$P(D|A) = P(D)\frac{P(A|D)}{P(A)} \tag{3.14}$$

$$P(D|\overline{A}) = P(D)\frac{P(\overline{A}|D)}{P(\overline{A})} \tag{3.15}$$

The weights W^+ and W^- of binary patterns can be calculated by means of the following formulas:

$$W^+ = \log\frac{P[A|D]}{P[A|\overline{D}]} \tag{3.16}$$

$$W^- = \log \frac{P[\overline{A}|D]}{P[\overline{A}|\overline{D}]} \tag{3.17}$$

$$\sigma(W^+) = \sqrt{\frac{1}{A \cap D} + \frac{1}{A \cap \overline{D}}} \tag{3.18}$$

$$\sigma(W^-) = \sqrt{\frac{1}{\overline{A} \cap D} + \frac{1}{\overline{A} \cap \overline{D}}} \tag{3.19}$$

$$\sigma(Total) = \sqrt{\sigma^2(W^+) + \sigma^2(W^-)} \tag{3.20}$$

where A denotes numbers of the area enclosed by patterns indicating presence of mineral occurrences; $\overline{A}$ denotes the area not enclosed by the patterns; D and $\overline{D}$ indicate the presence and absence of mineral occurrences, respectively; and $\sigma(W^+)$, $\sigma(W^-)$ and $\sigma(Total)$ represent the standard deviation of all types of weights. The contrast C is a measure of the spatial association between points and patterns, and the corresponding studentized value of the contrast, t provides a measure of its statistical significance. The contrast C and t-value can be expressed as follow:

$$C = W^+ - W^- \tag{3.21}$$

$$t = C/\sigma(Total) \tag{3.21}$$

where C is the contrast of weights and t is the studentized value of contrast. In this work, the t value is the parameter for validation by comparison of the spatial association

coefficients of all patterns of identified geo-information.

In the aspect of integration, the odds form, O is involved, prior probability of which is $O=P/(1-P)$. Posterior odds can be expressed to the presence and absence of binary patterns:

$$O(D|A) = O(D)\frac{P(A|D)}{P(A|\overline{D})} = O(D)\times W^{+} \tag{3.23}$$

$$O(D|\overline{A}) = O(D)\frac{P(\overline{A}|D)}{P(\overline{A}|\overline{D})} = O(D)\times W^{-} \tag{3.24}$$

The formulation introduced above is only for one set of binary patterns. Identified geo-information in mineral exploration is often multiple. The posterior odds of the combination of patterns indicating presence of mineral occurrences can be calculated by:

$$O(D|A_1 \cap A_2 \cap ... A_n) = O(D)\times e^{W_1^{+}+W_2^{+}+...W_n^{+}} \tag{3.25}$$

More detailed introduction and applications of WofE can be found in Bonham-Carter (1994).

Chapter 4. Granitic intrusion characterization by geophysical data analysis

4.1. Introduction to geophysical data analysis

Geophysical exploration has been greatly aided over past decades by the development in computer sciences and the availability of multi-source geophysical data which has become an important geo-information source in engineering, environment study, and resource exploration (Nabighian et al., 2005a, b). From a geological perspective, mineralization related geological bodies can arouse geophysical anomalies (Zhao, 1999). Interpreting geophysical anomalies from various observational datasets is not only beneficial to recognition of the presence and spatial distribution of underneath geological bodies (i.e., causative bodies), but also significant to knowledge of geological settings and mineral potential mapping issues (Cheng, 2012; Cianciara and Marcak, 1979). Among various geophysical datasets, gravity and magnetic data are broadly employed in mineral resource exploration. Although these two typical observational datasets are distinctive in potential fields, measured parameters, and operative physical properties, they are processed by similar and even same ways during data processing in many cases (e.g., wavelength filter, upward continuation, vertical derivative, directional filter, etc.) (Bhattacharyya, 1965; Hood and McClure, 1965; Hood and Teskey, 1989; Kearey et al., 2002; Wang et al., 2010).

Gravity and magnetic data detect spatial variations of gravitational and geomagnetic fields caused by causative bodies. In practice, regional anomalies caused by large or deeply buried sources are of low-frequency with long wavelength (e.g., sedimentary basin), while local anomalies caused by small or shallow sources are of high-frequency with short wavelength (e.g., anticline and salt dome) (Kearey et al., 2002). Anomaly interpretation requires gravity/magnetic data to be decomposed into two constituent parts, so called regional-residual separation (Agarwal and Sivaji, 1992; Li and Oldenbur, 1998). Spatial and frequency analysis are popular in geophysical exploration, methods of which involving Fourier transformation are mostly utilized. Meanwhile, many world-wide borehole measurements show that source (e.g., density or susceptibility) distribution is fractal (Dimri, 2000). Therefore, fractal and multifractal methods which consider both frequency distribution and spatial self-similar properties of causative bodies are effective on analyzing causative bodies as well (Cheng, 2007a; Li and Cheng, 2006).

Since the concept of fractal/multifractal introduced by Mandelbrot (1977; 1989), numerous studies have been carried out to understand complex natural properties. Researches in various fields were focused on characterizing measures with scale independence (Agterberg, 2012a; Cheng 2007b; Dimri and Srivastava, 2005). Natural processes with fractal behaviors like rainfall (Veneziano and Furcolo, 2002), flooding (Cheng, 2008; Malamud et al., 1996), cloud formation (Schertzer and Lovejoy, 1987) and mineralization (Cheng, 2007a, b) exhibit non-linear characteristics that satisfy fractal or multifractal statistics. Comparing with the classic geophysical data analysis, fractal/multifractal methods are advanced to characterize the spatial distribution of

underground causative bodies with arbitrary shapes. Dimri and Srivastava (2005) used modified Voronoi tessellation to generate fractal geometry of the causative bodies and provided an irregular realistic final model. Thorarinsson and Magnusson (1990) defined the fractal dimension as roughness of Bouguer anomaly surface, and by minimizing the roughness they used a new method to determine density values for the Bouguer reduction. Based on a series of experiments, Lovejoy et al. (2001) and Pecknold et al. (2001) concluded that the multifractality and scaling anisotropy as two essential components cannot be ignored in geophysical modeling. Cheng (2007b) introduced some multifractal imaging filtering and decomposition methods in space, frequency, and eigen domains, in which the singularity theory (Cheng, 1999) was applied to quantify the local scaling property in space domain and used as a high-pass filter to enhance high frequency patterns. The study in the current chapter applies a singularity theory-based technique integrated in GeoDAS software (Cheng, 2000) to characterize Bouguer gravity and aeromagnetic anomalies in southeastern Yunnan district, China. The spatial information of the causative bodies of these anomalies can be further used to support mineral exploration in the study area.

4.2. Physical properties of granitic intrusions in the study area

Since the significance of magmatism to mineralization, most researches used the geo-information of granitic intrusions as a main component in mineral exploration modeling (Cheng et al., 2011; Wang et al., 2011; Wang et al., 2012; Xiong and Shi, 1994). Among these efforts, Xiong and Shi (1994) demonstrated a physico-geological exploration model

to delineate spatial distribution of igneous rocks in this area by using geophysical data; nowadays, it still provides an important clue to distinguish various rock types based on specific geophysical properties. As described by Xiong and Shi (1994), the density of sedimentary rocks are uniform without significant variations (2.7-2.75 g/cm^3), while the igneous rocks show a wide density range. Specifically, the density of granitic intrusions are the lightest among all rock types (<0.15-0.24 g/cm^3); mafic (around 3.00 g/cm^3) and ultra-mafic (around 3.10 g/cm^3) igneous rocks are much denser than the sedimentary rocks and with the increase of femic constituents the rocks become denser. Ore bodies are the densest. In the aspect of magnetism of rocks in this area, sedimentary rocks with low or no magnetism do not arouse magnetic anomalies; mafic rocks can cause distinctive magnetic anomalies due to the high content of ferromagnetic minerals; granitic intrusions without sufficient ferromagnetic minerals show flat gradients or low magnetic anomalies in the aeromagnetic map of this area (Xiong and Shi, 1994). Therefore, a typical geophysical character for recognition of the granitic intrusions is the intersection of low gravity and low magnetic anomalies. Furthermore, in many cases, the patterns with high magnetic anomalies distributed around the round shape areas with low magnetic anomalies are probably caused by mineralization of magnetite and pyrrhotite around and/or in the contact zones between the granitic intrusions and their surroundings (Xiong and Shi, 1994).

Demonstrated by former researches, magmatic-hydrothermal mineralization in southeastern Yunnan mineral district is highly associated with granitic intrusions (Zhuang et al., 1996). Delineating outlines of the granitic intrusions is essential for better

understanding of their spatial association with mineralization and predicting Sn-Cu polymetallic deposits in this area. Bouguer gravity and aeromagnetic datasets are currently available to delineate the spatial distribution of granitic intrusions in the study area.

4.3. Geophysical data analysis

By ground-based gravity measurements, lateral variations in the gravity field at different points (P) are recorded in gravity data. After subtracting a regional field and relative corrections (Ervin, 1997), currently used Bouguer gravity data records gravitational variations related to causative bodies with different density. The Bouguer gravity anomalies (g_b) can be expressed as

$$g_b(P) = g_{obs}(P) - \gamma(P) \tag{4.1}$$

where, $g_{obs}(P)$ is the observed gravity at point P and $\gamma(P)$ is a model value or reference gravity and Bouguer anomaly related corrections.

Similar to gravity measurements, magnetic differences (ΔB) between the observed magnetic field and the modeled magnetic field at various locations (P) are recorded by magnetometers. It can be expressed as

$$\Delta B(P) = H\mu_0 k(P) \tag{4.2}$$

where, μ_0 is the magnetic permeability of a vacuum, H is the magnetization force in a homogeneous and infinite magnetic field, and k is the magnetic susceptibility of causative bodies. The variation of the magnetic field (i.e., magnetic anomalies) is caused by the contrast of magnetic susceptibility of subterranean materials. In addition, magnetic anomalies are influenced by other issues consisting of the inclination and declination of local magnetic fields and causative bodies' magnetization, and the orientation of causative bodies with respect to the magnetic north (Nabighian et al., 2005a). In general, the vector of H is not normal to the Earth's surface except in the north or the south poles. It is often difficult to interpret the magnetic field due to polarity effects. Therefore, a Reduction to pole (RTP) transformation (Cooper and Cowan, 2005) is applied, and observed ΔB is accordingly transformed into anomalies with vertical magnetization and ambient fields measured at magnetic poles to satisfy interpretation.

4.3.1. Band-pass filter

The foundation of differentiating granitic intrusions from their surroundings in this area is their distinctive contrast of density and magnetism with the sedimentary rocks (Xiong and Shi, 1994). In order to delineate the main granitic intrusions on the basis of gravity/magnetic fields and attenuate influences of relatively small geological bodies near the surface, a combination of filter operation (i.e., band-pass filter) is currently used.

Using the bouguer gravity anomaly as an example, the upward-continuation can be expresses as:

$$g_{continuation}(\xi,\eta) = -\frac{z}{2\pi}\int_{-\infty}^{\infty}\int_{-\infty}^{\infty}\frac{g_b(\xi,\eta)}{[(x-\xi)^2+(y-\eta)^2+z^2]^{3/2}}d\xi d\eta \tag{4.3}$$

where, (ξ, η) is the ground location of the mass point P, and $z > 0$ is the distance of upward-continuation while the $z < 0$ is the distance of downward-continuation.

The second-order vertical derivative can be expressed as:

$$\frac{\partial^2 g_b(\xi,\eta)}{\partial z^2} = -\frac{\partial^2 g_b(\xi,\eta)}{\partial x^2} - \frac{\partial^2 g_b(\xi,\eta)}{\partial y^2} \tag{4.4}$$

where, 2 represents the second-order of the vertical derivative.

Implemented in frequency domain, the calculation for the upward-continuation and vertical derivative will be greatly simplified:

$$G_{continuation} = G_b(\xi,\eta)\cdot e^{-z\sqrt{u^2+v^2}} \tag{4.5}$$

$$\frac{\partial^n g_b(\xi,\eta)}{\partial z^n} = (\sqrt{u^2+v^2})^n \cdot G_b(\xi,\eta) \tag{4.6}$$

where, G_b is the Fourier transformation of g_b, and u and v are the wave numbers in the directions of x and y. Therefore, the band-pass filter can be expressed as:

$$G_{band-pass} = G_b(\xi,\eta)\cdot(\sqrt{u^2+v^2})^n \cdot e^{-z\sqrt{u^2+v^2}} \tag{4.7}$$

It is consisted of the high-pass operator $(\sqrt{u^2+v^2})^n$ and the low-pass operator $e^{-z\sqrt{u^2+v^2}}$. For the analysis of aeromagnetic data, the same operation is applicable as well.

Both Bouguer and aeromagnetic data are firstly processed by upward continuation (i.e., low-pass filter) to remove the high-frequency anomalies aroused by small/shallow geological bodies and noisy signals and to retain the low-frequency anomalies caused by the large and deeply buried geological bodies. In this chapter, different upward-continuation distances from 4 km to 12 km at an interval of 2 km are used. Secondly, both the first- and second-order derivative (i.e., high-pass filter) are applied to enhance local anomalies and to outline boundaries of the causative intrusions. Therefore, currently used band-pass filters consisting of upward continuations using various continuation distances and the first-/second-order vertical derivatives can minimize the influences caused by small source bodies near surface and highlight variations of gravity/magnetic gradients of large and deeply buried granitic intrusions. Results by band-pass filters are demonstrated in Figs. 4.1, 4.2, 4.3 and 4.4. Zero-value contour lines (Figs. 4.1f, 4.2f, 4.3f and 4.4f) depicting edges of deeply buried granitic intrusions are supported by gravity and magnetic anomalies, respectively. The intrusions delineated by both gravity and magnetic data with second-order vertical derivative (Figs. 4.2 and 4.4) are more detailed than the ones by the first-order vertical derivative (Figs. 4.1 and 4.3). It is coincident with the fact that the second-order derivative has more resolving power than the first-order derivative. Simultaneously, the shapes of the contours are altered when the upward-continuation distances change (Figs. 4.1f, 4.2f, 4.3f and 4.4f). It can be noticed that

currently used band-pass filtering technique is depended on upward-continuation distances (i.e., scale dependence). Therefore, the parameters to define the model of band-pass filters require geophysical interpreters' judgment which is somehow subjective.

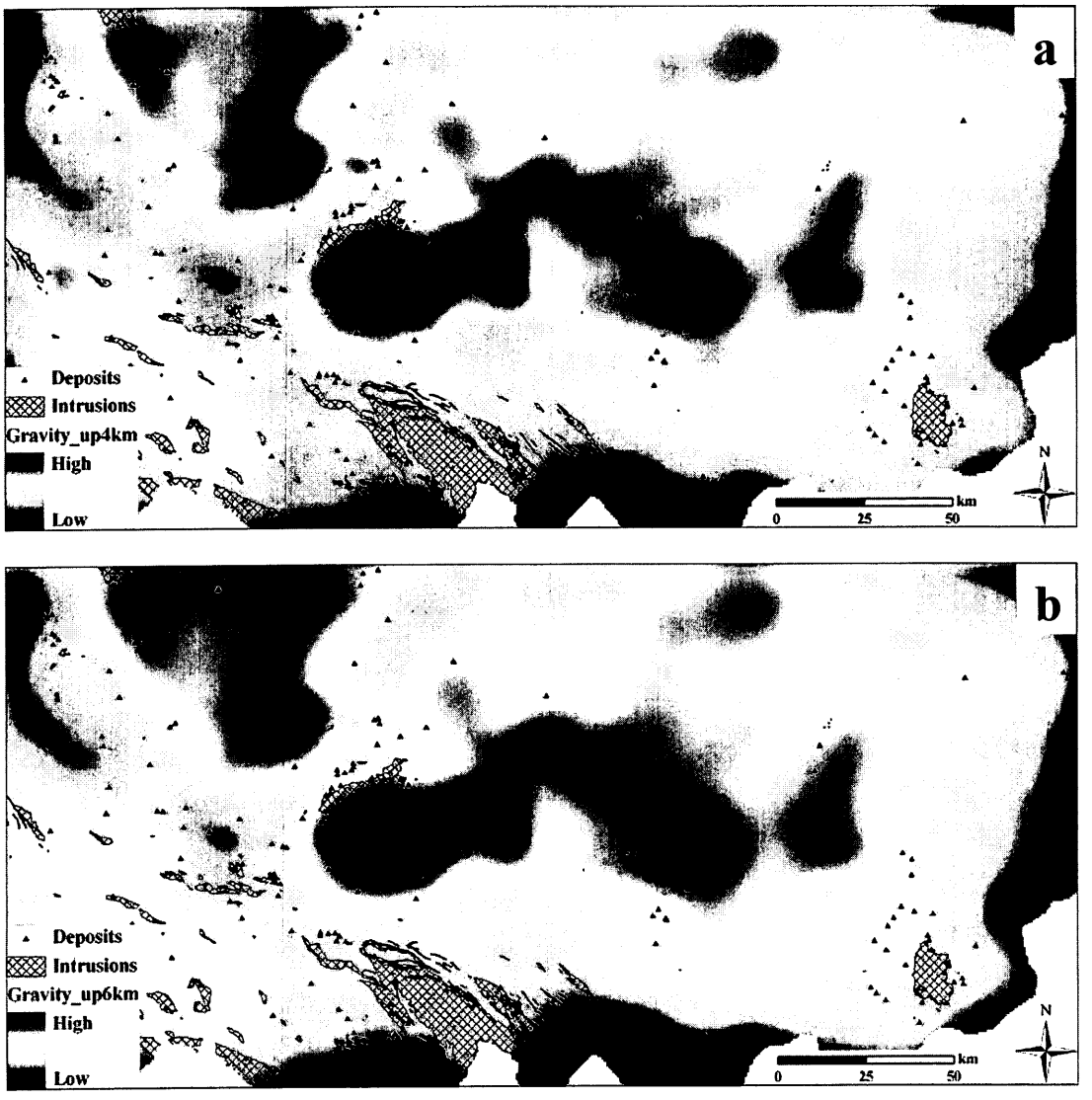


c
Deposits
Intrusions
Gravity_up8km
High
Low
N
km
0
25
50


d
Deposits
Intrusions
Gravity_up10km
High
Low
N
km
0
25
50

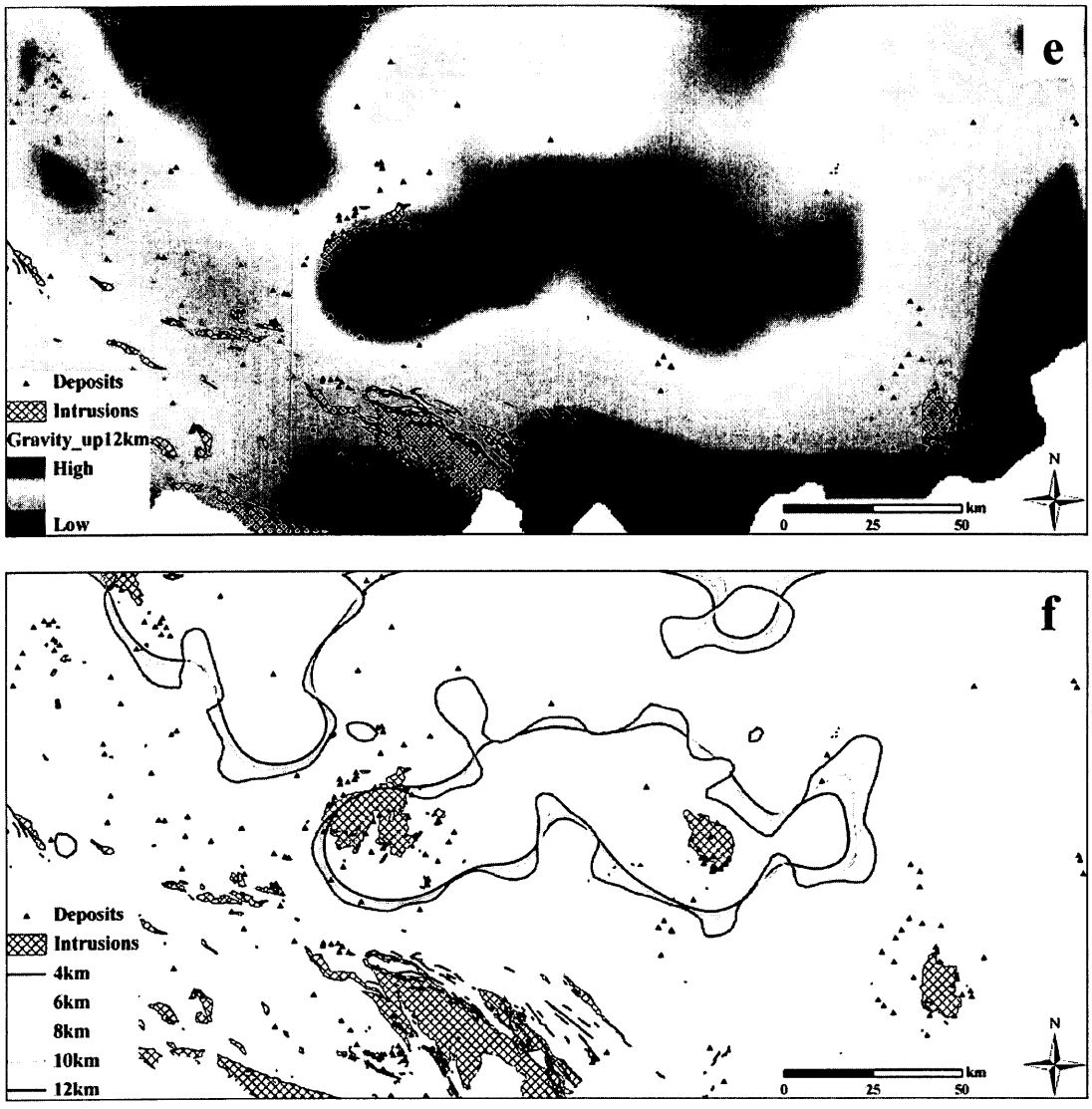

Fig.4. 1. The spatial distribution of Bouguer anomalies by means of a band-pass filter consisting of upward continuation using distances from 4 km to 12 km at an interval of 2 km and the first-order derivative. Zero-contour lines are shown here to highlight edges of deeply buried granitic intrusions. **a**: Band-pass filter with upward continued 4 km; **b**: Band-pass filter with upward continued 6 km; **c**: Band-pass filter with upward continued 8 km; **d**: Band-pass filter with upward continued 10 km; **e**: Band-pass filter with upward continued 12 km; **f**: Zero-contour lines of Figs. a to e.


a
Deposits
Intrusions
Gravity_up4km
High
Low
N
km
0
25
50


b
Deposits
Intrusions
Gravity_up6km
High
Low
N
km
0
25
50

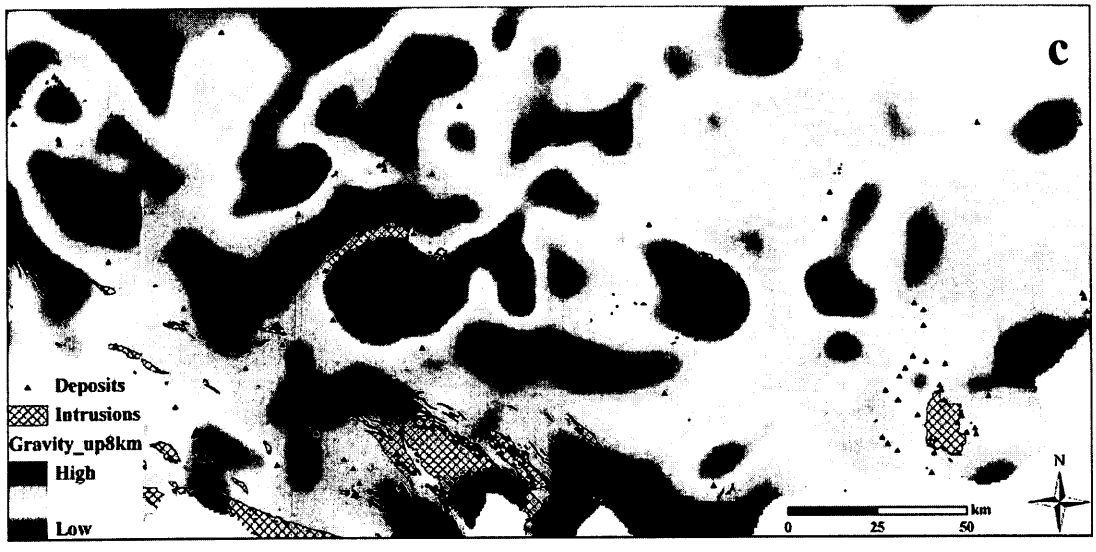
c
Deposits
Intrusions
Gravity_up8km
High
Low
N
km
0
25
50

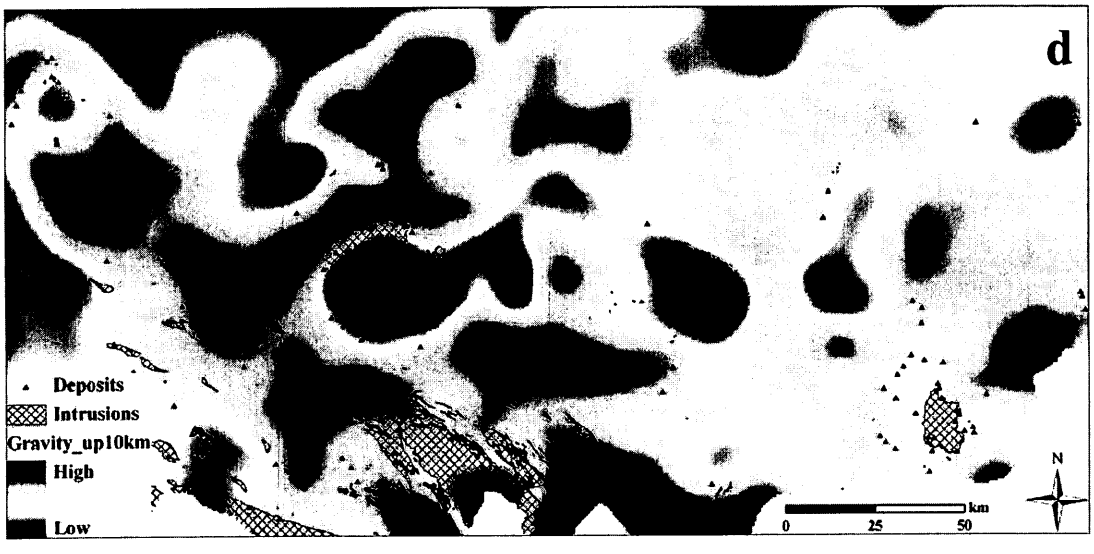
d
Deposits
Intrusions
Gravity_up10km
High
Low
N
km
0
25
50

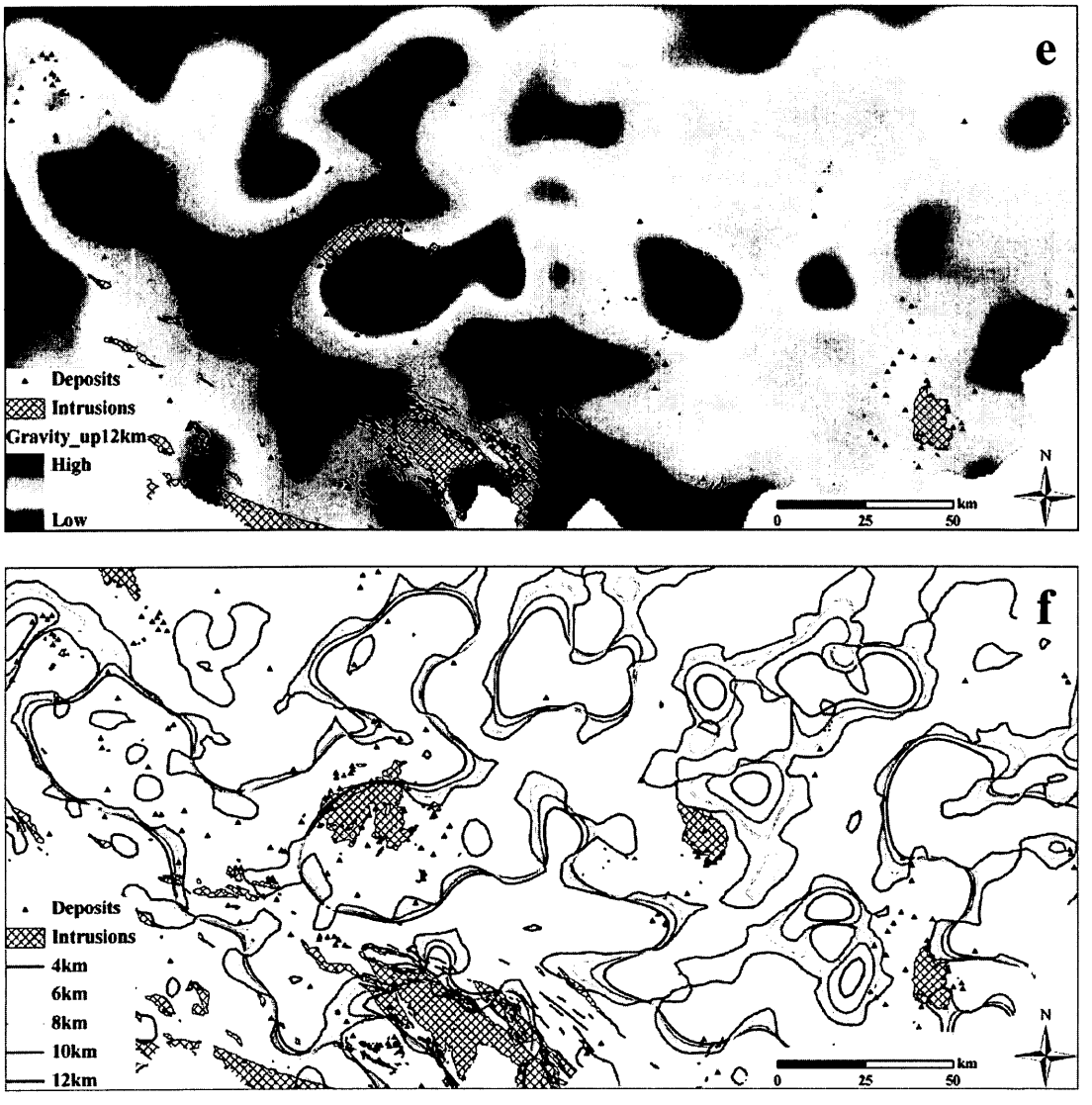

Fig.4. 2. The spatial distribution of Bouguer anomalies by means of a band-pass filter consisting of upward continuation using distances from 4 km to 12 km at an interval of 2 km and the second-order derivative. Zero-contour lines are shown here to highlight edges of deeply buried granitic intrusions. a: Band-pass filter with upward continued 4 km; b: Band-pass filter with upward continued 6 km; c: Band-pass filter with upward continued 8 km; d: Band-pass filter with upward continued 10 km; e: Band-pass filter with upward continued 12 km; f: Zero-contour lines of Figs. a to e.


a
Deposits
Intrusions
Aeromagnetic_up4km
High
Low
N
km
0
25
50


b
Deposits
Intrusions
Aeromagnetic_up6km
High
Low
N
km
0
25
50

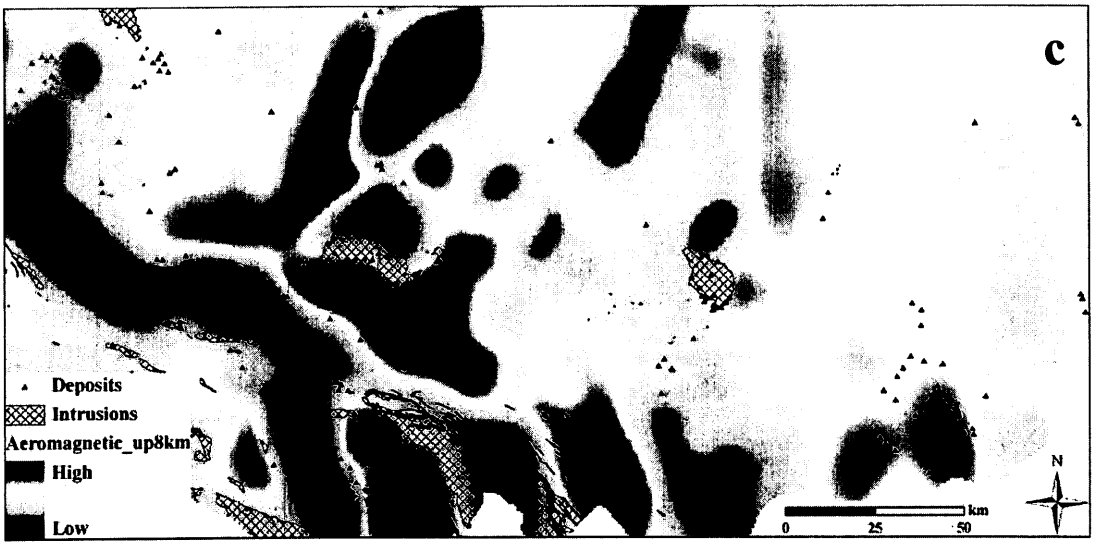
c
Deposits
Intrusions
Aeromagnetic_up8km
High
Low
N
km
0
25
50

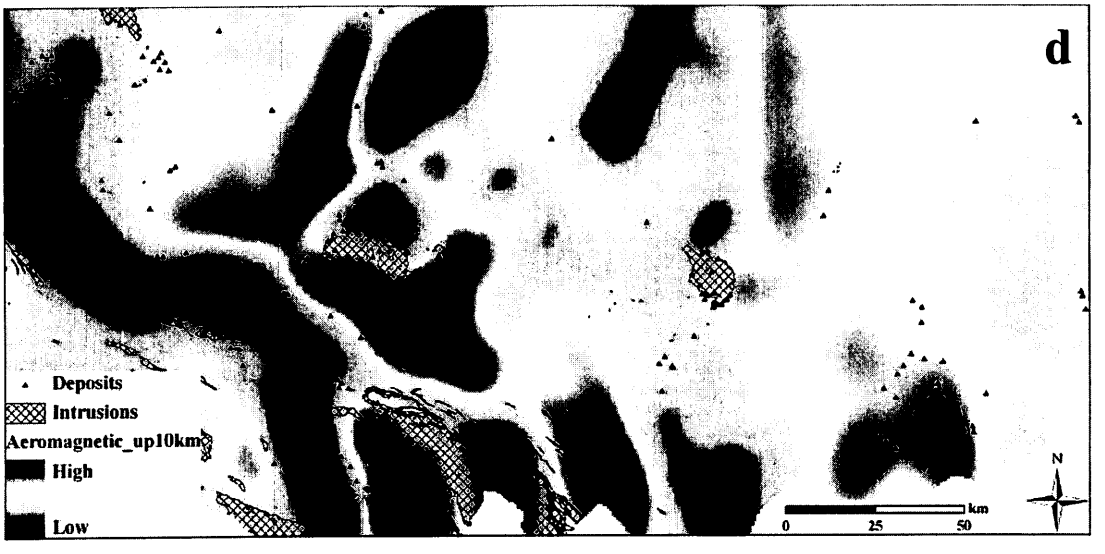
d
Deposits
Intrusions
Aeromagnetic_up10km
High
Low
N
km
0
25
50

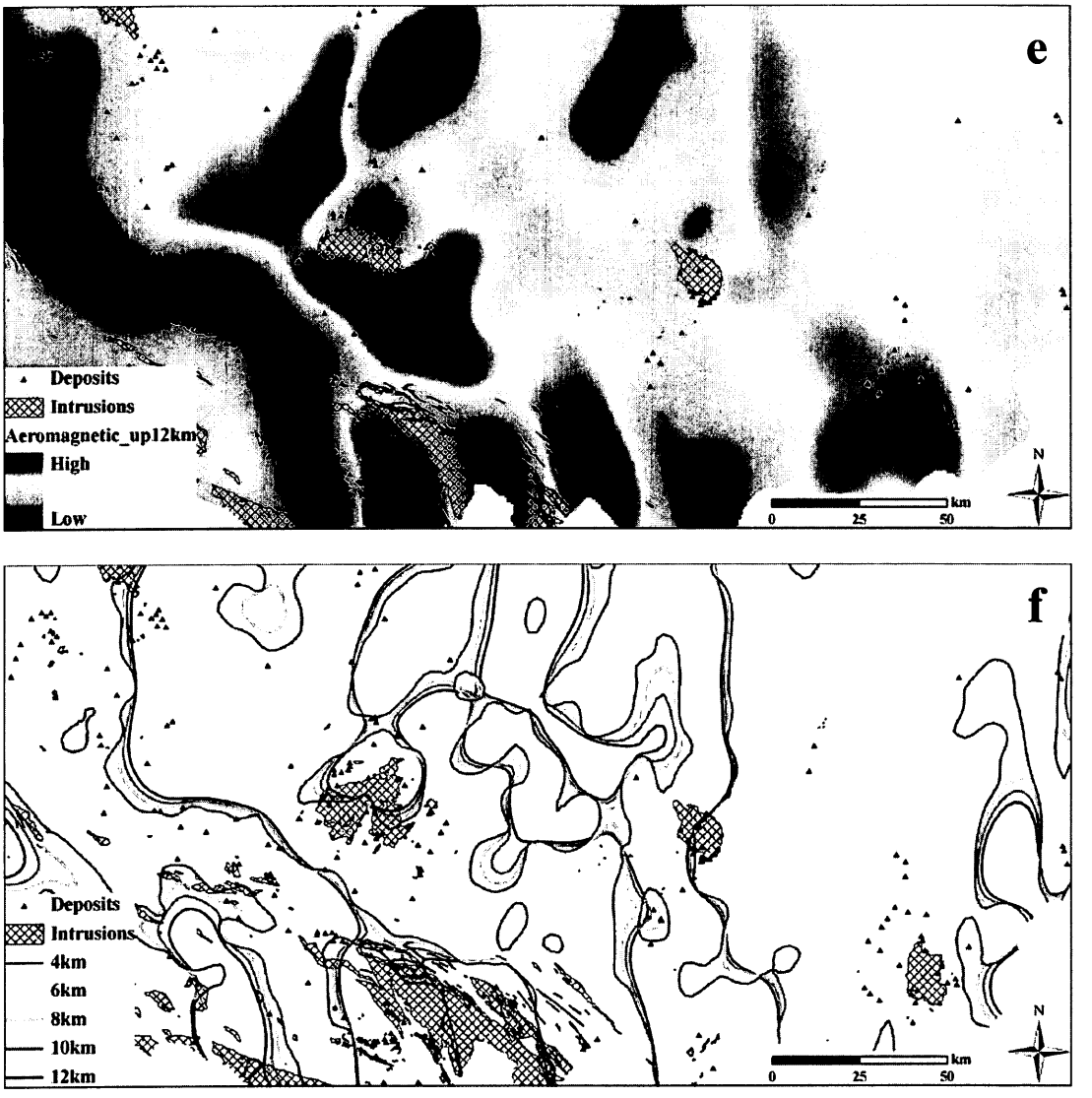

Fig.4. 3. The spatial distribution of aeromagnetic anomalies by means of a band-pass filter consisting of upward continuation using distances from 4 km to 12 km at an interval of 2 km and the first-order derivative. Zero-contour lines are shown here to highlight edges of deeply buried granitic intrusions. a: Band-pass filter with upward continued 4 km; b: Band-pass filter with upward continued 6 km; c: Band-pass filter with upward continued 8 km; d: Band-pass filter with upward continued 10 km; e: Band-pass filter with upward continued 12 km; f: Zero-contour lines of Figs. a to e.


a
Deposits
Intrusions
Aeromagnetic_up4km
High
Low
N
km
0
25
50


b
Deposits
Intrusions
Aeromagnetic_up6km
High
Low
N
km
0
25
50

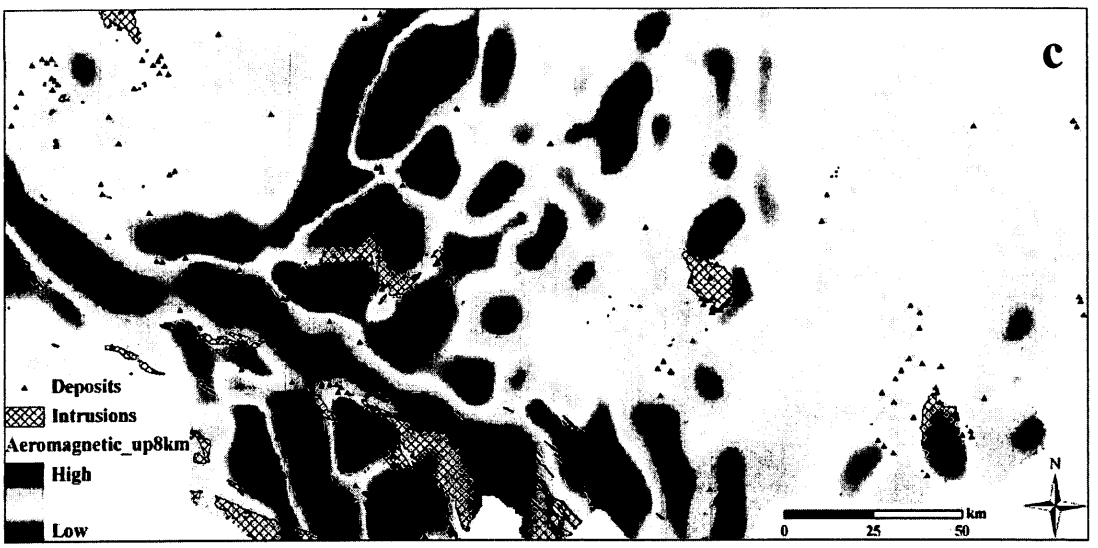
c
Deposits
Intrusions
Aeromagnetic_up8km
High
Low
N
km
0
25
50

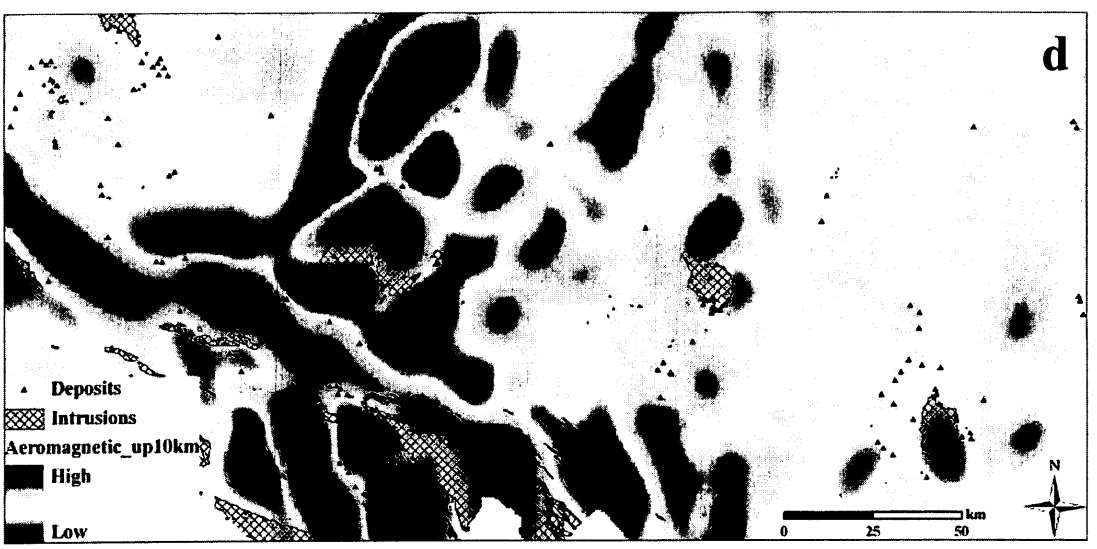
d
Deposits
Intrusions
Aeromagnetic_up10km
High
Low
N
km
0
25
50

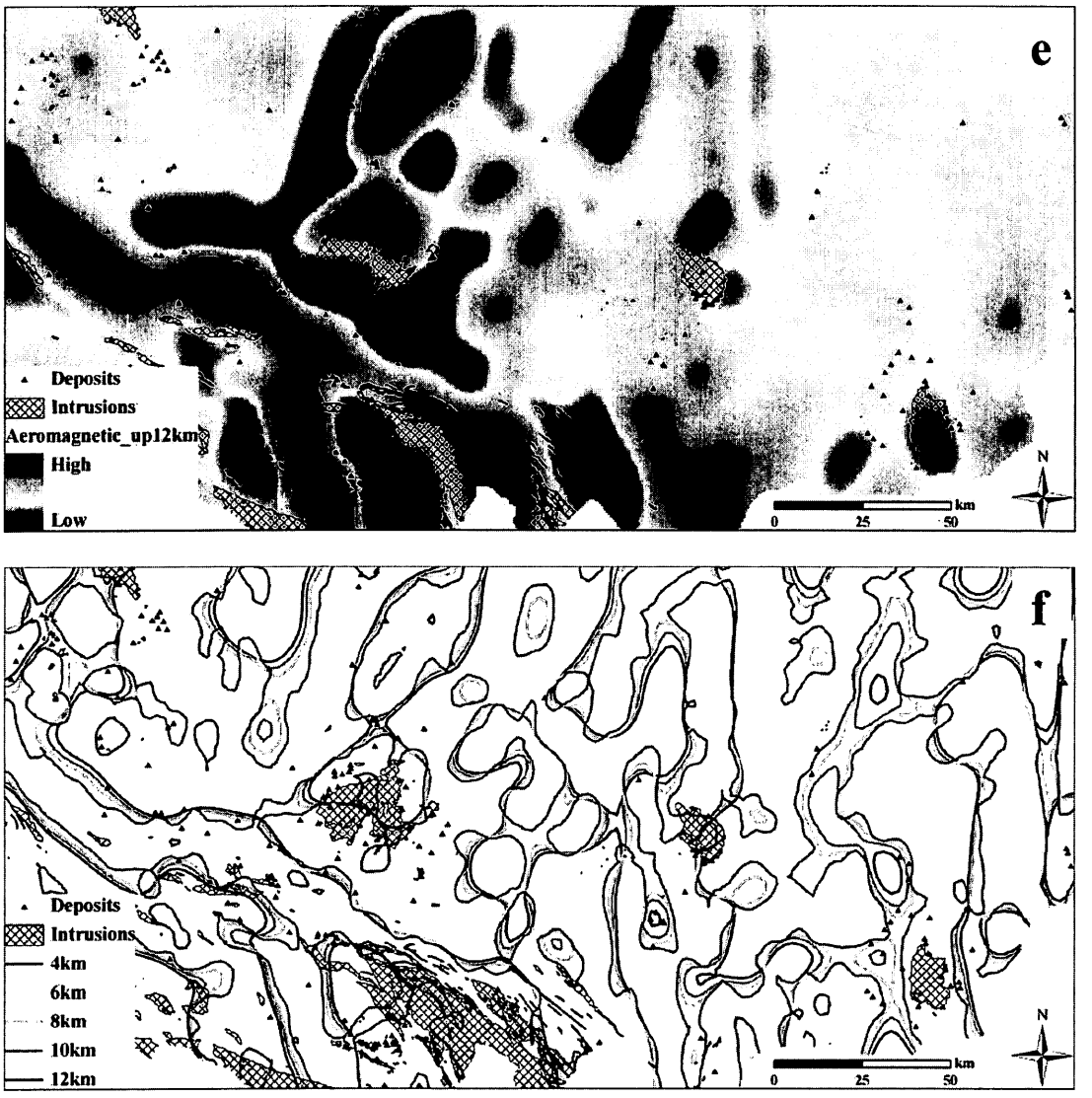

Fig.4. 4. The spatial distribution of aeromagnetic anomalies by means of a band-pass filter consisting of upward continuation using distances from 4 km to 12 km at an interval of 2 km and the second-order derivative. Zero-contour lines are shown here to highlight edges of deeply buried granitic intrusions. a: Band-pass filter with upward continued 4 km; b: Band-pass filter with upward continued 6 km; c: Band-pass filter with upward continued 8 km; d: Band-pass filter with upward continued 10 km; e: Band-pass filter with upward continued 12 km; f: Zero-contour lines of Figs. a to e.

4.3.2. Singularity index mapping

The formation of the granitic intrusions by magmatic activities is accompanied with energy release and material accumulation. This geo-process satisfies the definition of non-linear theory for singular processes (Cheng, 1999), and singularity index mapping is therefore applicable to characterize abnormal distributions of density and magnetism of granitic intrusions in this area.

In order to apply the singularity index mapping technique to geophysical data, the negative values become an issue, since the input data is subjected to a logarithmic transformation. Consequently, positive values need to be added to the values of Bouguer anomaly and RTP transformed aeromagnetic data, respectively, so that modified values, $g_b + v > 0$ and $\Delta B + v > 0$, are positive.

The estimation for singularity indices of gravity data is by means of the window-based method. Averaged Bouguer gravity values within square windows $\overline{g_b}[A(r_i)]$ against window sizes r_i are plotted on a log-log graph. The slope of the linear trend can be used to estimate singularity indices. With the same process for each location, the spatial distribution of geophysical anomalies will be obtained by moving the window across the space. In order to demonstrate its scale independence, the maximum window sizes r_{max} from 17 km to 25 km at an interval of 2 km are currently used.

Applying the window-based singularity index mapping technique to the Bouguer anomalies, spatial distributions of gravity singularity indices by various r_{max} are

delineated (Fig. 4.5). Referring to properties of singularity indices and the granitic intrusions, areas with $\alpha > 2$ (i.e., depletion of gravity gradients) indicate low-density, which is presumably a symptom of granitic intrusions. Areas with $\alpha < 2$ (i.e., enrichment of gravity gradients) indicate objects with higher density. In addition, a cutoff (i.e., $\alpha = 2$) is used to separate the granitic intrusions with lower density from the country rocks with higher density (Fig. 4.5f). Similarly, estimated by the window-based mapping method, spatial distributions of singularity indices of RTP transformed aeromagnetic data by various r_{max} are shown in Fig. 4.6. Based on properties of the intrusions, areas with $\alpha > 2$ depict low magnetic susceptibility corresponding with the low- or non-magnetic granitic intrusions, while areas with $\alpha < 2$ depict regional tectonic structures and/or mafic/ultramafic rocks showing round shapes in the study area. The contour lines with $\alpha = 2$ separating positive and negative singularity indices serve as zero-value contour lines in the previously used high-pass filter (Fig. 4.6f).

In comparison with band-pass filters, the singularity index mapping method preserves the shapes of granitic intrusions when the r_{max} change. The fact well demonstrates its advantages of scale independence (Figs. 4.5f and 4.6f). In addition, singularity indices of both gravity and aeromagnetic anomalies in Figs. 4.5 and 4.6 provide more detailed results than most of the band-pass filtered patterns do in Figs. 4.2 and 4.4, respectively; meanwhile, the singularity index mapping method produces similar but not exactly same delineations (Figs. 4.5f and 4.6f) as some results by the band-pass filters (Figs. 4.2f and 4.4f). It is because that the first-order derivative transformation of the $\mu(A)$ introduced in singularity index model (4) serves as a high-pass filter. In addition, the definition of

window sizes (r_i) is based on intentions to pursue a regional or local singularity index. In other words, processed Bouguer and aeromagnetic data in model (4) are mean values (i.e., $C(A_i)$) within square windows (A_i) that implies a moving average operation included during the singularity index estimation process. Therefore, currently achieved singularity indices by a window-based method are products of the first-order derivative of gravity and aeromagnetic fields accompanying with a moving average operation to attenuate signals of small causative bodies near surface and highlight anomalies of the large and deeply buried granitic intrusions.

Based on the models and results of currently used methods, the singularity index mapping technique is related to a first-order derivative and moving average operation, but its results are much more detailed than a band-pass filter consisting of the upward continuation and first-order vertical derivative; meanwhile it provides similar but not exactly same results as a band-pass filter consisting of the upward continuation and the second-order vertical derivative. That might be due to two reasons: (1) both the second-order vertical derivative and singularity index mapping have more resolving power than the first-order vertical derivative. More detailed variations can be identified by these two approaches; (2) the objectives of both singularity mapping and the second-order vertical derivative are proposed to outline boundaries of large and deeply buried granitic intrusions, the patterns which depend on the shapes of the granitic intrusions might be delineated similarly.

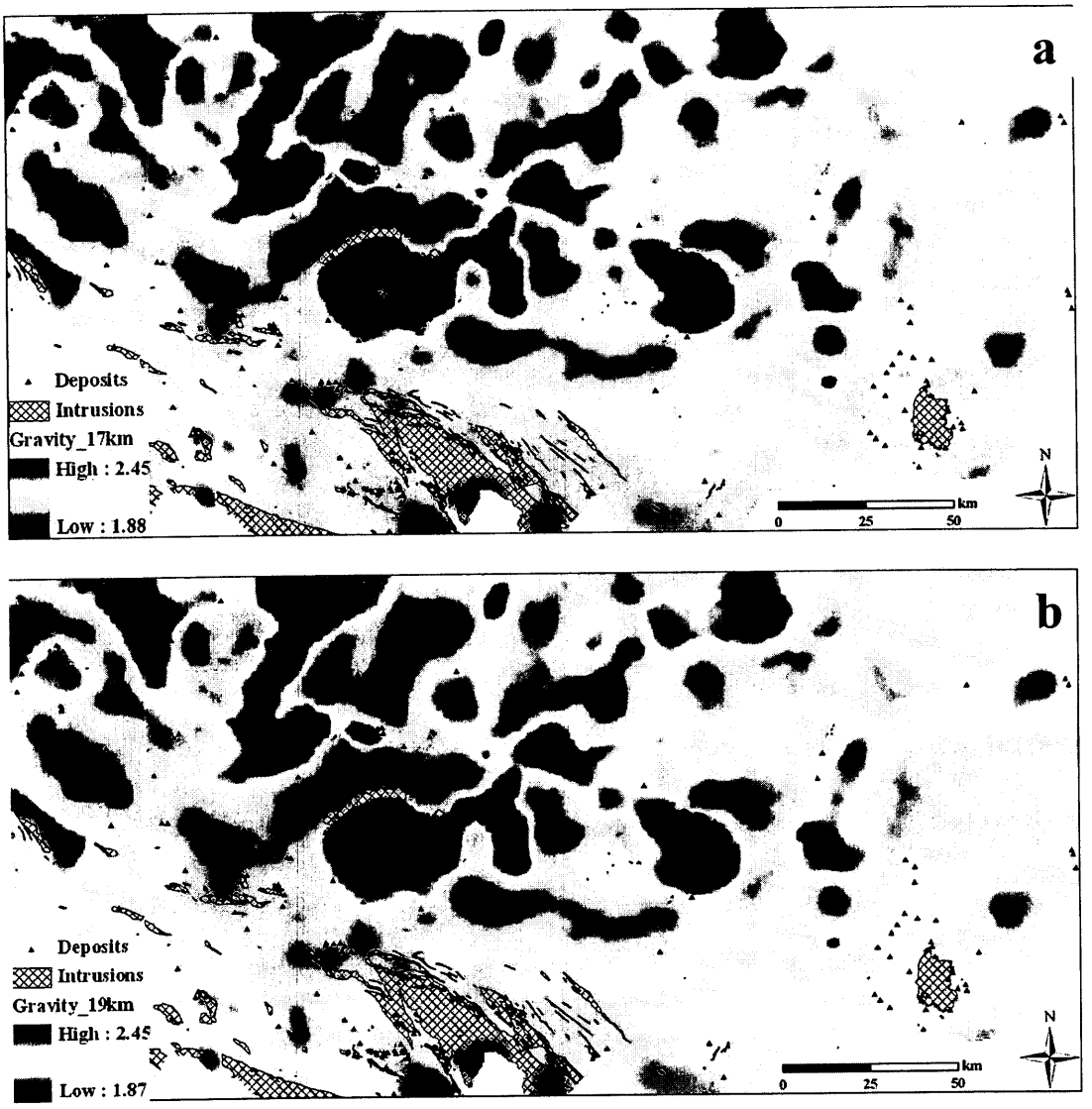
a
Deposits
Intrusions
Gravity_17km
High : 2.45
Low : 1.88
N
km
0
25
50
b
Deposits
Intrusions
Gravity_19km
High : 2.45
Low : 1.87
N
km
0
25
50


c
Deposits
Intrusions
Gravity_21km
High : 2.45
Low : 1.87
N
km
0
25
50

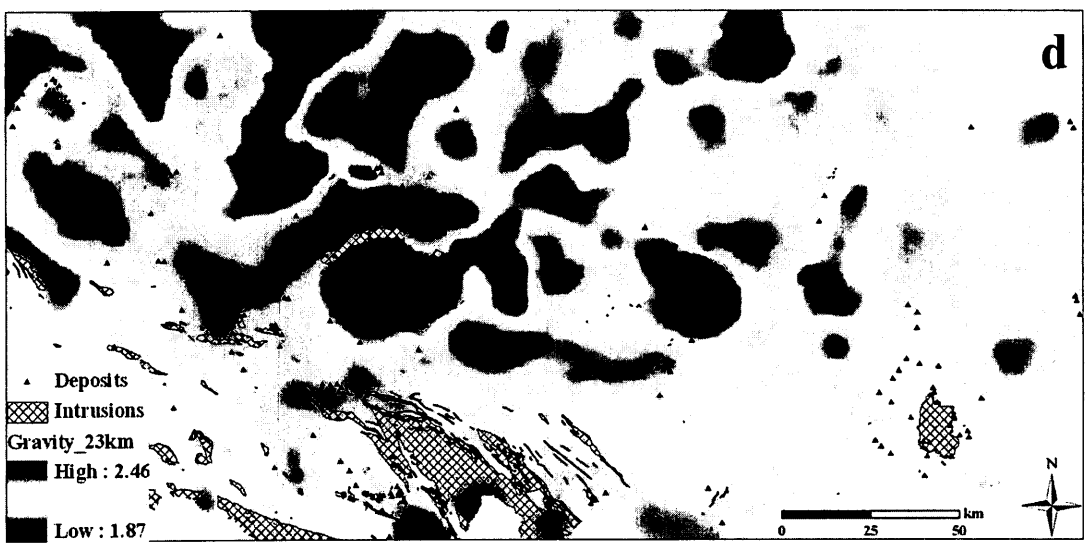
d
Deposits
Intrusions
Gravity_23km
High : 2.46
Low : 1.87
N
km
0
25
50

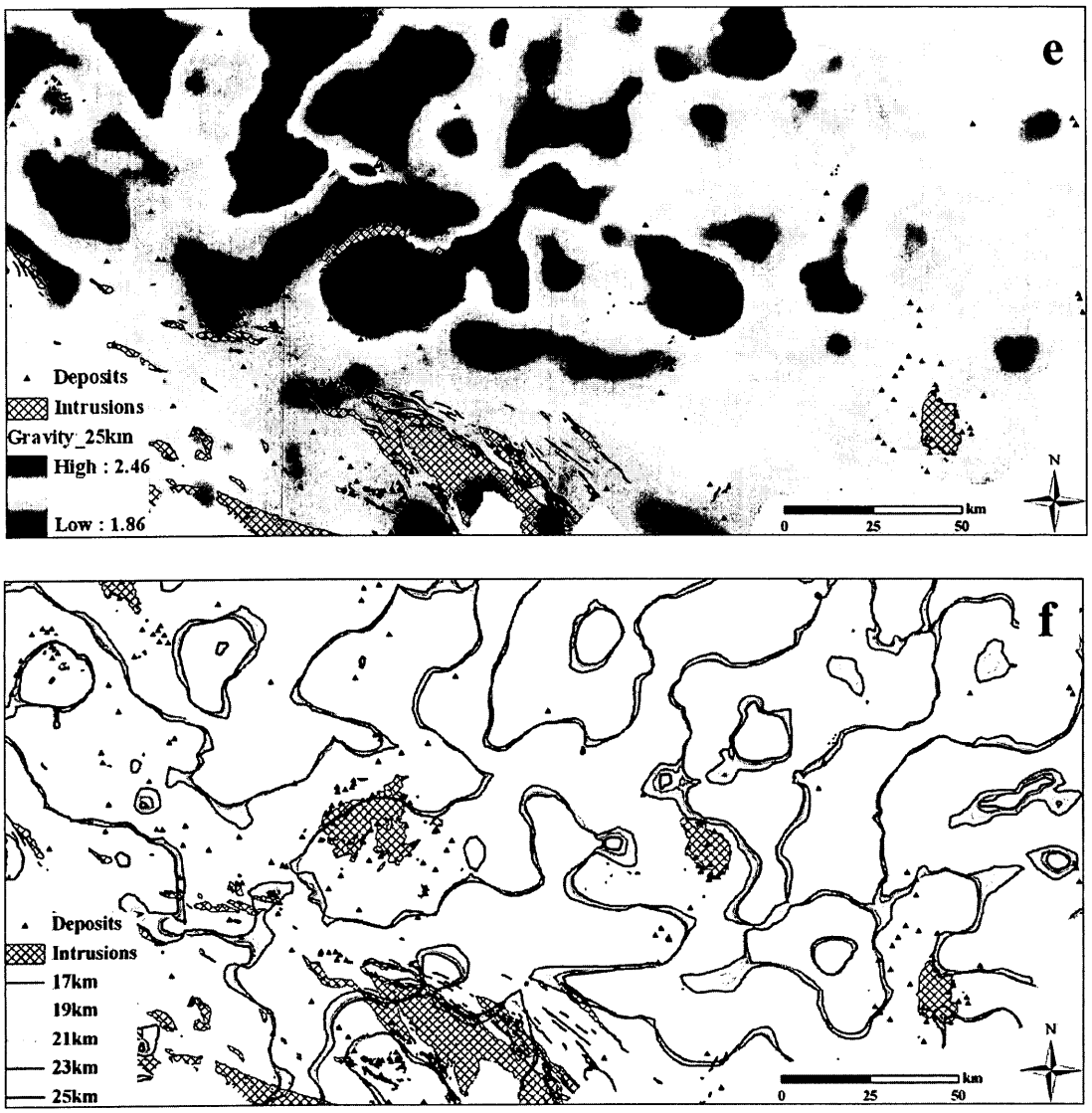

Fig.4. 5. The spatial distribution of singularity indices of Bouguer anomalies by a window-based method with r_{max} from 17 km to 25 km. Contour lines (i.e., $\alpha = 2$) separating the positive ($\alpha < 2$) and negative ($\alpha > 2$) singularity outline edges of deeply buried granitic intrusions. **a**: r_{max} = 17 km; **b**: r_{max} = 19 km; **c**: r_{max} = 21 km; **d**: r_{max} = 23 km; **e**: r_{max} = 25 km; **f**: $\alpha = 2$ contour lines of Figs. a to e.

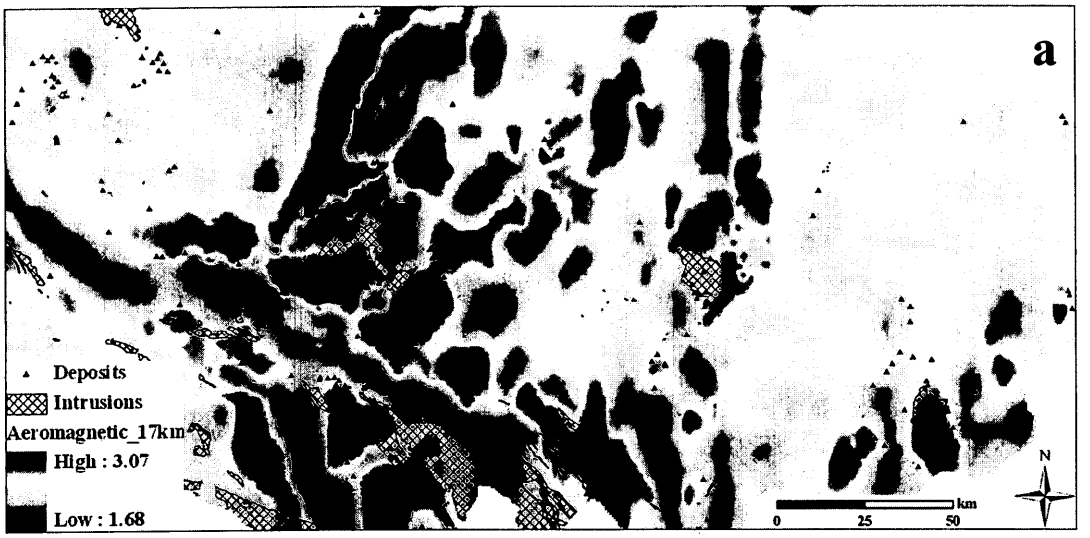
a
Deposits
Intrusions
Aeromagnetic_17km
High : 3.07
Low : 1.68
N
km
0
25
50

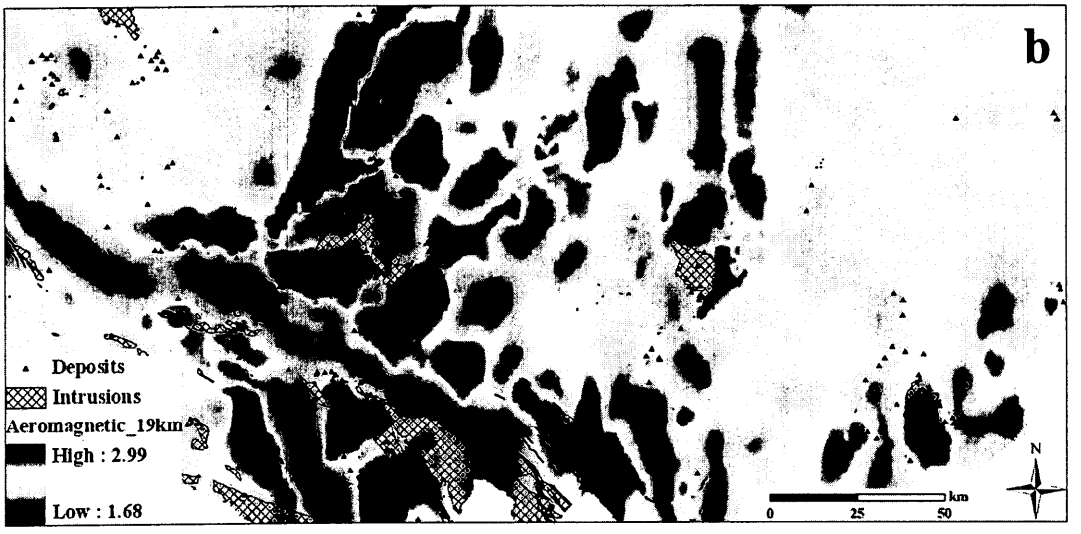
b
Deposits
Intrusions
Aeromagnetic_19km
High : 2.99
Low : 1.68
N
km
0
25
50


c
Deposits
Intrusions
Aeromagnetic_21km
High : 2.96
Low : 1.68
N
km
0
25
50


d
Deposits
Intrusions
Aeromagnetic_23km
High : 2.95
Low : 1.68
N
km
0
25
50

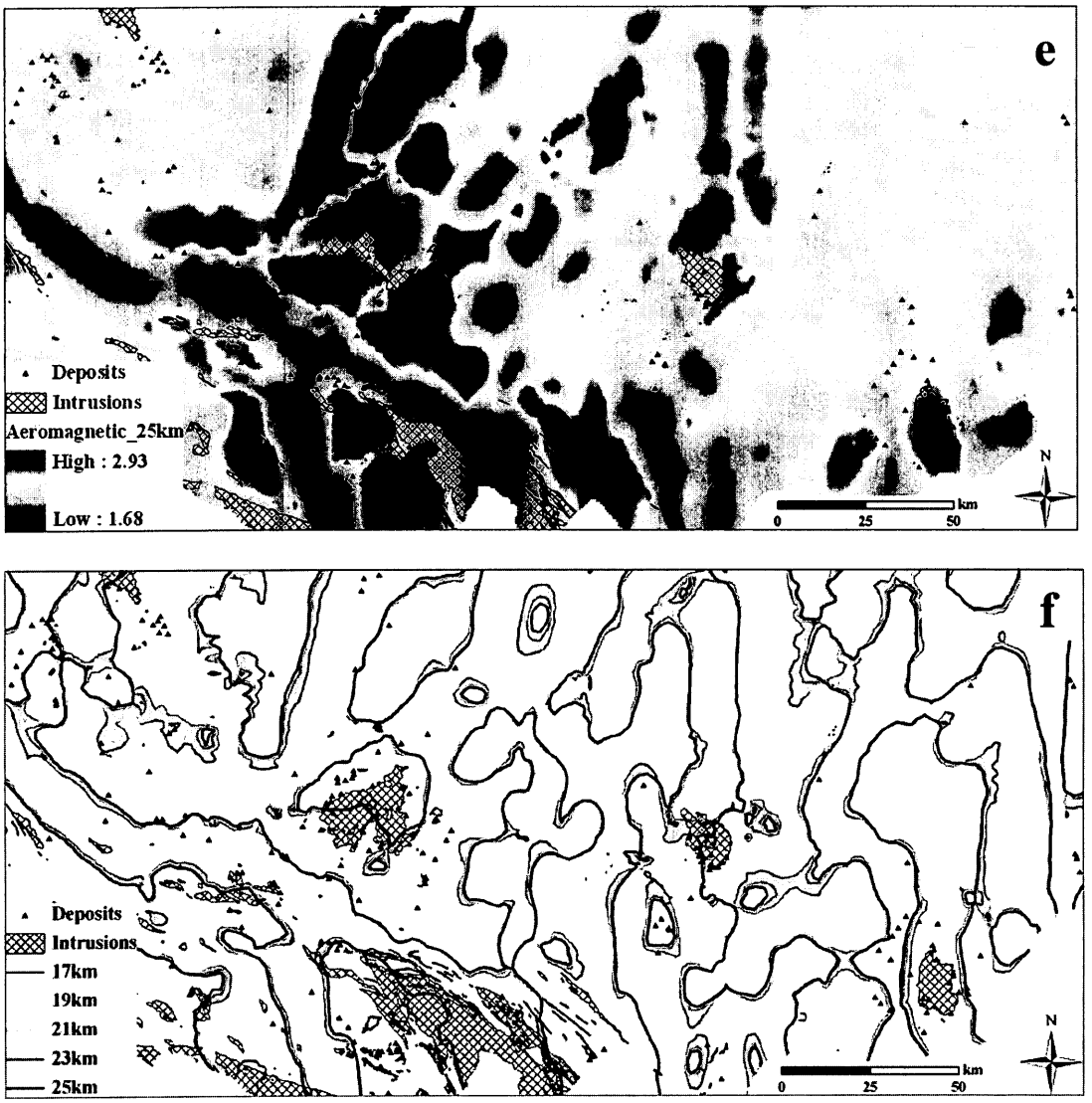

Fig.4. 6. The spatial distribution of singularity indices of aeromagnetic anomalies by a window-based mapping method with r_{max} from 17 km to 25 km. Contour lines (i.e., $\alpha = 2$) separating the positive ($\alpha < 2$) and negative ($\alpha > 2$) singularity outline edges of deeply buried granitic intrusions. **a**: r_{max} = 17 km; **b**: r_{max} = 19 km; **c**: r_{max} = 21 km; **d**: r_{max} = 23 km; **e**: r_{max} = 25 km; **f**: $\alpha = 2$ contour lines of Figs. a to e.

4.4. Summary and conclusions

Through current applications, band-pass filters consisting of a combination of upward continuations and the vertical derivatives have not only shown their advantages to interpret causative bodies, but also exposed their shortages in scale dependence that makes interpretations are somehow subjective. In contrary, the fractal/multifractal based singularity index mapping technique provides an improved and simplified approach for band-pass filtering in geophysical data analysis. Operated in space domain, the results produced by singularity index mapping method are scale independent (i.e., results are not influenced by changing the scale of measurement). After achieving geo-information regarding to singular aggregation of ore-forming elements by former researchers, studies introduced in this chapter extend the application of singularity theory to delineate geophysical potential fields. Spatial distributions of density and magnetic susceptibility characterized by singularity index mapping are more suitable geo-information in support of future mineral exploration in southeastern Yunnan mineral district. Furthermore, according to the similar geo-information extracted by both the band-pass filter (i.e., upward-continuations and the second-order derivative) and the singularity index mapping technique in some cases, it is concluded that the currently used singularity filter can be used to identify the granitic intrusions in the study area. Advantages of this method over traditional band-pass filters need to be further discussed by according to more applications and studies in future work.

A comprehensive mineral exploration modeling requires geo-information extracted and integrated from multi-sources. Magmatic-hydrothermal mineralization in this area is associated with other issues besides granitic intrusions. Mineralization related non-linear geo-processes (e.g., magmatic activities, tectonic activities, sedimentary processes, etc.) satisfy definition of singularity theory, and the products of these processes can be characterized by singularity index mapping technique that will provide various indicators to mineralization. Therefore, a singularity theory based modeling process is suggested here to enhance the efficiency of mineral exploration.

Chapter 5. Tectonic-geochemical anomaly identification by geological and geochemical data analysis

5.1. Introduction to tectonic and geochemical analysis

Recognition and mapping of geochemical signatures of the presence of mineralization plays an important role in mineral exploration modeling. Directed by metallogenic features, data-driven, knowledge-driven, and hybrid methods are applied to integrate geochemical anomalies with other indicators for investigating mineral targets of interest. Similar procedures can be applied to clarify geological processes associated with mineralization (Wang et al., 2011). Exploration for hydrothermal ore deposits is one of the examples benefitting from the advances in mineral exploration modeling. Geochemical anomaly indicates the spatial distribution of associated ore-forming elements, and mineral deposits are frequently discovered within geochemical haloes. However, mineralization is a complex process in an anomalous environment (Yu, 2002). Concerns about exploration of hydrothermal ore deposits are therefore comprehensive (e.g., igneous rocks, tectonics, wall rocks, etc.).

Tectonic activities provide spaces for transportation and precipitation of ore-forming materials (Zhai et al., 1999). Tectonics features (e.g., faults, folds, etc.) are important for the migration of hydrothermal solutions during mineralization. From the point of view of economic geology, tectonics as a process is highly related with the spatial and mechanical

properties of ore deposits in terms of two controlling factors (Zhai et al., 1999). One controlling factor is scale. Tectonics at regional scales controls the spatial distribution of mineral deposits as well as their properties; whereas tectonics at local scales controls the spatial distribution, shape and interior structures of ore bodies (Faulkner et al., 2010; Micklethwaite et al., 2010; Zhai et al., 1999). The other controlling factor is stage of tectonism. Tectonic stages may play an even more essential role in mineralization than scales. Tectonic stages linked with mineralization may be referred to as pre-mineralization, syn-mineralization or post-mineralization (Zhai et al., 1999). Pre-mineralization faults, for example, provide spaces for migration of ore-bearing fluids. In addition, faults facilitate precipitation and storage of ore minerals. Syn-mineralization faults release pressure in rocks and create more migration spaces. As a result, structures and components of ore bodies become complicated. During space-filling and metasomatism of wall rocks, chemical and physical properties of fluids are changed gradually; consequently, within spaces created by faults, wall rock alterations and mineral assemblages change dramatically both in vertical and lateral extents. Post-mineralization faults affect deposits more mechanically rather than in chemical ways such that ore bodies are destroyed, re-shaped or more strongly influenced by supergene enrichment (Faulkner et al., 2010; Micklethwaite et al., 2010; Zhai et al., 1999). Since post-mineralization faulting of a deposit might be a continuation of pre- or syn-mineralization faulting related with another deposit, fault activities can support thermodynamic power for fluid migration in this case (Zhai et al., 1999). It is sometimes difficult to differentiate types of faulting activities without detailed field observations and

mineralogical and isotope geochemical studies. Tectonic activities discussed in this paper are focused on pre-mineralization and syn-mineralization faulting activities.

To outline areas favorable for mineralization of a certain type, comprehensive research on related geological processes is necessary (Wang et al., 2011). This chapter applies advanced geo-information extraction and integration techniques in GeoDAS GIS software (Cheng, 2000) to construct a tectonic-geochemical exploration model for southeastern Yunnan ore district, China. Anomalous distributions of tectonic and geochemical signatures are mapped and integrated to investigate the relationship between tectonics and ore-forming element association. Furthermore, ore-controlling properties of geological structures are analyzed to map locations favorable for mineralization.

5.2. Geo-anomaly recognition

5.2.1. Geochemical anomalies

Hydrothermal ore deposits are characterized by high concentrations of certain metals, distributions of which have fractal or multifractal properties. As previously introduced, main ore-forming elements in the southeastern Yunnan district, China, are Au, Ag, Cu, Pb, Sn, W and Zn. In order to delineate anomalous areas likely containing mineral deposits in this area, singularity theory is currently used to characterize geochemical distributions of these ore-forming elements.

Using the window-based method in GeoDAS GIS software, singularity indices (α) of the distribution of ore-forming elements are estimated (Fig. 5.1). According to the properties of α, areas with $\alpha < 2$ (or positive singularity) indicate distributions of intensely concentrated ore-forming elements, spatially coincident with known deposits (i.e., mineral occurrences) of certain elements; whereas, areas with $\alpha \geq 2$ (or negative singularity) represent geochemical background and/or depletion of ore-forming elements (Fig. 5.1).

In order to characterize mineralization better, PCA is applied to determine geochemical signatures based on singularity indices of elements in an association of ore-forming elements (instead of original concentrations of elements) in the study area. A scree plot (Fig. 5.2a) shows the distribution of eigenvalues representing relative importance of each component. The first principal component (PC1) accounts for 55% of the total variance. PC1 with an eigenvalue >1 (Kaiser, 1960) can be retained for interpretation. Positive loadings (Fig. 5.2b) indicate that PC1 mainly reflects the singular association of ore-forming elements. In comparison with singularity maps of individual ore-forming elements, areas with high PC1 scores (Fig. 5.3) have stronger coincidence with known mineral occurrences (Fig. 5.3). This goes to show that integrated singularity indices (α) of elements in an association of ore-forming elements reflect more accurately geochemical anomalies linked with hydrothermal mineralization. Furthermore, there is a noticeable spatial correlation between fault traces and intermediate to high PC1 scores, implying that fluid-rock interactions along faults resulted in enrichment of a suite of elements similar to those in the known occurrences of hydrothermal mineral deposits (Fig. 5.3).

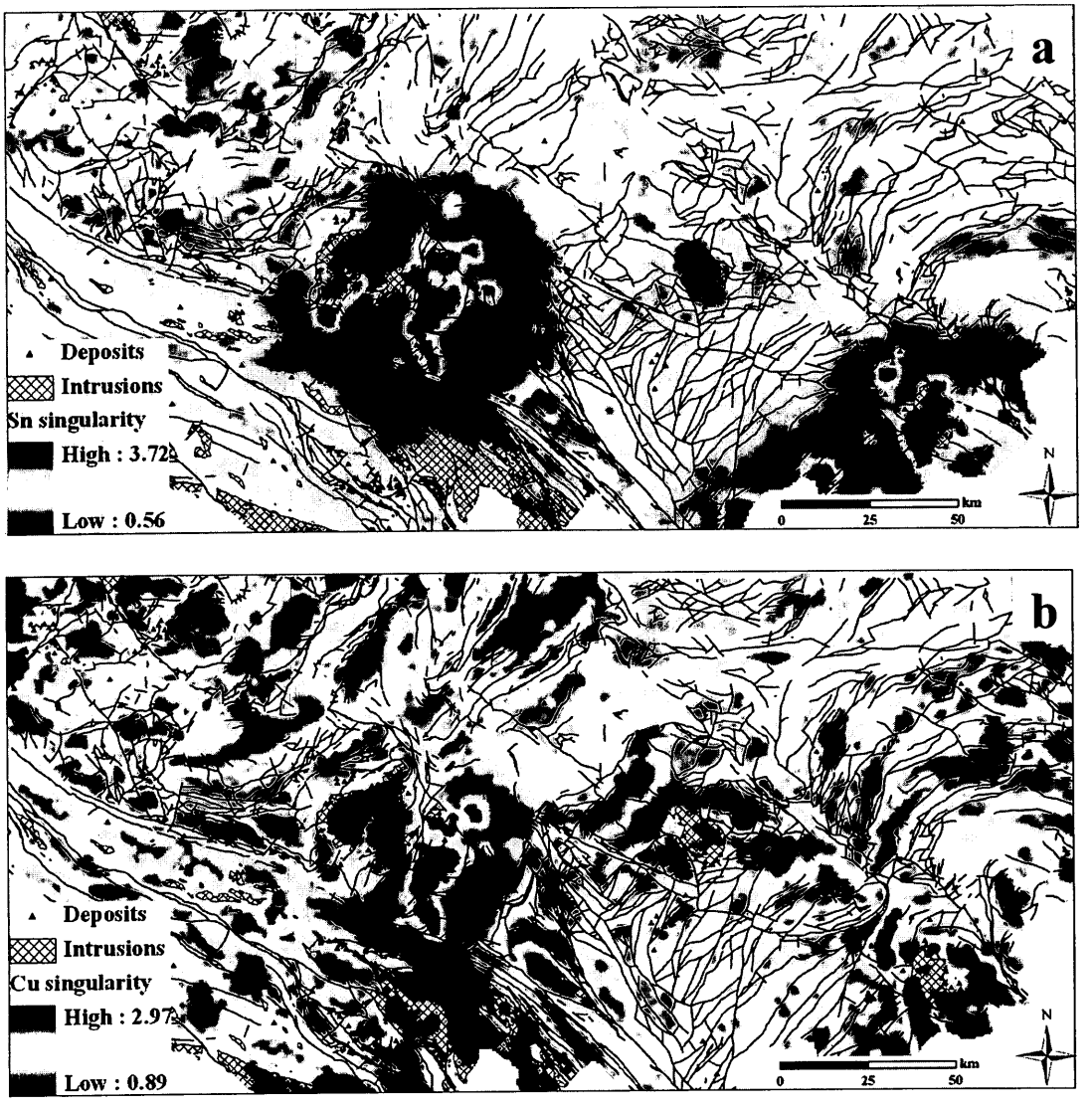

Fig.5. 1. Spatial distributions of singularity indices for Sn (**a**) and Cu (**b**) are shown as examples for demonstration the efficiency of singularity index mapping in anomaly identification. Mineral occurrences, fault traces and boundaries of felsic intrusions are shown for reference.

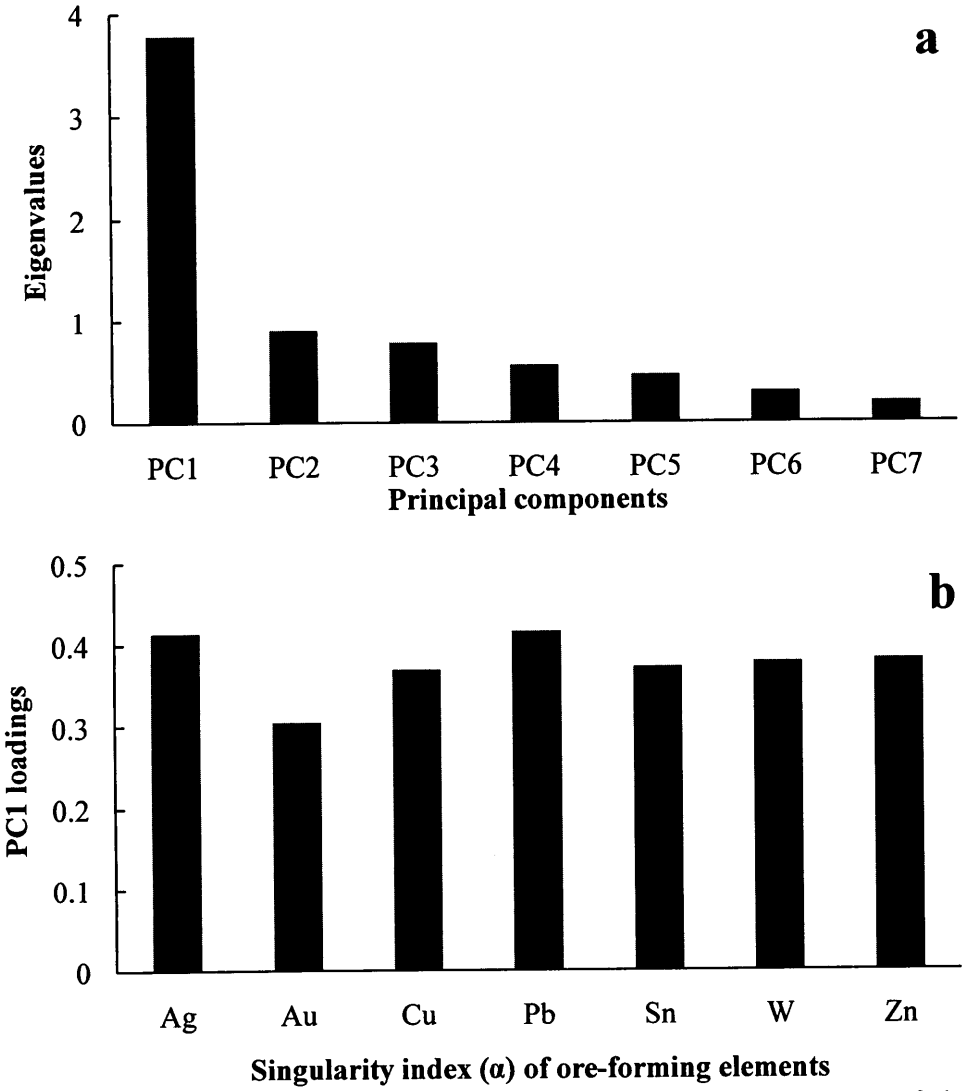

Fig.5. 2. **a:** Scree plot of eigenvalues of principal components (PC1-PC7) of singularity indices of ore-forming elements. **b:** Loadings of ore-forming elements on the first principal component (PC1), which represents 55% of the total variance in singularity indices of ore-forming element data.

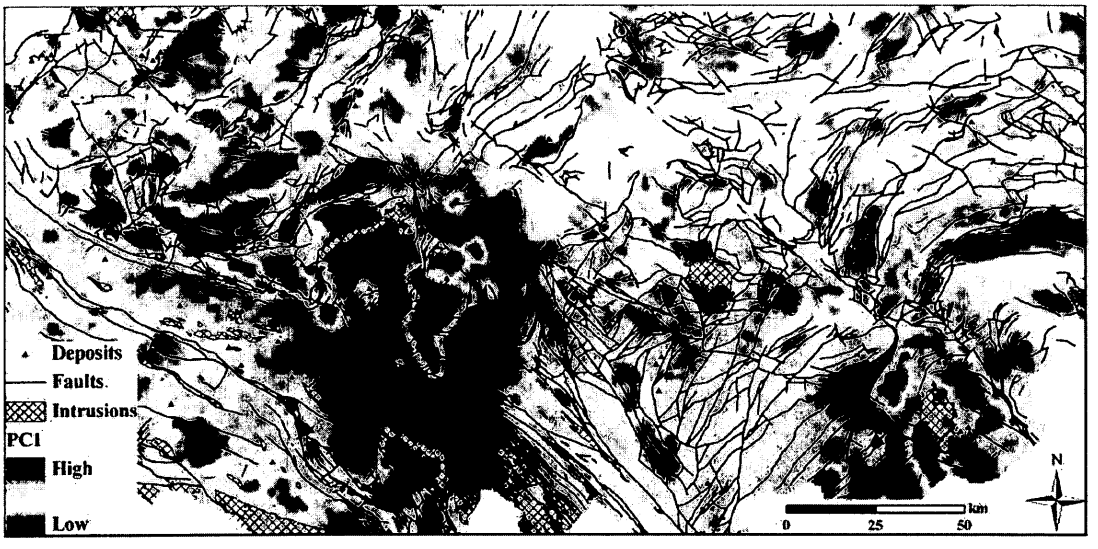

Fig.5. 3. Spatial distribution of PC1 scores of singularity indices the stream sediment geochemical data for the ore-forming elements. Mineral occurrences, fault traces and boundaries of felsic intrusions are shown for reference.

By cross referencing the simplified geological map (Fig. 2.1) and the map of PC1 scores (Fig. 5.3), areas with enrichment of the ore-forming elements are those within and/or along major fault zones. The anomalous areas (i.e., with $\alpha < 2$) in Gejiu, Wenshan and Dulong districts are characterized by high-density mineral occurrences and intersections of regional faults, intensely developed local faults, and granite intrusions (Fig. 5.3). These characteristics are in accordance with regional metallogenic features (i.e., regional faults confine magmatic activities to certain scales and ranges; hydrothermal fluids permeate rocks through local faults; metasomatism and mineralization occur within fault/fracture zones). Therefore, the complexity of fault systems is significant to mineralization in the study area (Ford and Blenkinsop, 2008; Zhao et al., 2011): well developed fault systems provided spaces for hydrothermal fluid flow and mineralization.

5.2.2. Fault anomalies

Fault systems as products of non-linear geo-processes (i.e., faulting activities) are frequently accompanied by energy released within short spatial-temporal intervals and increase in numbers and total length of parallel or intersecting faults. Fault density (I) defined as total length L of fault traces per unit area A (i.e., $I = L/A$) can be currently used to describe development extent of a fault system in 2-D (Xypolias and Koukouvelas, 2004). High fault density indicates intensely developed fault systems, which benefit migration of ore-bearing fluids and permit accumulation of ore-forming elements. From a multifractal point of view, $I(A)$ follows a power-law relationship with A:

$$\langle I(A) \rangle = cA^{\alpha/2-1} \qquad (5.1)$$

where c is a constant. The singularity index (α) characterizes singular distributed fault density (i.e., intensely developed fault systems). An example is shown here to demonstrate a well developed fault system characterized by a singularity index $\alpha < 2$ at a local scale (Fig. 5.4), which is favorable for mineralization. In contrast, singularity index $\alpha \geq 2$ stands for depletion or non-singular distribution of fault density, and will not be discussed here.

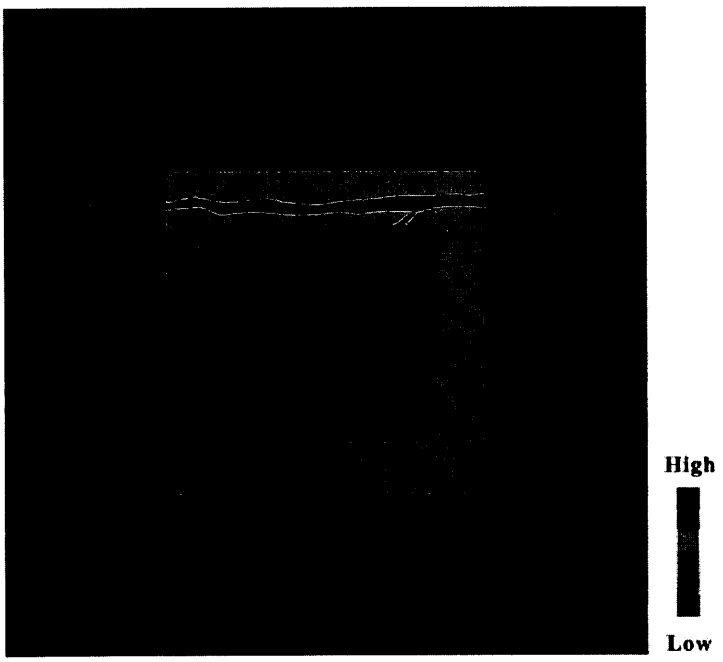

Fig.5. 4. Conceptual diagram of positive singularity of fault density. It corresponds to a special case where fault traces (grey lines) are well developed at a local scale. The background squares with different colors represent fault density within areas (After Wang et al., 2012).

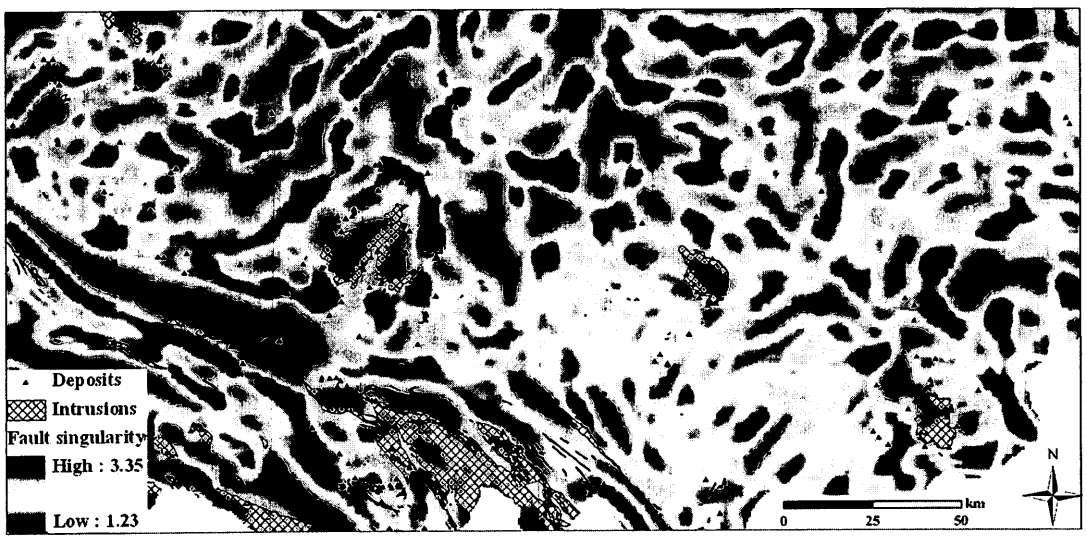

Fig.5. 5. Spatial distribution of singularity indices ($\alpha < 2$ for positive fault singularity, $\alpha > 2$ for negative fault singularity) of fault density. Mineral occurrences, fault traces and boundaries of felsic intrusions are shown for reference.

The estimated singularity indices of fault density (Fig. 5.5) clearly indicate areas with high fault density by $\alpha < 2$. All positive singularity indices (i.e., $\alpha < 2$) are coincident with areas where local faults intersect and/or where regional faults intersect with local faults. From a geological point of view, positive singularity describes drastic enhancement of fault density. The changes of fault density are represented by increase of broken spaces where the internal pressure-temperature conditions of passing hydrothermal fluids will be reduced abruptly, which benefits crystallization, differentiation and mineralization of hydrothermal fluids (Zhai et al., 1999). In addition, most hydrothermal-type mineral occurrences are located in and/or nearby areas with $\alpha < 2$ (Fig. 5.5). These findings show that hydrothermal mineralization in this area is positively correlated with degree of development of fault systems. Mineralization was favored by spaces provided by fault systems modeled by positive singularity indices (i.e., $\alpha < 2$). Furthermore, based on student's *t*-values of the singularity indices of fault density (Fig. 5.6a) and of the fault density (Fig. 5.6b) estimated by WofE method, two binary maps are constructed (Fig. 5.7). Anomalies identified by using singularity indices of fault density indicate well areas with fault intersections; whereas, anomalies identified by using only fault density are spread overwhelmingly in the study area. Singularity indices of fault density can, thus, be used to efficiently characterize enhancement of fault density, and can be accepted as a suitable geo-information in support of mineral exploration modeling.

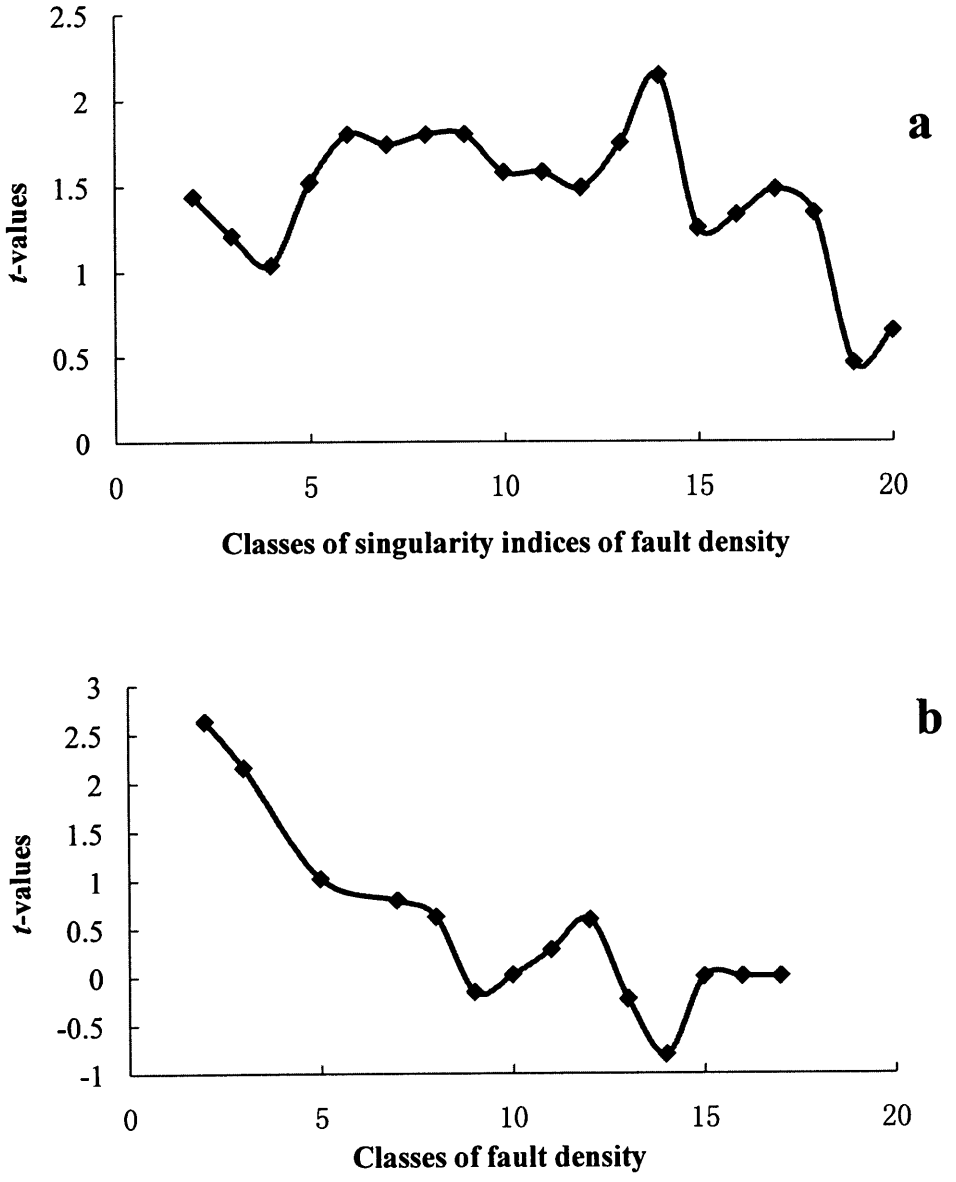

Fig.5. 6. Student's *t*-value calculated by weights of evidence method for measuring the spatial correlation between deposits and (**a**) singularity indices of fault density, and (**b**) fault density. The value of the *x*-axis with variable corresponding with the highest *t*-value is considered as a threshold to define binary patterns.

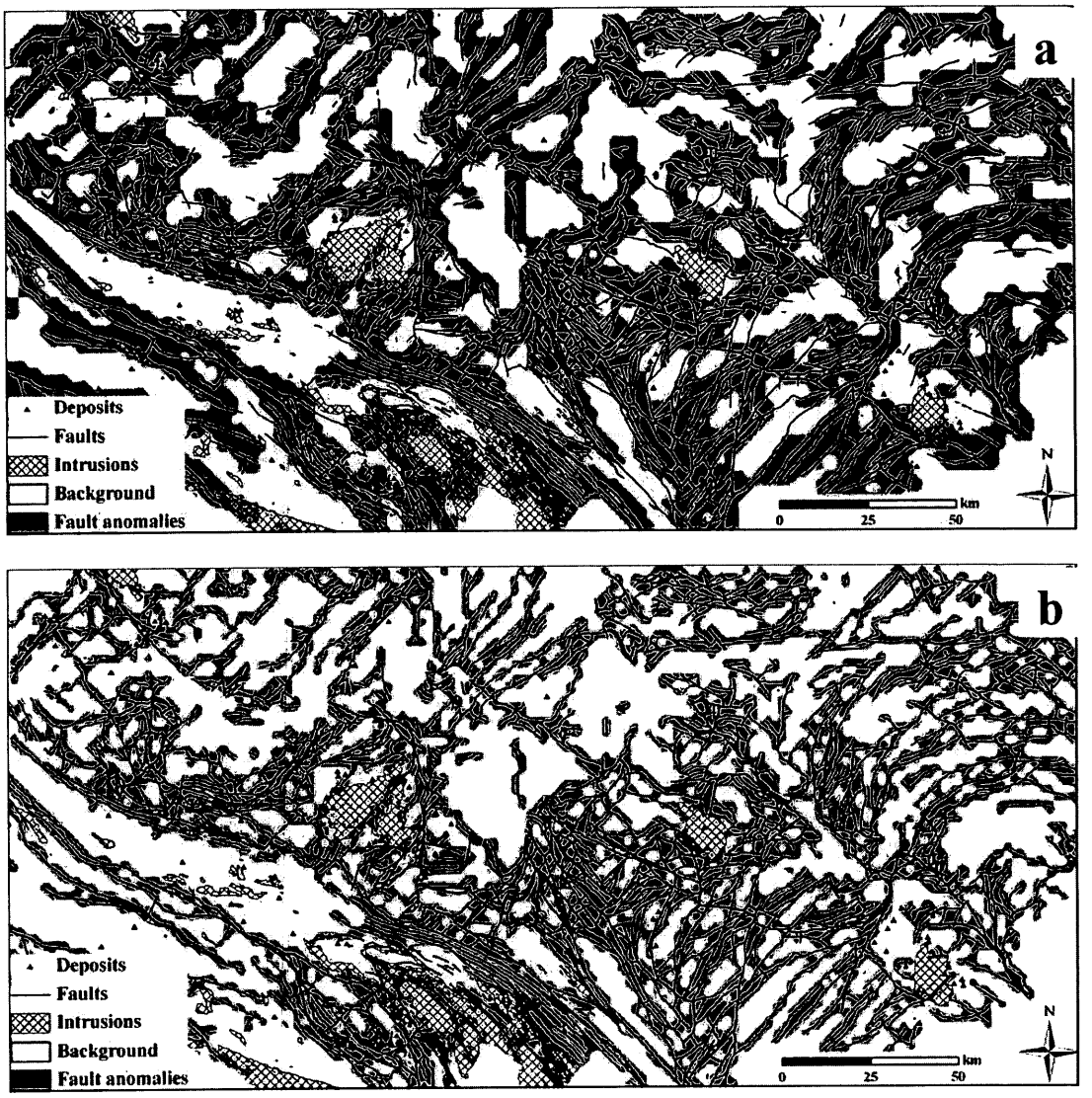

Fig.5. 7. Binary maps indicating areas highly correlated with mineral occurrences based on the highest *t*-values for (**a**) singularity of fault and (**b**) fault density. Mineral occurrences, fault traces and boundaries of felsic intrusions are shown for reference.

5.2.3. Anomaly integration

The positive singularity indices ($\alpha < 2$) of the association of ore-forming elements (Fig. 5.3) likely represent geochemical anomalies related to geochemical haloes of mineralization in the study area. According to the relationship between faults and mineralization introduced at the beginning of this chapter, the positive singularity indices of fault density (Fig. 5.5) likely represent anomalous faulted areas (i.e., faults in these areas are intensive) where fluid-rock interactions may have occurred resulting in mineralization. In order to study the interrelation of mineralization and faults, it is instructive to integrate the previously achieved two layers of geo-information (i.e., geochemical and fault anomalies).

In current study, PCA is further used to integrate previously achieved geo-information (i.e. singularity of the element association and fault intensity). The PC1 with an eigenvalue > 1 is retained, and positive loadings of the two geo-variables (i.e., fault singularity and geochemical anomalies of the element association) in PC1 support that low PC1 scores are indicative to the hydrothermal mineralization (Fig. 5.8). Representing 54% of the total variances of these two geo-variables, the reasonable integration delineates geochemical and tectonic anomalies, simultaneously (Fig. 5.9). The integration result properly reveals the regional metallogenic features; that is, mineral occurrences are spatially coincident with intensively faulted areas. Geo-information related to mineral occurrences not previously indicated (Fig. 5.3) is enhanced by geo-information of faults (Fig. 5.5). From the result, favorable spaces for migration of ore-forming fluids along

faults and accumulation of ore-forming elements within fracture zones can be tracked. Compared with the singularity of fault intensity, highly faulted areas without supporting mineralization are constrained by geochemical anomalies.

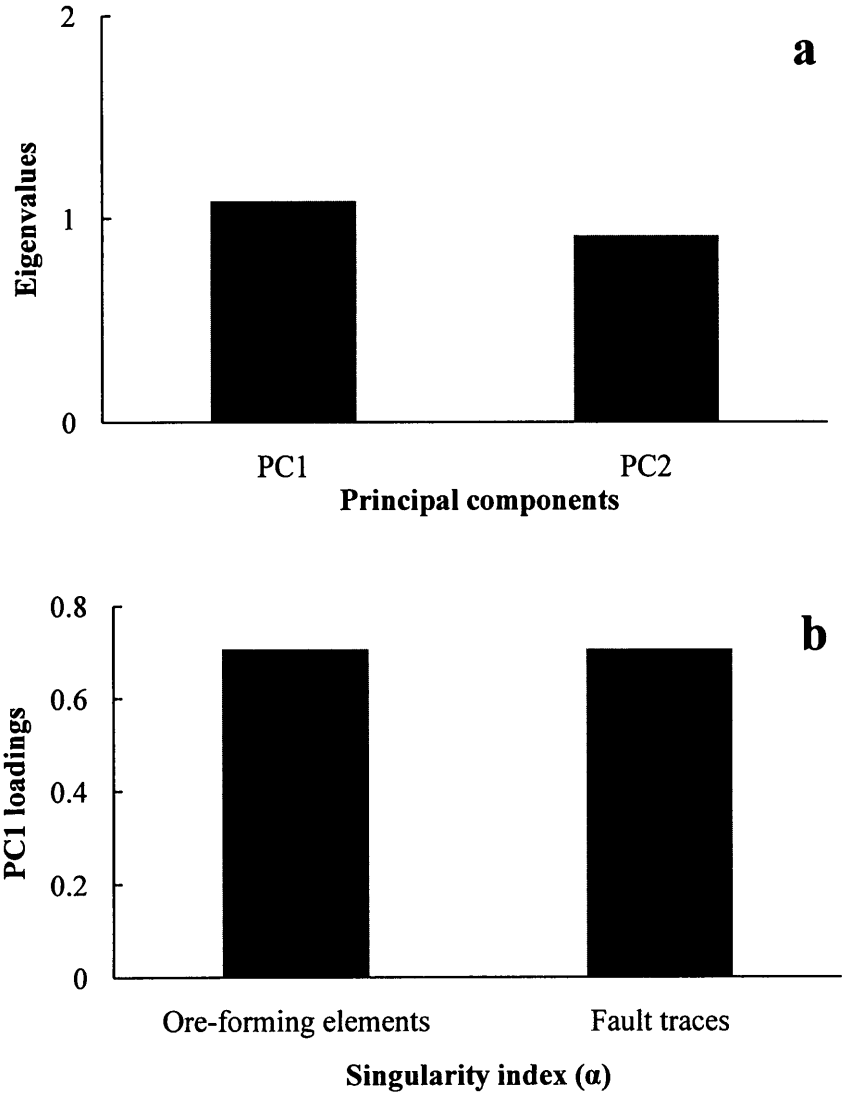

Fig.5. 8. **a**: Scree plot of eigen values of principal components of the ore-forming element assemblage and fault singularity. **b**: Loadings of ore-forming element assemblage and fault singularity, which represents 54% of the total variances of these two geo-variables.

Fig.5. 9. Spatial distributions of PC1 scores by integrating geochemical anomalies of ore-forming the element association and fault singularity indices. Mineral occurrences, fault traces and boundaries of felsic intrusions are shown for reference.

5.3. Summary and discussions

Strong enrichment of an association of ore-forming elements is an important precondition of mineralization in the area; meanwhile, fault systems played significant roles in mineralization by controlling the spatial distributions of magmatic intrusions, hydrothermal fluid flow and wall rock metasomatism. The tectonic-geochemical model constructed in this paper, supported by the application of the singularity theory for geo-information extraction and principal component analysis for geo-information integration, is useful and efficient for identifying and locating areas most favorable for the occurrence of mineralization. Those areas are characterized by the combination of fault and geochemical anomalies, which exhibit strong spatial association with known locations of

mineral deposits. The results support mineral exploration, and provide suggestions for future research on fault systems in the southeastern Yunnan district, China.

The formation of hydrothermal mineral deposits is a complex process produced by various geological processes. The tectonic-geochemical exploration model discussed in this study is based on fault and geochemical anomalies. This model focuses on fault-controlled and geochemical halo-associated deposits. Identification of areas favorable for the occurrence of other types of hydrothermal mineral deposits that are not relevant to the discussed model (e.g., known mineral deposits in the study area located within the range of magmatic intrusions) could rely on a comprehensive mineral exploration model constructed through similar procedures described in this study. However, other issues (e.g., spatial characteristics of intrusions, ore-hosting strata, etc.) must be taken into consideration. In addition, integration of other multidisciplinary datasets (e.g., remote sensing-geochemical exploration; geophysical-geochemical exploration; etc.) into the currently introduced tectonic-geochemical exploration model can be applied to enhance the efficiency of mineral exploration.

Chapter 6. Characterization of interrelations between tectonic and geochemical signatures

6.1. Introduction to interrelations of tectonic and geochemical signatures

Mineralization is a complex and non-linear dynamic process (Cheng, 2007a; Cheng and Agterberg, 2009; Yu, 2002; Zhao, 1999). As an end product of mineralization, formation of mineral deposits is caused by multiple geo-processes consisting of ore-forming element activation/transportation, ore-bearing fluid formation, migration, accumulation and precipitation, etc. Furthermore, these geo-processes are associated with many issues respectively. Interactions between fluids and tectonism believed as important ones mostly influence mineralization, and concerns to these two are thus significant to mineral exploration (McCaffrey, et al., 1999). Fluid as a major medium to extract and transport ore-forming materials from their original positions can facilitate dispersion and accumulation of ore-forming materials (Zhai et al., 1999). Meanwhile, tectonism within the metallogenetic environment plays an important role in influencing the physical and chemical properties of ore-forming fluids (McCaffrey, et al., 1999; Zhai et al., 1999). First of all, the prominent decrease of tectonic stress within the faults (e.g., the dilatant faults) can benefit alteration of the thermodynamic equilibrium among various components of fluids when they passing through the faults system. Consequent variations

in component concentration and saturation which further disturb the physical-chemical stability of fluids may cause the occurrences of mineralization. Secondly, the variation of tectonic stress can cause dissolution, activation and migration of ore-forming materials from ore-bearing strata to hydrothermal fluids. In addition, dilatant structures with high permeability can advantage dispersion of ore-forming materials and provide space for mineralization. Therefore, proper analysis for tectonic system will benefit understandings of mineralization, especially hydrothermal mineralization.

Hydrothermal mineralization is an important mineralization type in geosciences, the occurrence of which is normally dominated by three controlling factors consisting of igneous intrusions, mineralization-favored wall rocks and tectonic systems, (Cheng, 2007a; Heinrich, 1995; Wang et al., 2011, 2012; Zhao et al., 2012). The previous two factors determine chemical reactions during mineralization, which confine occurrences of metasomatism within the mineralization system (Yuan et al., 1979). Controlling effects of tectonic systems on spatial and mechanical characteristics of hydrothermal deposits are undertaken by two properties: tectonic scales and stages (Zhai et al., 1999). In general, local tectonics influence the local distribution, shapes and interior structures of hydrothermal ore bodies, while regional tectonics influence the spatial distribution and properties of hydrothermal deposits (Faulkner et al., 2010; Micklethwaite et al., 2010; Zhai et al., 1999). Chronologically, tectonic stages involve pre-, syn- and post-mineralization tectonics which provides spaces for ore-bearing fluid flow, releases pressure in wall rocks and affects deposits mechanically (e.g., re-shaped, disassemble or supergene enrichment), respectively (Zhai et al., 1999). Since the effects of tectonic

system on hydrothermal fluid flow and ore formation, properties of tectonic activities (e.g., types and spatial distributions) have long been noticed. Fault as one of the most significant productions of tectonic activities is the focus of many researches (Faulkner et al., 2010; Kim and Sanderson, 2005; Torabi and Berg, 2011). By analyzing fault properties (e.g., fault length, population, and displacement, etc.), knowledge regarding to various mineralization-associated issues can be derived to support further studies (Agterberg et al., 1996; Wang et al., 2012; Zhao et al., 2011).

It is broadly understood that the formation of faults and geochemical haloes are caused by multiple non-linear geo-processes, the distributions of which are consequently complex and anisotropic (Agterberg et al., 1996; Agterberg, 2012b; Cheng, 2007a; Zhao et al., 2011). As the description in Zhai (2003), migration of geochemical elements cannot be occurred without force and power. Forced by tectonic stress, geochemical elements are transported within the spaces of faults toward certain positions and further mineralized accompanying with heterogeneously distributed geochemical anomalies, rock deformation and/or metamorphism of wall rocks. As a result, the geochemical anomalies are spatially confined within certain tectonic units, and faults can be accordingly identified by the long axis of anomalous patterns in some cases (Zhai et al., 1999). The tectonic stress-related deformation and geochemical element accumulation constitute a uniform physical-chemical system, so-called as tectonic-geochemical system (Zhai et al., 1999). Therefore, concerns of interrelations between geochemical signatures and tectonic features are necessary to understand the tectonic-geochemical associated mineralization.

Interpretation of the interrelations requires the collaboration of geochemistry and tectonics in many cases.

With the development of computer sciences (De Paor, 1996) and constructions of geo-database all over the world (Darnley, 1995), multidisciplinary approaches nowadays are flourishing. Geosciences as the beneficiary have been greatly progressed in geo-information integration for datasets from multi-source and at multi-scale (Harris et al., 1998; Wang et al., 2011; Cheng, 2012). Among these interdisciplinary collaborations, tectonic-geochemical exploration is the one employed frequently (Zhai, 2003; Zhai et al., 1999; Wang et al., 2012). Statistical methods are popular and effective to frequency domain rather than spatial domain, by which optimal buffers of fault traces and their intersections are often applied as indicators to mineralization-favored spaces (Bonham-Carter, 1994; Cheng et al., 2009; Koch and Link, 1980). Since the concept of 'fractals' proposed by Mandelbrot (1972), fractal and multifractal approaches taking care of both frequency and spatial properties of geological signatures have been widely used to fault analysis (Agterberg et al., 1996; McCaffrey, et al., 1999; Wang et al., 2012; Zhao et al., 2011). There is an increasing interest in applying fractal dimension and multifractal spectra to describe complexity and self-similarity of fault systems. In fractal/multifractal point of view, active and complex fault system corresponding with high fractal dimension can benefit ore-bearing fluid flow and provide favorable environment for mineralization (Zhao et al., 2011). Furthermore, the multifractal based singularity index mapping technique (Cheng, 2007a) has proven to be efficient in qualitatively and quantitatively

characterizing spatial variations of fault density and delineating mineralization-favored spaces provided by fault systems (Wang et al., 2012).

After characterizing spatial distribution of fault intensity and modelling hydrothermal mineralization-associated tectonic-geochemical signatures in southeastern Yunnan mineral district, China in chapter 5, this chapter as a successor to the previous research intends to apply an interdisciplinary collaboration method to characterize anisotropic distributions of geochemical signatures in Gejiu area (i.e., a sub-district of this dissertation) (Fig. 6.1). In addition, current results will define a new fault property based on variations of geochemical signatures or mineralization favorability along the directions of fault traces.

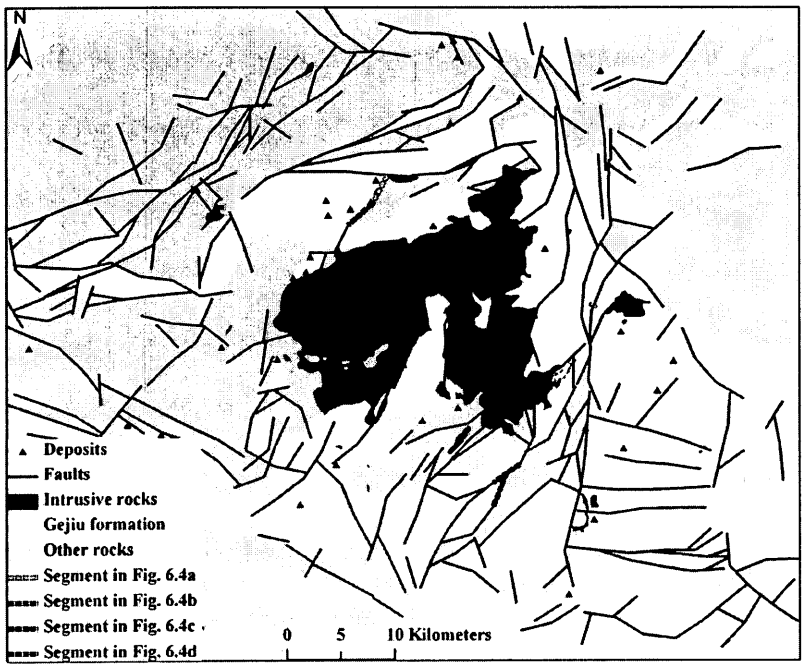

Fig.6. 1. A simplified geological map of the Gejiu mineral district, China (after Cheng, 2007a). Segments used in following analysis are shown for reference.

6.2. Geological settings of Gejiu area

Similar to southeastern Yunnan mineral district, China, Gejiu mineral district (Fig. 6.1) approximately 200 km south of the city of Kunming, the capital of Yunnan Province, China, chosen for current research is well-known for its world class Sn-Cu polymetallic deposits, the centre of which is at a longitude of 103°09'26"E and a latitude of 23°22'40"N. Located in the suture zone of the Indian Plate and the Eurasian plate on southeastern of China sub-plate, tectonic-magmatism is well developed and provides a mineralization-favored environment.

As a major type of mineral deposits, magmatic-hydrothermal polymetallic deposits (e.g., Sn, Cu, Pb, Zn, W, et al.) are spreading in this district (Zhuang et al., 1996). Recognized by previous researches (Zhuang et al., 1996), main controlling factors of the mineralization are tectonic settings, magmatism (e.g., intrusions and hydrothermal activities) and wall rocks. The interactions of these factors are believed to be important for metallic mineralization. The Middle Triassic Gejiu formation (i.e., the wall rocks) consisting of limestone and minor dolomites is the main ore-bearing strata (Qin et al., 2008; Zhuang et al., 1996). Magmatic activities in the Gejiu mineral district experienced medium- to small-scale ultramafic-felsic extrusions in the period of the Jinning epoch (1000-800 Ma) to the Hercynian epoch (386-257 Ma), massive mafic intrusions in the Indo-China epoch (257-205 Ma) and felsic intrusions in the Yanshanian epoch (205-135 Ma). Among these magmatic activities, the Yanshanian intrusions (i.e., the Gejiu Batholith) supplied both heat and material resources to the Sn-Cu polymetallic

mineralization in the Gejiu mineral district (Guan, 1993; Zhuang et al., 1996). Tectonic activities controlled the spatial-temporal distribution of both mineralization and diagenesis not only in the Gejiu mineral district but also in southeastern Yunnan region (Qin et al., 2008; Zhuang et al., 1996; Wang et al., 2012).

In general, faults in the Gejiu mineral district are shown as an annular structure around the Gejiu Batholith in the center of the study area (Fig. 3). They can be sorted into four orientations (i.e., the NS, NW, EW and NE trending faults) with different mechanic properties and stratigraphy- and mineralization-controlling effects. The distinct NS trending Gejiu fault as a part of the regional Xiaojiang fault located in the east of the Gejiu Batholith divides the study area into two parts, the eastern and the western districts. Mineral resources discovered in the eastern district are much more than which were explored in the western district. The NW trending faults (e.g., the Red river fault) are well developed in the western district rather than in the eastern district, which dominate the mineralization in the southwestern area. The EW trending faults are broadly developed in the eastern district and control the spatial distribution of ore fields (Zhuang et al., 1996). The NE trending faults were produced by tectonic activities in the Hercynian, Indo-China, and Yanshanian epochs. They are considered as the most significant stratigraphy- and mineralization-controlling structures. Most of the discovered mineral occurrences are located within their buffer zones (Cheng et al., 2009).

In the Gejiu mineral district, interrelations between faults and ore-forming fluids or mineralization can be derived from lithological analysis, discussions of which are mostly

qualitative rather than spatially quantitative (Qin et al., 2008; Zhuang et al., 1996). In fact, quantitative analysis on faults was formerly attempted. According to statistical approaches, Cheng et al. (2009) used buffer analysis on fault traces and intersections of fault traces to identify mineralization-favored spaces. In addition, singularity index mapping technique was applied to indicate mineralization-favored spaces by characterizing variations of fault density (Wang et al., 2012). However, the influences of faults to ore-forming fluids and mineralization were not explained quantitatively, especially the spatial variations of controlling effects of faults. Therefore, according to a tectonic-geochemical collaboration, current research contributes a new effort to this topic by using the anisotropic singularity index mapping technique which was introduced in the former section.

6.3. Singularity index mapping and results

In the Gejiu mineral district, China Sn-Cu polymetallic mineralization is accompanied with the accumulation of Sn, Cu, Pb, W, and Zn. In this study, geochemical distributions of these elements are selected for singularity index mapping. Integrated geochemical distribution of these elements by the principal component analysis (PCA) method (Table 6.1) is used as well to represent ore-forming elemental association (Fig. 6.2). As shown by these geochemical distributions (Fig. 6.2), patterns of both geochemical anomalies of individual elements and the association are controlled by tectonic-magmatism related granitic intrusions and fault structures. In the eastern district, geochemical anomalies of individual elements are extensively distributed, which are constrained by the EW

trending faults. In addition, the junctions of the faults striking along different orientations are the most important places for mineralization, where intensive release of tectonic stress is occurred. It is coincident with the occurrences of the known deposits located around the intersections of the EW trending faults and the NS trending Gejiu fault. Without presenting distinct geochemical anomalies, the Gejiu Batholith in the western district may not have great mineralization potentials due to the insufficiency of ore materials. However, the apparent geochemical anomalies around the intersections of the granitic intrusions and the fault structures (e.g., the northwestern edge of the Gejiu Batholith) may be caused by the interactions between wall rocks and the hydrothermal fluids during their migration within the fault systems. As the source of heat, these hydrothermal fluids, which were probably differentiated from the Gejiu Batholith, altered the chemical properties of the carbonate wall rocks and boosted the directed migration and accumulation of ore-forming materials in the wall rocks. Therefore, faulted areas with less geo-stress dominating the physical-chemical reactions between hydrothermal fluids and wall rocks provide a mineralization-favored environment in the Gejiu mineral district.

By the square window-based singularity mapping technique, a set of window sizes (i.e., ε_i) ranging from 6 to 26 km are defined, and fault traces can be classified based on the values of the singularity index α which describes the geochemical behaviors (i.e., enrichment and depletion) of the elements in space (Fig. 6.3). Since the isotropic nature of the square window-based singularity mapping technique, identified geochemical behaviors of the elements are the end products by combined effects of multiple geo-

processes (e.g., magmatism and tectonic activities). The influences of each geo-process to mineralization cannot be recognized and reflected by the singularity index. Without emphasizing to certain geo-processes, the isotropic singularity indices are not supportive to describe mechanism of mineralization (i.e., interrelations of mineralization related controlling factors), although they are efficient to indicate locations of both weak and strong geochemical anomalies for geological exploration.

Table 6. 1 Results of PCA of selected geochemical distributions and loadings of PC1 representing the spatial distribution of ore-forming fluids.

	PC1	**PC2**	**PC3**	**PC4**	**PC5**
Component Variance	3.04	0.91	0.52	0.32	0.21
Cumulative Importance of Components	0.61	0.79	0.89	0.96	1.00
	Cu	**Pb**	**Sn**	**W**	**Zn**
PC1 Loadings	0.40	0.48	0.46	0.42	0.46

In order to apply currently introduced fault trace-oriented singularity index mapping techniques to characterize anisotropic geochemical signatures, fault traces in the study area are divided into equal segments (i.e., r = 3 km). Furthermore, a set of rectangular windows with half window sizes ranging from 3 km to 13 km at an interval of 1 km are predefined (i.e., ε_i = 6 km, 8 km, ..., 26 km). Consequently, 11 rectangular windows with sizes $r \times \varepsilon_i$ (i.e., 3×6 km^2, 3×8 km^2, ..., 3×26 km^2) will be used. During the singularity estimation process, element concentration $C[A(r\times\varepsilon_i)]$ is calculated by averaging the values of all geochemical samples within the window. Plotting ε_i and $C[A(r\times\varepsilon_i)]$ on a log-log graph, a linear trend can be achieved by means of the least square method. The slope of the regression is the value of $\alpha_r - 1$ (Fig. 6.4). From the spatial distributions of

singularity indices of selected ore-forming elements and elemental association (Fig. 6.5), the positive fault segments ($\alpha_r < 1$) are well coincident with the mineral occurrences. Comparing with the isotropic singularity indices (Fig. 6.3), the newly estimated anisotropic singularity indices (Fig. 6.5) with more physical-chemical meanings support understandings to mechanism of mineralization (i.e., interrelations between hydrothermal fluids, fault spaces, and wall rocks), and the variations of patterns of fault segments are more delicate.

Due to the variations of tectonic stress, faults with diverse mechanical properties can provide various influences on fluids or mineralization. Through currently achieved results (Fig. 6.5), the influences of an individual fault on hydrothermal fluids or mineralization are characterized by the continuous chemical reactions between wall rocks and fluids at different segments along the fault trace. The EW trending faults controlling the spatial distributions of the ore fields in the eastern mineral district possesses positive singularity indices ($\alpha_r < 1$). Especially, the segments intersecting with the NS trending faults with even smaller α_r are corresponding with the accumulation of individual elements and elemental association. It is coincident with the fact that areas near/around the intersections are the major mineralized positions in the eastern district. For the EW trending segments in a longer distance from the intersections, the medium singularity indices indicate that the reactions of fluids and wall rocks within these segments are not sufficient to facilitate mineralization. In the western district, positive segments (i.e., $\alpha_r < 1$) are mainly trending along the NE direction that satisfies former discussions (i.e., the NE trending faults dominated the spatial distributions of mineral deposits). However, the

negative segments (i.e., $\alpha_r > 1$) indicate that hydrothermalism is inactive at the positions far away from the intrusions (Fig. 6.5). Without fluids passing through the faults, hydrothermal mineralization is not well developed in these areas. From the patterns of these faults, segments of an individual fault trace possess different singularity indices. It might be due to the differences of interchange of materials between fluids and wall rocks during the fluids passing through the fault structures and the migration of ore-forming material toward the segments with positive singularity indices. These segments are mainly located near/around the intersections of the faults in different orientations and the intersections of the faults and intrusions.

6.4. Discussions

Singularity index mapping technique efficient in identifying heterogeneity of geochemical signatures had been utilized to identify geochemical anomalies in many cases. As an example of interdisciplinary collaboration, this chapter applies a newly proposed fault trace-oriented singularity index mapping technique to characterize anisotropic geochemical signatures associated with hydrothermal mineralization. According to a case study in Gejiu area, it can be considered as a supplement to the formerly introduced square window-based isotropic singularity index mapping technique. The fault trace-oriented singularity index assigned to its corresponding fault segment provides an inspiring way to qualitatively and quantitatively explain the interrelations between fault activities and hydrothermal fluids or mineralization. In comparison with frequently employed fault properties (e.g., length, density, types, etc.), the fault trace-

oriented singularity index as an new fault attribute is applicable to describe variations of physical-chemical reactions between ore-forming fluids and wall rocks along fault traces that benefit the interpretation to metallogenic mechanism.

Because of currently used geochemical data at a 2 km spatial resolution, fault traces are predefined at a longer unit (i.e., 3 km) which is advantage to employ sufficient geochemical samples for the singularity index estimation (i.e., regression) and to preserve geo-information of 2 km resolution geochemical data. If fault traces can be divided by a finer unit and cooperate with geochemical data at a higher resolution, more detailed variations of interrelations between fault systems and hydrothermal fluids or mineralization will be expected.

Mineralization which is mentioned again is complex and controlled by various non-linear geo-processes. Geochemical signatures of mineralization-favored spaces inherited from these geo-processes are anisotropic. The fault trace-oriented singularity index properly depicts the anisotropy associated with fault systems. Other controlling factors including wall rocks, intrusions, and their contact zones influence the formation of anisotropic geochemical signatures as well. If the anisotropy of these controlling factors can be characterized by other interdisciplinary collaborations (e.g., tectonics-geophysics, geochronology-geochemistry, etc.), then approaches like regression analysis can be employed to examine the anisotropic influences of each controlling factor on mineralization, and more comprehensive understandings to cascade mineralization process is expected.

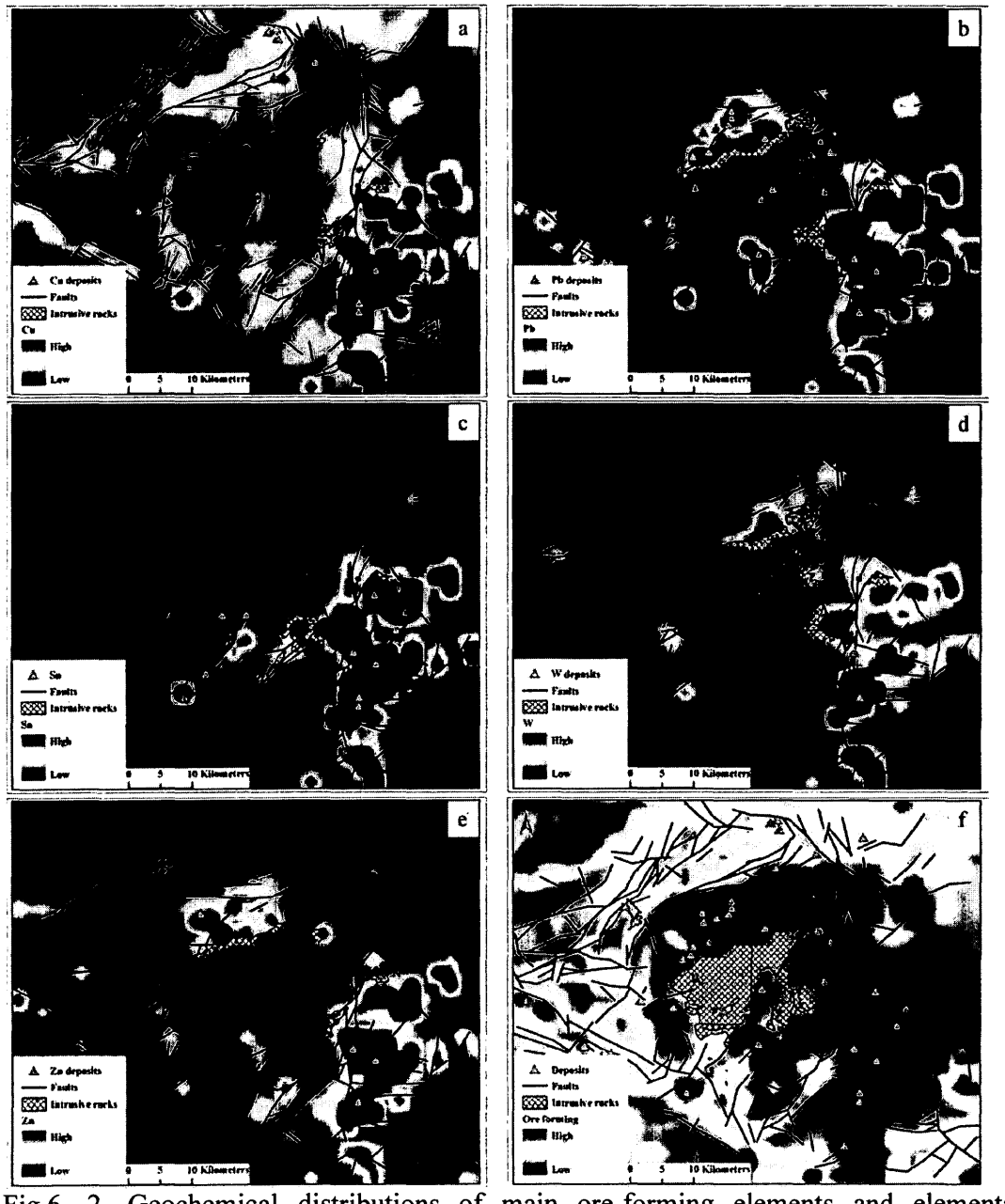

Fig.6. 2. Geochemical distributions of main ore-forming elements and elemental association. **a**: Cu; **b**: Pb; **c**: Sn; **d**: W; **e**: Zn; **f**: the ore-forming element association. Occurrences of mineral deposits (i.e., Cu, Pb, Sn, W, and Zn), fault traces, and outcrops of intrusions are shown for reference.

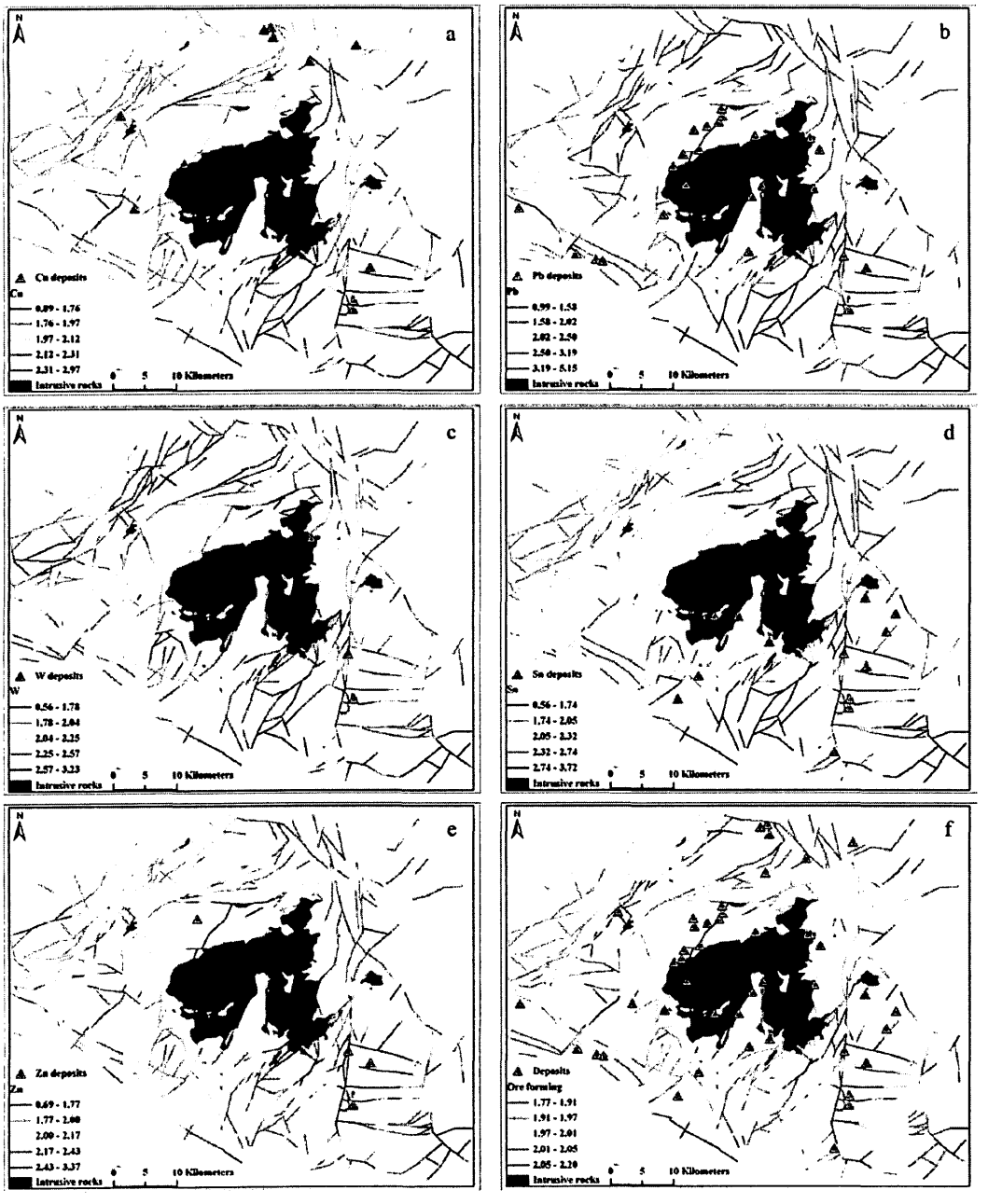

Fig.6. 3. Spatial distributions of isotropic singularity index estimated by the square window-based method. Various α in a 2-dimensional scenario estimated based on ore forming elements and elemental association are demonstrated in **a**: Cu; **b**: Pb; **c**: Sn; **d**: W; **e**: Zn; **f**: element association.

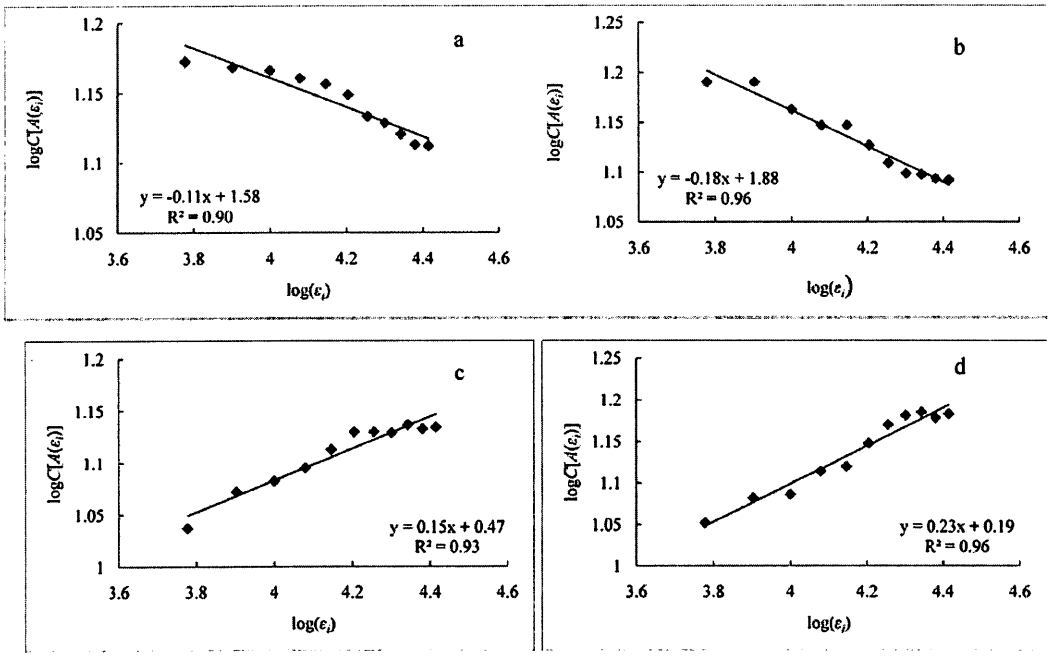

Fig.6. 4. Example fault segments in the Gejiu mineral district are provided to demonstrate how the anisotropic singularity index is estimated for individual fault segment. Locations of these four segments can be found in Fig. 6.1. a: $\alpha_r = 0.89$; b: $\alpha_r = 0.82$; c: $\alpha_r = 1.15$; d: $\alpha_r = 1.23$.

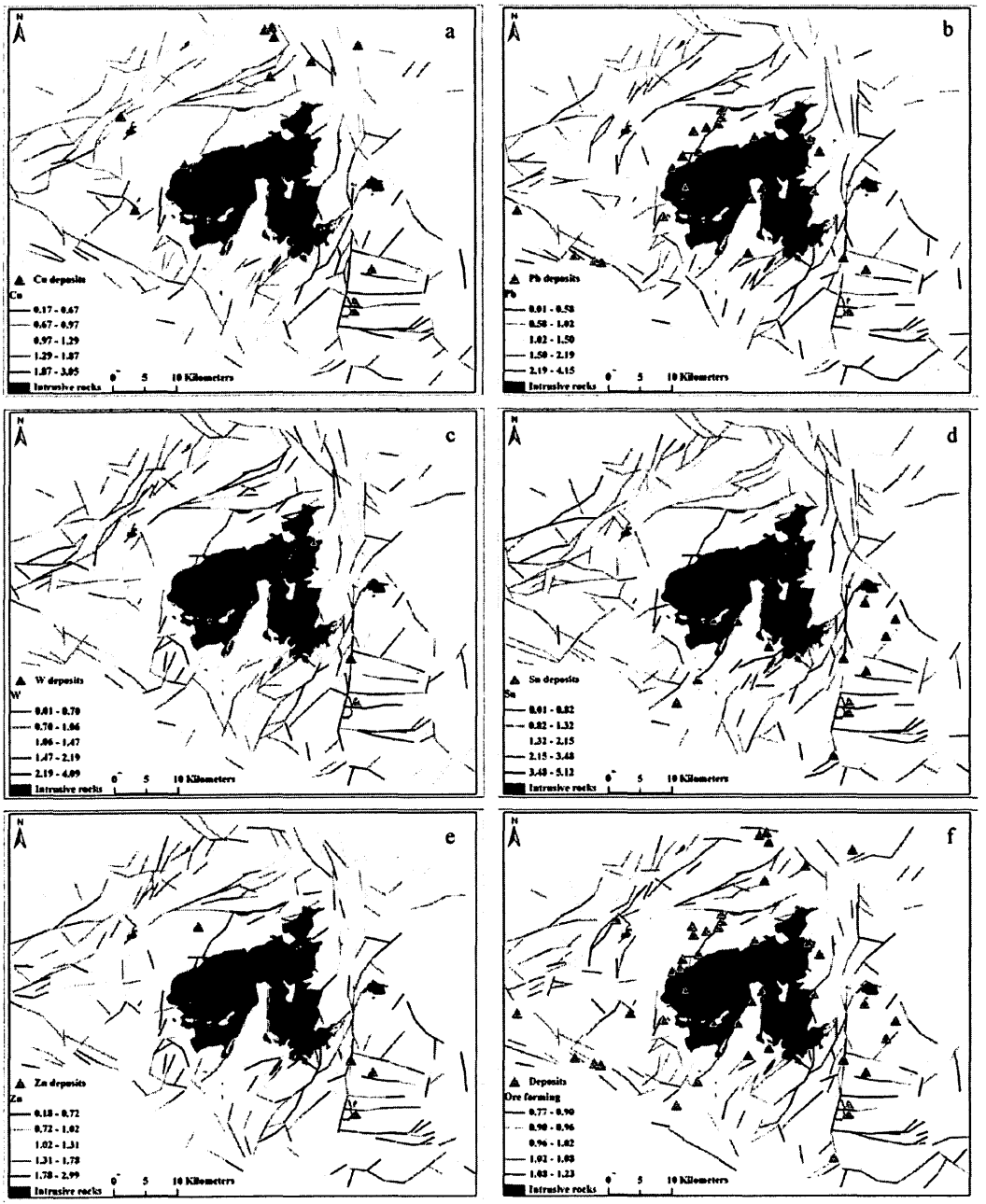

Fig.6. 5. Spatial distributions of anisotropic singularity index indicate the spatial variations of interrelations between faults and fluids or mineralization. Various α_r in a 1-dimensional scenario estimated based on ore forming elements and elemental association are demonstrated in **a**: Cu; **b**: Pb; **c**: Sn; **d**: W; **e**: Zn; **f**: elemental association. Positive and negative fault segments are defined by $\alpha_r < 1$ and $\alpha_r > 1$, respectively.

Chapter 7. Gejiu formation characterization by geochemical data analysis

7.1. Introduction to geological feature identification by geochemical data analysis

As introduced in former chapters, the hydrothermal mineralization accompanied with formation of various geological bodies is produced by a series of geological activities. Knowledge of these geological bodies assistant to characterize these geological activities is consequently significant to mineral exploration (Agterberg et al., 1996; Bonham-Carter, 1994; Cheng et al., 2011, 2012). Based on detailed field observations and studies of mineralogy and isotope geochemistry, controlling effects of the geological bodies or activities can be analyzed; however, achieved knowledge of these geological issues in terms of types, distributions and geneses are only qualitatively interpretable rather than spatially and quantitatively (Wang et al., 2011). Nowadays, advancements in computer sciences and geo-databases (e.g., geological, geophysical and geochemical data) have greatly improved the knowledge (i.e., geo-information) acquisition of these concerns.

Geological database consisting of location information of geological occurrences provide spatial distributions of various outcropping geological bodies (e.g., mineral deposits, earthquakes, etc.). For hydrothermal mineral exploration modeling, spatial distributions of fault traces, intrusions and wall rocks as three important controlling factors can be

interpreted from their location information and further considered as main components of an exploration model (Bonham-Carter, 1994). Buffer analysis is a typical data processing method commonly employed in mineral exploration. Based on distance from locations of a certain geological bodies (i.e., controlling factors), its controlling effects to mineralization can be estimated. For hydrothermal mineralization, areas surrounding igneous rocks (e.g., intrusions), close to fault traces or their intersections, and within ore-bearing strata (e.g., wall rocks) are believed as mineralization favored spaces. In addition to the intuitive characterization of mineral potentials by creating buffers, based on their spatial association with discovered mineral occurrences, spatial statistical approaches (e.g., student's *t*-value) further reclassify these multiple buffers to binary patterns that are influence areas of corresponding geological bodies to hydrothermal mineralization and the background, respectively. With more geological guidance, the interpretation to the new characterization are more quantitative; however, due to the variations of geological, geophysical and geochemical signatures of these geological bodies or activities across the space, their controlling effects to mineralization are spatially varying (Wang et al., 2013b); therefore, The optimal buffer may not properly indicate the influenced areas of the controlling factors, and delineations from more detailed observations are necessary.

Geophysical and geochemical data as two primary geo-information resources can be utilized to indicate geological bodies by characterizing their physical and chemical properties. Geophysical data efficient in identifying underground objects is frequently employed to depict spatial distributions of geological bodies (Cheng and Xu, 1998; Nabighian et al., 2005a, 2005b; Wang et al., 2011, 2013a). As introduced in chapter 4,

granitic intrusions can be outlined base on spatial variations of geophysical anomalies. Geochemical data as another important geo-information resource is applicable to describe presence and absence of geological bodies as well. In mineral exploration, geochemical data analysis plays a significant role in indicating spatial distributions of mineralization associated geo-anomalies. Numerous advanced analysis methods have been employed to characterized spatial distributions of geochemical signatures (Cheng et al., 1994; Cheng, 2007a; Xie et al., 2007; Zuo et al., 2009). Reviewing applications of geochemical data analysis to mineral exploration, it can be noticed that most published researches mainly focused on characterizing ore-forming elements or element assemblages, results of which were used to represent geochemical signatures of mineralization (e.g., identified mineralization in Chapter 5); whereas, geological bodies associated with geological activities which constitute the cascade process of mineralization are not often concerned by geochemical data analysis. Consequently, geo-information integration without geochemical signatures of these geological bodies may not be a comprehensive indication to mineralization (Cheng, 2012; Wang et al., 2011, 2012; Zhao et al., 2012).

Until recent years, several efforts have been attempted to delineate mineralization associated geological bodies according to their spatially distributed geochemical signatures (Cheng, 2012; Cheng et al., 2011; Wang et al., 2011, 2012; Zhao et al., 2012). Cheng et al (2011) and Zhao et al (2012) employed major oxides to describe geochemical signatures of intrusions in southeastern Yunnan and eastern Tianshan mineral districts, China, respectively. These results are more interpretable and well delineate spatial distributions of mineralization associated intrusions. As a follow-up research of

geological body identification, the Gejiu formation as main ore-bearing strata in the study area is identified by using PCA to integrate geochemical signatures of several selected elements and oxides. As a comparison, singularity index mapping technique is applied to characterize spatial variations of selected elements and oxides, results of which are further integrated by PCA to describe spatial variations of geochemical signatures of the Gejiu formation. Detailed information about these two processes can be found in the following sections.

7.2. Characterization of Gejiu formation

7.2.1 Geochemical signatures identification for Gejiu formation

Pointed out by former researches (Zhuang et al., 1996), the Middle Triassic Gejiu formation is mainly composed of carbonate rocks (e.g., dolostone and limestone) (i.e., high contents of CaO and MgO, low content of SiO_2, K_2O, and Na_2O); furthermore, as the main ore-bearing strata, ore-forming elements are accumulated in the Gejiu formation, concentrations of which are higher than other formations in the study area (Zhuang et al., 1996). Therefore, current research chooses four oxides associated with carbonate rocks (i.e., CaO, SiO_2, K_2O and Na_2O) and five typical ore-forming elements (i.e., Ag, Cu, Pb, Sn, and Zn) to delineate spatial distributions of the Gejiu formation, by which both general and specific geochemical signatures can be characterized by PCA, simultaneously.

Table 7. 1 Results of PCA of selected geochemical elements and oxides.

Principal Components (PCs)	PC1	PC2	PC3	PC4	PC5	PC6
Component variance (Eigenvalues)	3.57	1.95	1.43	0.84	0.53	0.52
Standard Deviation	1.89	1.40	1.20	0.92	0.73	0.72
Relative Importance of Components	0.36	0.20	0.14	0.08	0.05	0.05
Cumulative Importance of Components	0.36	0.55	0.70	0.78	0.83	0.88

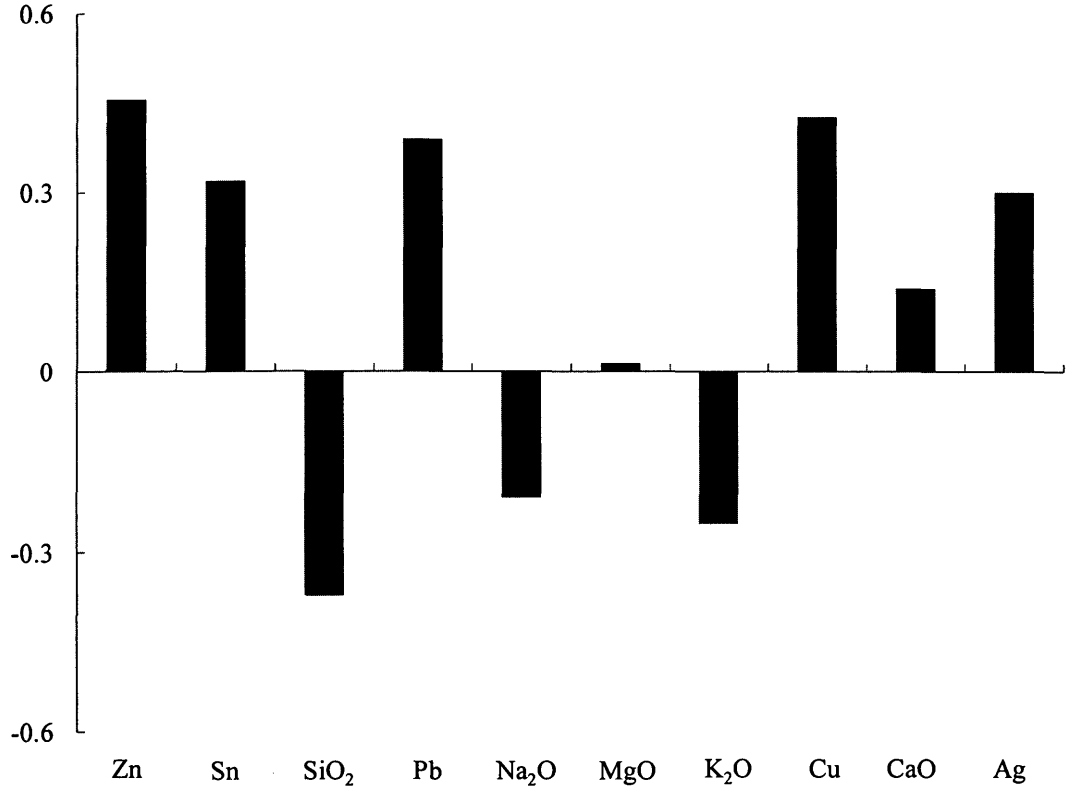

Fig.7. 1. PC1 loadings of the Gejiu formation associated elements and oxides. It supports the PC1 can represent geochemical signatures of the Gejiu formation.

According to the results shown in Table 7.1, the first three principal components (PCs) with eigenvalues greater than 1 (Kaiser, 1960) can be retained for interpretation. Positively loadings of selected oxides and elements are consistent with geochemical signatures of the Gejiu formation while negative loadings correspond to geochemical signatures of felsic rocks (Fig. 7.1). Geo-information interpreted from the loadings

satisfies the metallogenetic model that the mineralization occurred within the Gejiu formation (i.e., wall rocks). Therefore, high scores of the PC1 can be suggested to indicate the presence of the Gejiu formation by spatial distributions of its geochemical signatures (Fig. 7.2). Overlaid with geological occurrences, outcrops of the Gejiu formation are well correspond to patterns with high PC1 scores. Most discovered mineral deposits are located in the high scores. Furthermore, the hydrothermal mineralization favored spaces provided by the Gejiu formation are delineated as well.

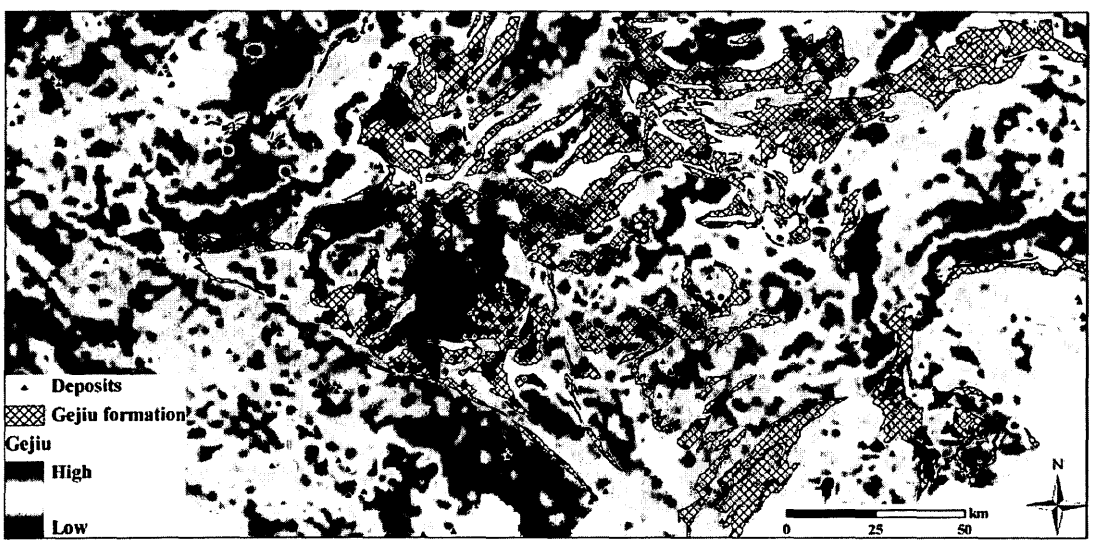

Fig.7. 2. PC1 scores to indicate spatial distribution of geochemical signatures of the Gejiu formation.

7.2.2 Spatial distributions of mineralization in the Gejiu formation

Stages of the hydrothermal mineralization include intrusions of magma, migration of ore-forming materials through fault systems, hydrothermal metasomatism, and mineralization in wall rocks, occurrences of which located in specific positions of wall rocks can cause variations of geochemical signatures, or so-called geo-anomalies, which are frequently

employed to locate mineral deposits. Former studies introduced that geochemical anomalies associated with these geo-processes are proper indicators of occurrences of mineralization (Cheng, 2007a; Wang et al., 2011, 2012, 2013a; Xie et al., 2007; Zhao et al., 2012; Zuo et al., 2009). Therefore, in addition to delineate spatial distributions of the ore-bearing strata, spatial variations of geochemical signatures of the Gejiu formation are necessary to be characterized to enhance exploration efficiency. Singularity index mapping technique formerly used to map geo-anomalies by characterizing spatial variations of physical or chemical quantities is currently utilized to analyze these selected oxides and elements, results of which are integrated by PCA to indicate the presence of mineralization within the Gejiu formation.

By singularity index mapping technique, areas with accumulation of selected elements and oxides are indicated by patterns with $\alpha < 2$. Similar to the interpretation of PCA for selected geochemical distributions (Table 7.1 and Fig. 7.1), the first three PCs with eigenvalues greater than one are retained (Table 7.2), and loadings of singularity indices of these elements and oxides in PC1 (Fig. 7.3) support the scores of PC1 can be used to represent spatial variations of geochemical signatures of the Gejiu formation. Indicated by patterns with low scores, areas with accumulations of ore-forming element association not only characterize spatial variations of geochemical signatures but also indicate specific locations of mineralization within the Gejiu formation (Fig. 7.4). The newly obtained geo-information by integrating singularity indices of these elements and oxides is more appropriate to be used theoretically and visually for hydrothermal mineral

exploration modeling. Statistical and quantitative comparisons of the results will be demonstrated in the following chapter of geo-information integration.

Table 7. 2 Results of PCA of singularity indices of selected geochemical elements and oxides.

Principal Components (PCs)	PC1	PC2	PC3	PC4	PC5	PC6
Component variance (Eignvalues)	3.45	1.76	1.56	0.74	0.71	0.53
Standard Deviation	1.86	1.32	1.25	0.86	0.84	0.73
Relative Importance of Components	0.35	0.18	0.16	0.07	0.07	0.05
Cumulative Importance of Components	0.35	0.52	0.68	0.75	0.82	0.88

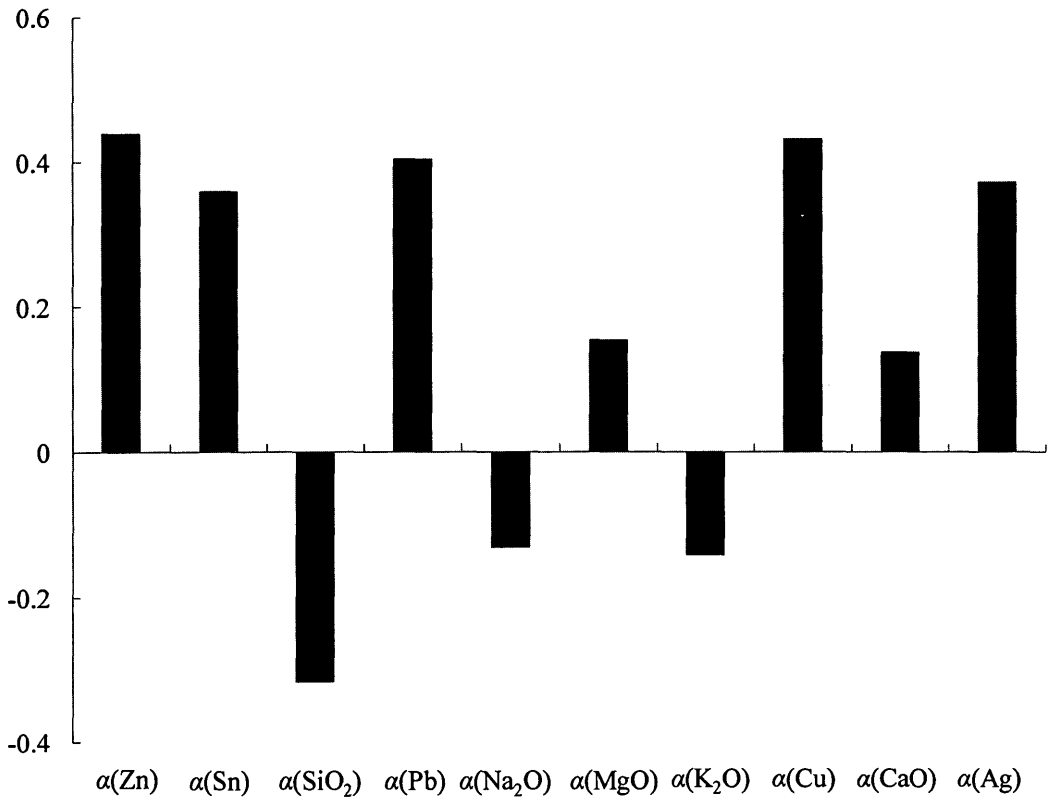

Fig.7. 3. PC1 loadings of singularity indices of the Gejiu formation associated elements and oxides. It supports the PC1 can represent spatial variations of geochemical signatures the Gejiu formation.

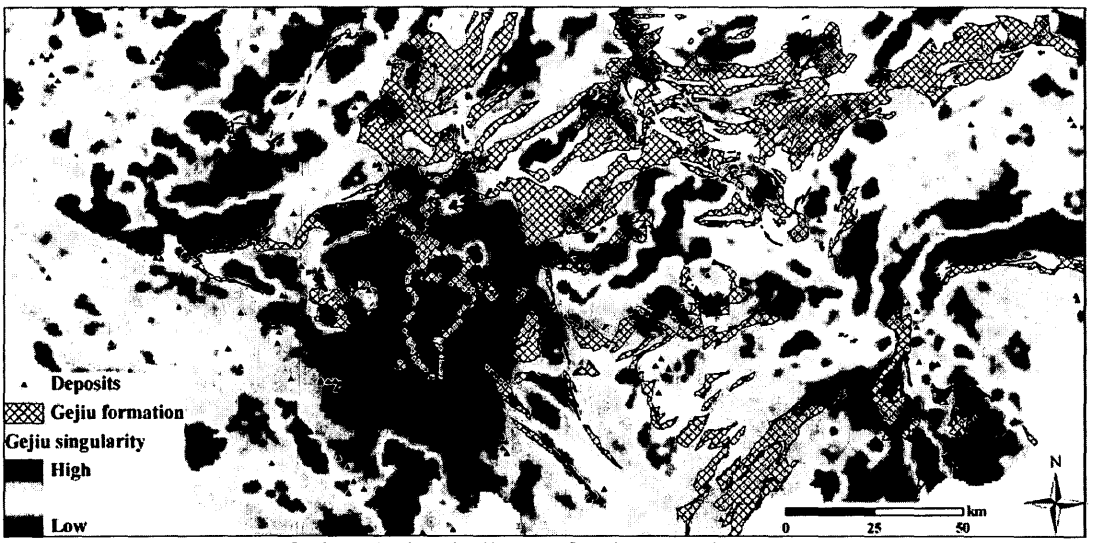

Fig.7. 4. PC1 scores of singularity indices of selected elements and oxides indicating spatial variations of geochemical signatures of the Gejiu formation that is coincident with mineralization in the Gejiu formation.

7.3. Discussions

In this chapter, both traditionally used integration of geochemical signatures and currently used integration of geochemical behaviors (i.e., spatial variations of geochemical signatures) are employed to characterize the Gejiu formation in support of mineral exploration modeling in the study area. In comparison with commonly used geo-information from geological database, currently achieved results are more reasonable to define influencing areas of geological bodies. Furthermore, identified from geochemical signatures, these results will benefit the interpretation to spatial variations of the controlling effects of various geological bodies across the space.

Spatial distributions of geochemical signatures of the ore-bearding strata generally delineate mineralization favored space (i.e., the Gejiu formation). Identified geochemical

anomalies coincident with the Gejiu formation are indicative to spatial variations of regional geochemical signatures. In other words, the result is suitable to classify the regional lithological units; whereas, within spaces of the Gejiu formation, occurrences of the hydrothermal mineralization are located on specific positions (i.e., localized spaces) where interactions of the controlling factors facilitated the mineralization. The integration of singularity indices of these elements and oxides delineate geo-anomalies caused by spatial variations of local geochemical signatures. It is more indicative to the specific positions corresponding to occurrences of the hydrothermal mineralization within the Gejiu formation. Therefore, chosen as an indicator to the presence of the hydrothermal mineralization occurred in wall rocks, geo-information of the Gejiu formation identified by singularity-based methods is involved in the mineral exploration modeling of this dissertation.

Chapter 8. Geo-information integration for mineral potential mapping

8.1. Introduction to the integration

With the development of Earth observation techniques, mineral exploration becomes more dependent on the geo-information identified from data. By interpreting observational datasets (e.g., geological, geophysical, geochemical and remotely sensed data), various Earth's properties can be inferred, the spatial variations of which can be further employed to concerns of diverse geological issues (Wang et al., 2011, 2012, 2013a; Zhao et al., 2012). In mineral exploration, uni-source datasets can be processed by advanced spatial analysis methods and provide geo-information in support of the exploration modeling, examples of which can be found in former chapters. In order to achieve comprehensive interpretation to mineralization, geo-information from multi-scale is required to be integrated frequently. For instance, regional tectonic features (e.g., fault traces) as one of causative bodies of magnetic anomalies can be tracked by aeromagnetic data in some cases (Kearey et al., 2002); whereas, the detection to tectonic features without geophysical anomalies is frequently assisted by remotely sensed data (Kowalik and Glenn, 1987). As introduced in former chapters, geological processes associated with the hydrothermal mineralization in the southeastern Yunnan mineral district, China were characterized based on the spatial analysis of geophysical and geochemical datasets that well demonstrated the efficiency of uni-source datasets in identifying geological features.

However, mineralization is a complex geo-process denominated by superposition of various associated geological activities (e.g., sedimentation, magmatism, tectonism, metamorphism, etc.). Uni-source geo-information interpretable to individual geological process may not properly indicate the characteristics of mineralization. Consequently, geo-information integration is necessary in the mineral exploration modeling.

Nowadays, improved accessibility to multi-source datasets strongly enhanced the knowledge of various Earth's properties that benefits interpreters to better understand geological settings from different aspects of geological signatures (e.g., physical and chemical). Furthermore, with the participation of GIS and its additional extensions in identifying target areas for mineral exploration, advantages of multi-source geo-information integration have been widely received by geologists (Harris and Sanborn-Barrie, 2006). In Cheng (2007a), identified geochemical anomalies of ore-forming elements by singularity index mapping technique were successfully integrated by PCA to indicate mineralization in Gejiu mineral district, China. In Harris et al (2006) weights of evidence (WofE) and logistic regression were applied to create gold prospectivity maps in the Red Lake mineral district, Canada. More comprehensive reviews regarding to geo-information integration can be found in Bonham-Carter (1994) and Harris and Sanborn-Barrie (2006).

As introduced in Chapter 1, the mineral exploration modeling is a dynamic process. With the improvements of data collection and processing technique, some formerly achieved geo-information (e.g., spatial distributions of geological features) will be modified or

retired. Using these geo-information as main components, the exploration modeling process can be updated accordingly, results of which will be replaced by more significant and accurate geo-information. In current chapter, geo-information associated with hydrothermal mineralization in the study area extracted from geological, geochemical and geophysical datasets to represent different controlling factors are integrated by selected methods. Moreover, geo-information identified by traditional approaches and the currently employed singularity mapping-based technique are compared to demonstrate the improvements of the updated mineral exploration modeling.

8.2 Geo-information preparation

Geo-anomalies (i.e., geo-information) of the hydrothermal mineralization associated controlling factors (i.e., Gejiu formation, fault traces and felsic intrusions) of the study area had been extracted by singularity index mapping-based spatial analysis methods from geochemical, geological and geophysical data in former chapters, respectively. In this chapter, three selected geo-information integration methods are employed. First of all, RGB composite image commonly used in remote sensing field is currently applied to combine geo-information of the three controlling factors. Secondly, principal component analysis (PCA) which is one of the most well-known multivariate statistical approaches to integrated geo-variables is currently chosen to mapping mineral potentials based on extracted geo-information by traditionally and currently used singularity mapping-based methods. Thirdly, weights of evidence method (WofE) as one of the most important prospecting methods in mineral exploration is employed as well. Before the integration,

there are several preparations need to be completed.

8.2.1. Fault traces

By traditionally used spatial analysis methods, geo-information of fault traces are often derived from the density analysis (e.g., total number of faults per area and total length of faults per area) (Xypolias and Koukouvelas, 2004). As introduced in chapter 5, the geo-information of fault length density was extracted from geological data (Fig. 8.1). Fault length density defined as an estimator of fault intensity can be used to evaluate if an area is favorable to the mineralization of hydrothermal deposits or not. Furthermore, as illustrated in chapter 5, the student's *t*-value assists to determine a threshold which reclassified the spatial distribution of fault length density (Fig. 8.1) to a binary pattern: one corresponds to mineralization favored fault anomalies, while the other corresponds to the background (Fig. 5.7b). By currently used the singularity index mapping technique, spatial variations of fault density (i.e., accumulation and depletion) had been characterized in chapter 5 (Fig. 5.5). As well as the spatial distribution of fault length density, spatial distributions of the fault singularity indices had been defined to be a binary pattern consisting of fault anomalies and the background (Fig. 5.7a). The spatial distributions of fault length density, fault singularity indices and their corresponding binary patterns will be used as geo-information of faults to be integrated with geo-information of the other two controlling factors.

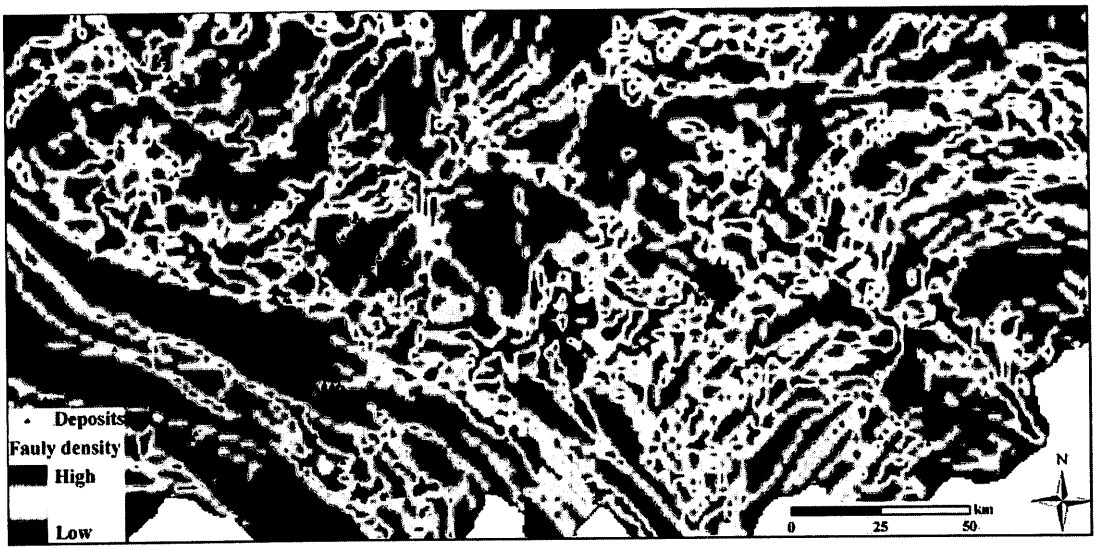

Fig. 8. 1. Fault length density of southeastern Yunnan mineral district, China. Areas with high density values are favor to the mineralization of hydrothermal mineralization.

8.2.2. The Gejiu formation

In the aspect of traditional analysis of the Gejiu formation, geochemical distributions associated with its geochemical signatures were selected and integrated by PCA. The spatial distribution of the ore-bearing strata had been depicted clearly (Fig. 7.1). In order to evaluate the spatial association between identified geo-information of the Gejiu formation and known mineral occurrences, student's *t*-value is used. Similar to the analysis to faults, a threshold can be estimated to define a binary map. Supported by the geo-information of the Gejiu formation, one class of patterns indicates spatial distributions of areas highly associated with the hydrothermal mineralization, while the other class of patterns corresponds to the background (Fig. 8.2).

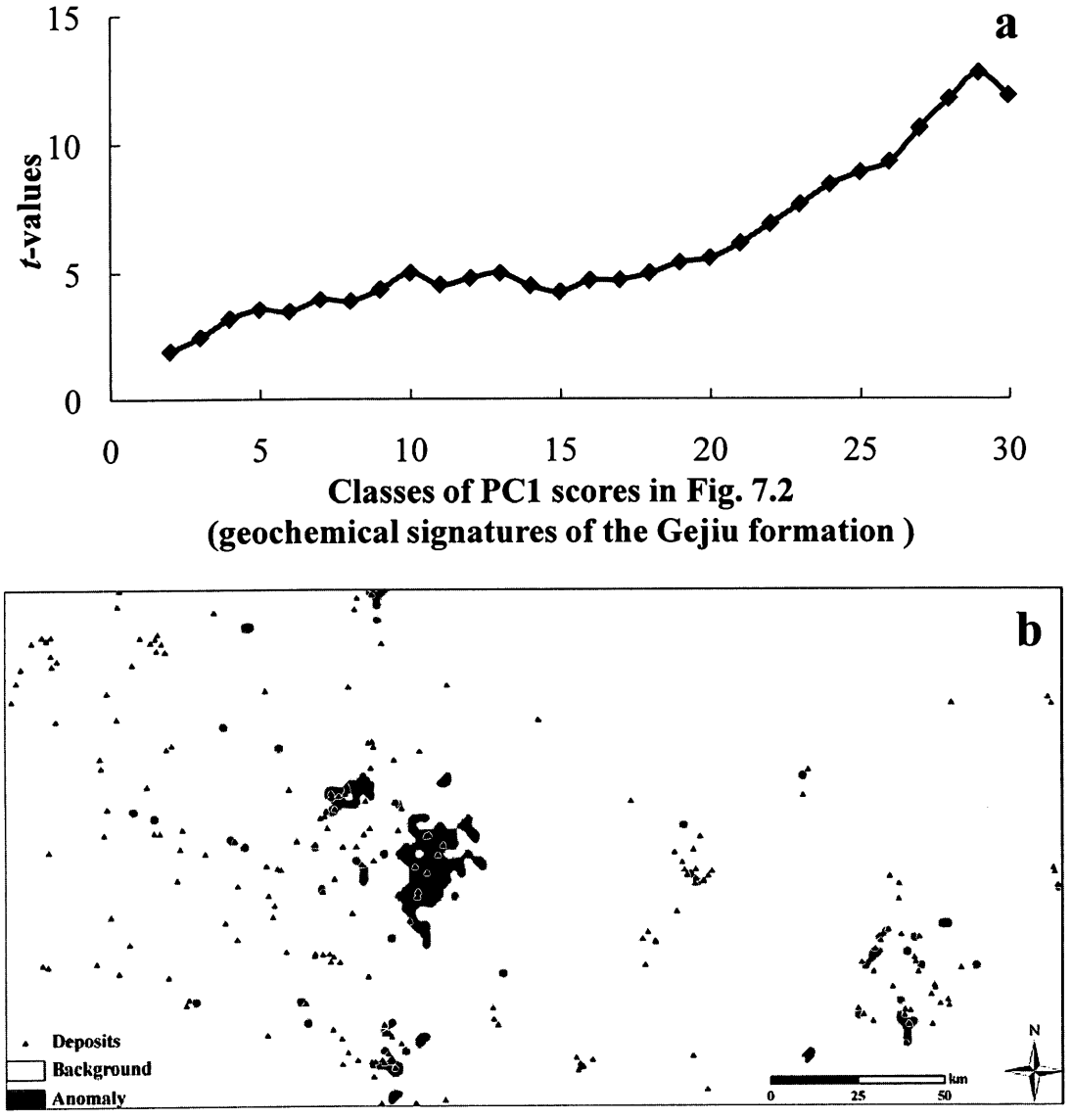

Fig. 8. 2. **a:** Student's *t*-values calculated by weights of evidence (WofE) method for measuring the spatial correlation between deposits and spatial distributions of geochemical signatures of the Gejiu formation. **b:** Binary map of the Gejiu formation indicating areas highly associated with mineral occurrences.

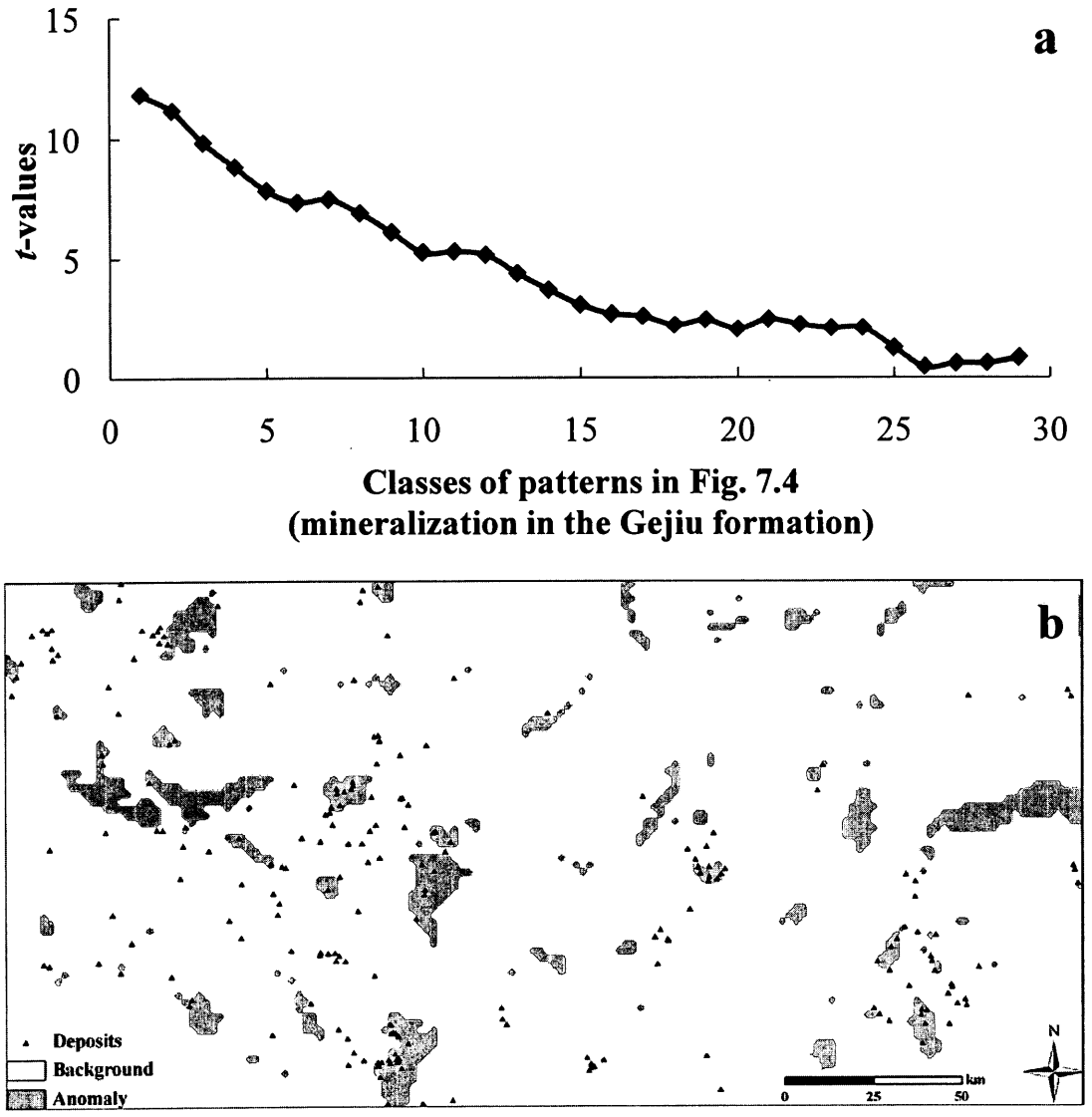

Fig. 8. 3. **a:** Student's *t*-values calculated by weights of evidence (WofE) method for measuring the spatial correlation between deposits and mineralization in the Gejiu formation. **b:** Binary map of mineralization in the Gejiu formation indicating areas highly associated with mineral occurrences.

Spatial distributions associated with singularity indices of geochemical signatures of the Gejiu formation were firstly derived, and then PCA was applied to integrate these identified spatial variations to characterized geochemical behaviors of

elements/compounds enriched in the Gejiu formation (Fig. 7.3). Similar to the analysis of geochemical signatures of the Gejiu formation, student's *t*-value is employed as well. Anomalous areas highly associated with known mineral occurrences are indicated in the binary map (Fig. 8.3). Furthermore, in comparison with the result supported by geochemical signatures of the Gejiu formation, newly achieved result improves the indication to mineral occurrences that well demonstrates the advantages of currently used singularity index mapping techniques. The spatial distributions of geochemical signatures (Fig. 7.1) and behaviors (Fig. 7.3) of element association enriched in the Gejiu formation and their corresponding binary patterns (Figs. 8.2 and 8.3) will be used as geo-information of the Gejiu formation to be integrated with geo-information of the other two controlling factors.

8.2.3. Granitic intrusions

As introduced in chapter 4, both traditionally used band-pass filter technique and currently applied singularity index mapping technique had been discussed. Advantages of singularity theory to scale independence are demonstrated in Figs. 4.5 and 4.6, respectively. In current study, spatial distributions of physical properties of granitic intrusions in the Gejiu mineral district, China are mainly delineated by the geo-information from gravity and aeromagnetic data. In order to integrate with the other geo-information of controlling factors, geo-information of rock density and magnetism are necessary to be pre-integrated for representing geo-information of granitic intrusions. For the traditionally used data analysis methods, Bouguer anomalies and aeromagnetic data

are integrated by PCA (Table 8.1). According to the loadings of the two PCs, both geo-information from gravity and aeromagnetic data are positively loaded in PC2 (Fig. 8.4a). It satisfies the fact that granitic intrusions are characterized by low values of both gravity and magnetism. Therefore, low PC2 scores can be accepted to represent spatial distributions of physical properties of granitic intrusions in current research (Fig. 8.4b). In order to delineate mineralization favored areas supported by geo-information of granitic intrusions, student's *t*-value is applied to estimate the threshold (Fig. 8.4c) which is further employed to define a binary map indicating anomalies and the background, simultaneously (Fig. 8.4d).

Table 8. 1 Results of PCA of Bouguer anomalies and aeromagnetic data.

Principal Components (PCs)	PC1	PC2
Component variance (Eignvalues)	1.08	0.92
Standard Deviation	1.04	0.96
Relative Importance of Components	0.54	0.46
Cumulative Importance of Components	0.54	1.00

Table 8. 2 Results of PCA of singularity indices of Bouguer anomalies and aeromagnetic data.

Principal Components (PCs)	PC1	PC2
Component variance (Eignvalues)	1.12	0.88
Standard Deviation	1.06	0.94
Relative Importance of Components	0.56	0.44
Cumulative Importance of Components	0.56	1.00

Correspondingly, spatial variations of rock density and magnetism which had been characterized by singularity index mapping technique need to be pre-integrated to represent spatial variations of physical properties of granitic intrusions. By PCA, the singularity indices of Bouguer anomalies and aeromagnetic data are integrated (Table 8.2). According to the loadings of the two PCs, these two variables are positively loaded

in PC1 (Fig. 8.5a). It satisfies that granitic intrusions are corresponding to high singularity indices (i.e., depletion) of both gravity and aeromagnetic data. Therefore, the high PC1 scores can be used to represent spatial variations of geo-physical properties of granitic intrusions (Fig. 8.5b). By student's *t*-value (Fig. 8.5c), a binary map is defined to indicate both anomalies and the background, simultaneously (Fig. 8.5d).

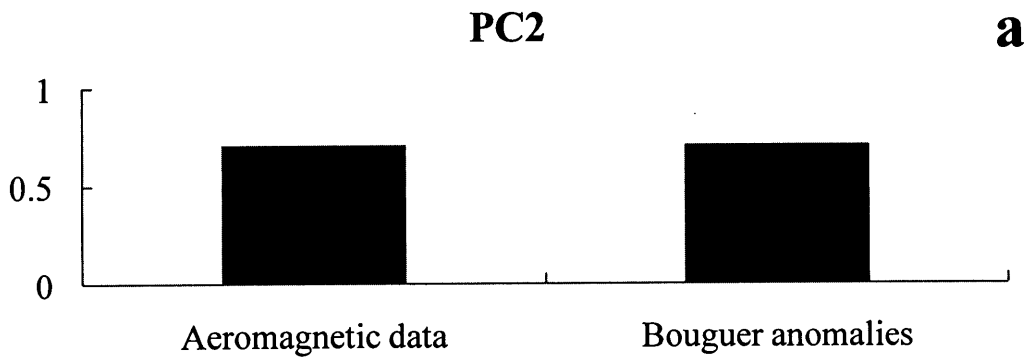

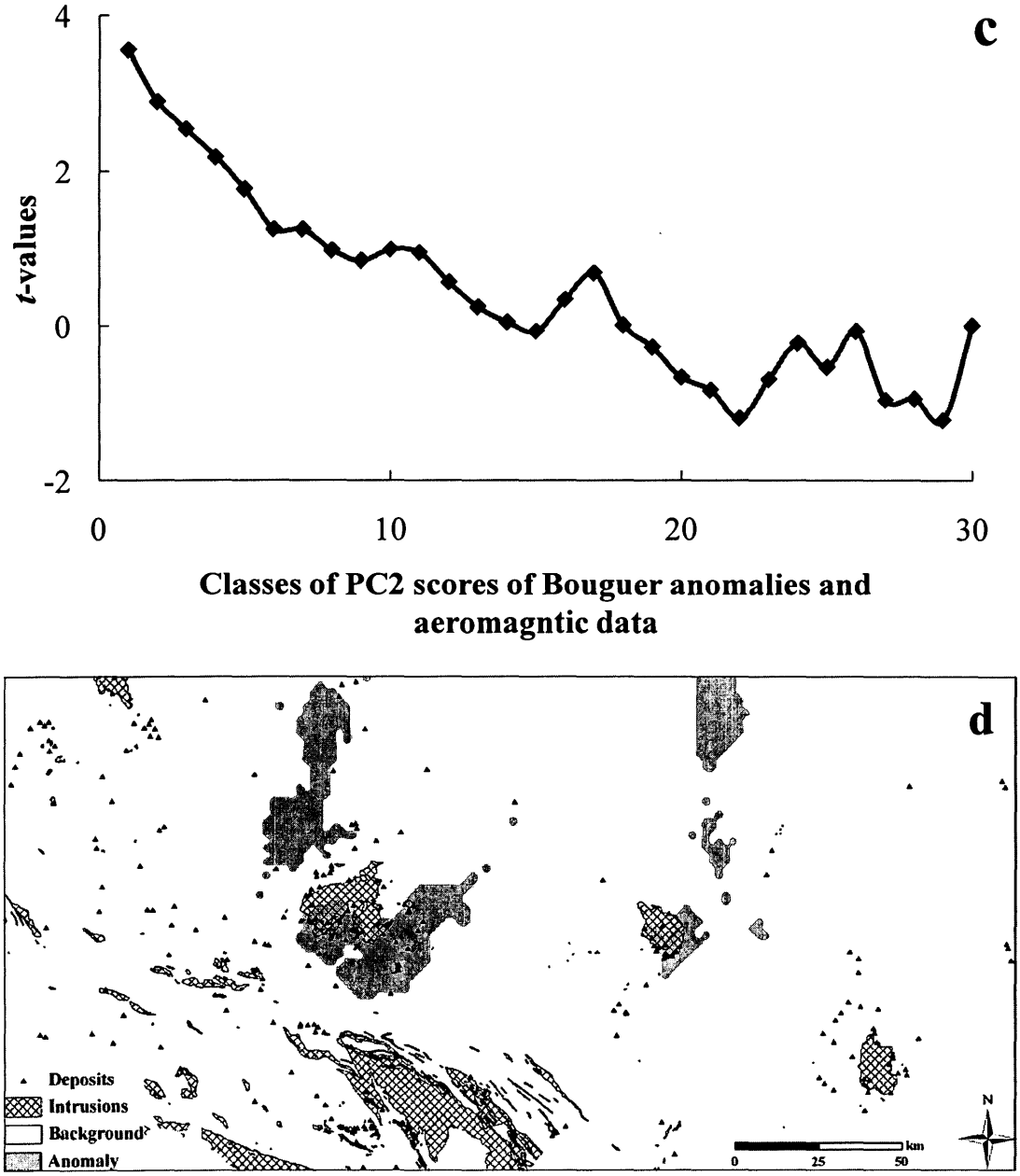

Fig. 8. 4. Geo-information extracted from geophysical data by PCA. **a:** PC2 loadings of gravity and magnetic data supporting that the PC2 can represent physical signatures of the granitic intrusions. **b:** Spatial distributions of PC2 scores of aeromagnetic and Bouguer anomalies. **c:** Student's *t*-values calculated by weights of evidence (WofE) method for measuring the spatial correlation between deposits and values of PC2 scores. **d:** Binary map of PC2 scores indicating areas highly associated with mineral occurrences.

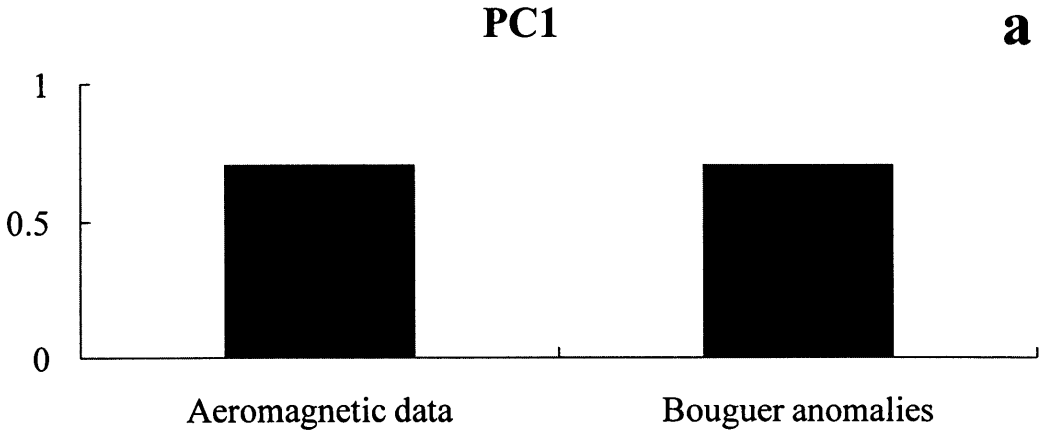
PC1
a
1
0.5
0
Aeromagnetic data
Bouguer anomalies

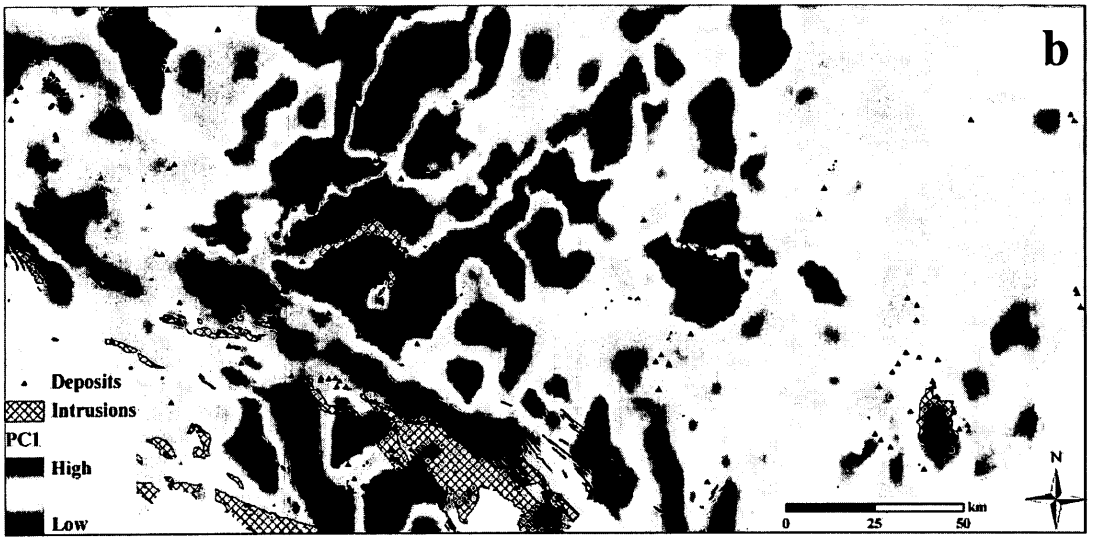
b
Deposits
Intrusions
PC1
High
Low
N
km
0
25
50

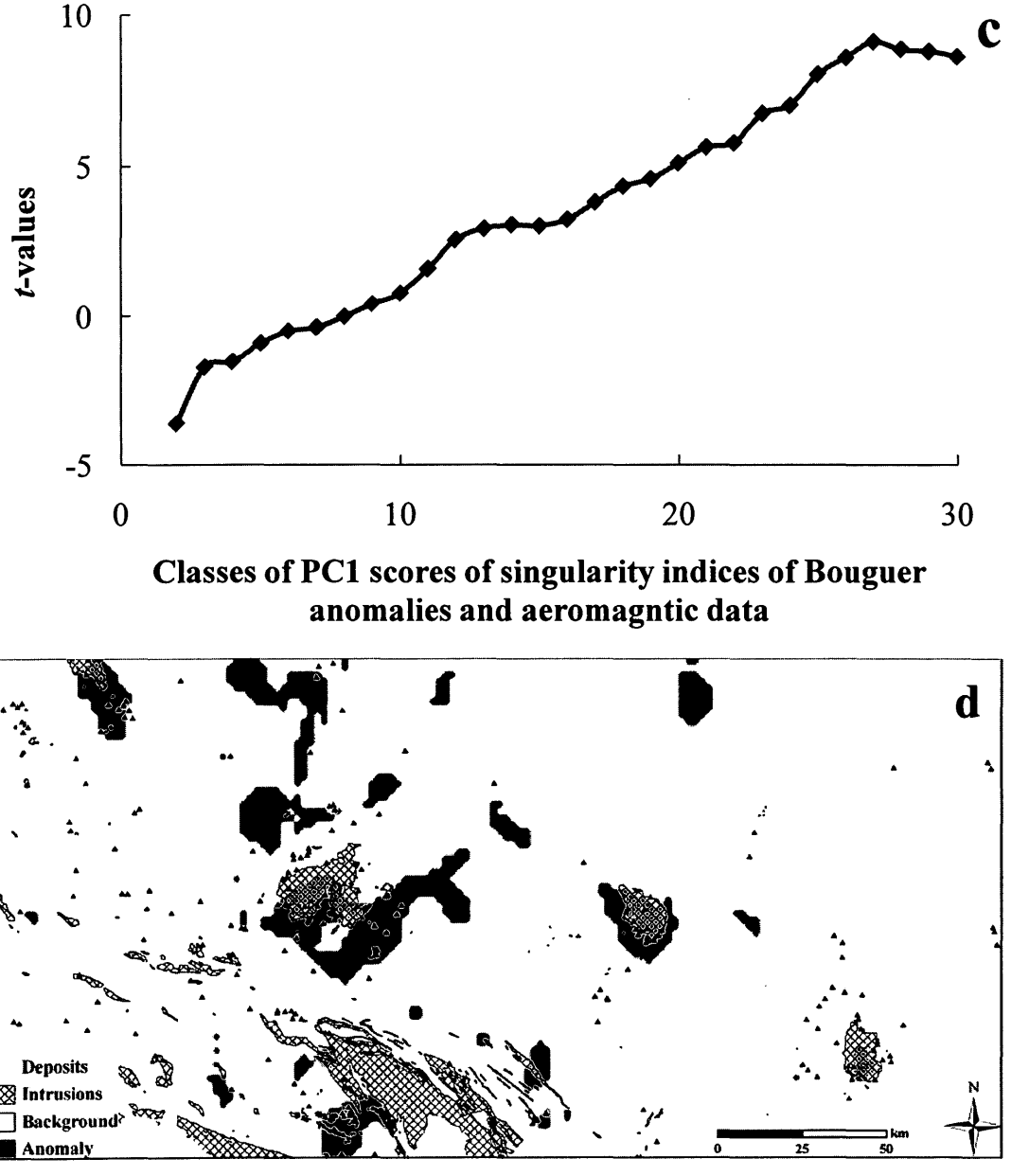

Fig. 8. 5. Geo-information extracted from singularity indices of geophysical data by PCA. **a:** PC1 loadings of singularity indices of gravity and magnetic data supporting that the PC1 can represent physical signatures of the granitic intrusions. **b:** Spatial distributions of the PC1 scores of singularity indices of aeromagnetic and Bouguer anomalies. **c:** Student's *t*-values calculated by weights of evidence (WofE) method for measuring the spatial correlation between deposits and values of the PC1 scores. **d:** Binary map of the PC1 scores indicating areas highly associated with mineral occurrences.

8.3. Geo-information Integration

After preparation, all geo-information of faults, the Gejiu formation and granitic intrusions are obtained for mineral exploration modeling. Due to the non-linear nature of mineralization and its associated geo-processes, influences of these controlling factors to the hydrothermal mineralization are diverse and varying. In addition to indicate areas with mineral potentials, all achieved geo-information are necessary to be integrated to demonstrate the variations (Fig.8.6).

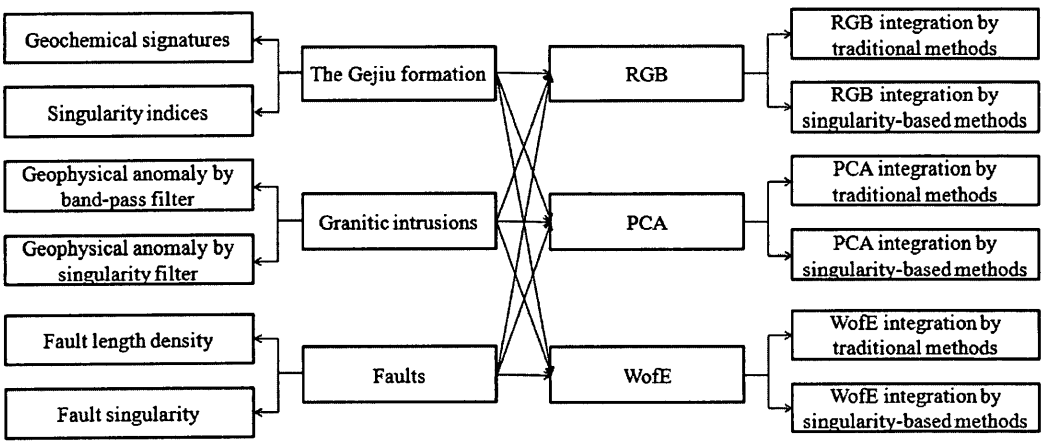

Fig. 8. 6. A concept model to indicate integration processes demonstrated in this chapter.

8.3.1 RGB composite image

As an important geo-information integration method in remote sensing, the RGB composite image of the three controlling factors is provided to exhibit mineral potentials and the influences of these controlling factors on mineralization. Before the combination, high values of all geo-information are defined to indicate presences of their

corresponding factors. Furthermore, since the former studies indicated that the hydrothermal mineralization mainly occurred within the contact zone of intrusions and wall rocks, the areas of outcrops of granitic intrusions identified from the geological map are masked from the geo-information of granitic intrusions (Figs. 8.4b and 8.5b) to indicate the buried ones. The red, green and blue transformations are applied to the geo-information of fault, the Gejiu formation and buried granitic intrusions, respectively (Fig. 8.7). According to the RGB color model, the reddish, greenish and bluish patterns imply that the hydrothermal mineralization is controlled by single corresponding factors, while the off-white patterns imply combining effects of all three controlling factors. Most of known mineral deposits located in the areas of secondary colors rather than primary colors satisfy the fact that hydrothermal mineralization was caused by interactions of multiple ore-controlling factors at specific locations, especially the bright patterns at the southeast of the Gejiu batholith demonstrating the mineralization caused by interactions of intensive influences of faults, granitic intrusions and hydrothermal alteration within the Gejiu formation. The cyan patterns as a combination of the Gejiu formation and granitic intrusions may correspond to the skarn mineralization at their contract zones caused by the emplacement of the intrusions to the carbonate strata. The magenta patterns as a combination of faults and granitic intrusions may correspond to the vein type mineralization caused by the migration of ore-bearing hydrothermal fluids within spaces produced by faults. The yellow patterns as a combination of faults and the Gejiu formation may correspond to mineralization favored spaces within the Gejiu formation produced by faults.

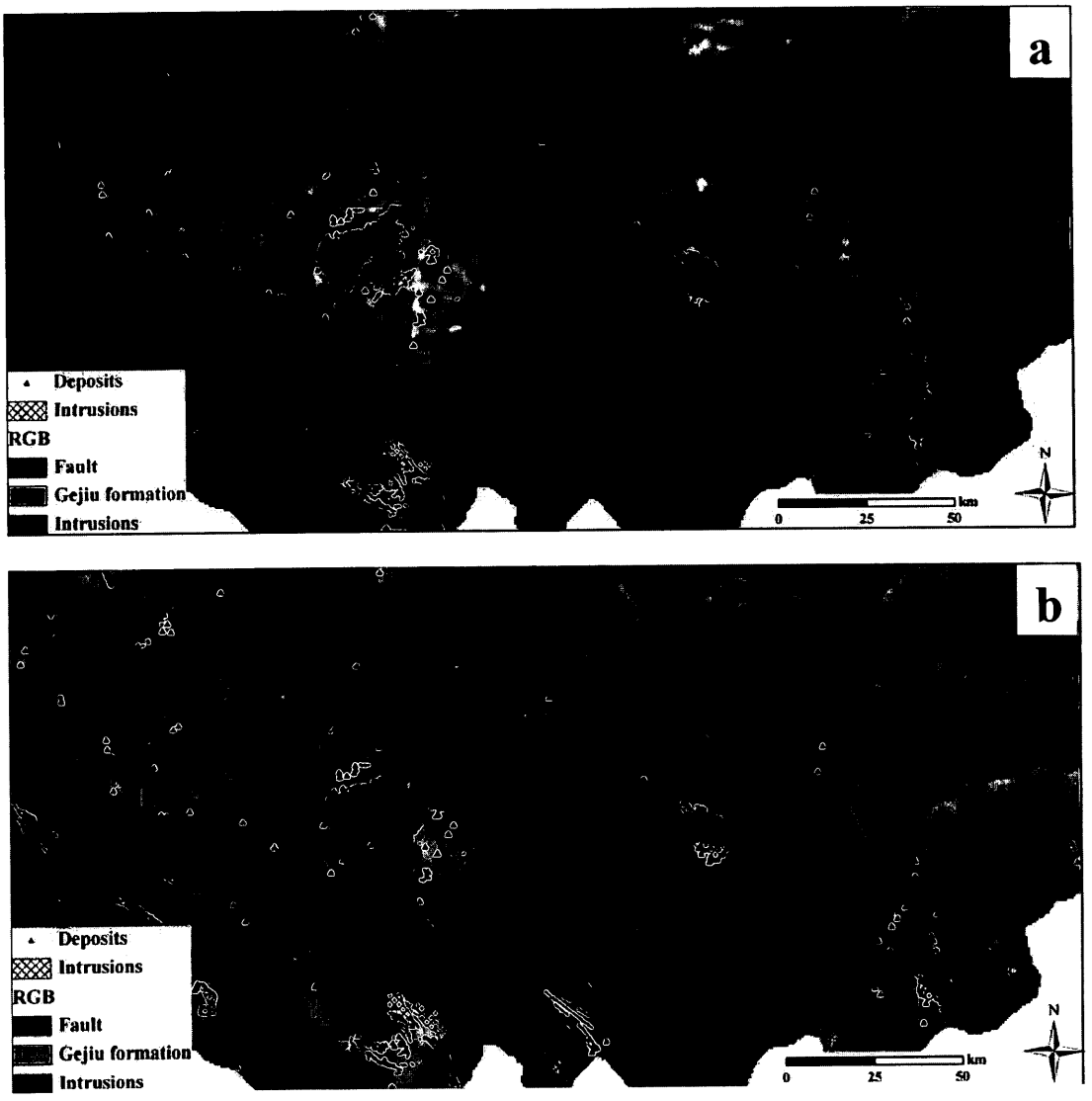

Fig. 8. 7. RGB composite images of geo-information of three controlling factors. Red, green and blue transformations are applied to geo-information of fault, the Gejiu formation and granitic intrusions, respectively. **a:** RGB image based on geo-information identified by traditional methods. **b:** RGB image based on geo-information identified by currently used singularity-based methods. Mineral occurrences and outcrops of granitic intrusions are shown for reference.

Through the comparison of these two RGB composite images, it can be noticed that the patterns by traditional methods are complicated to be interpreted. Interactions of three controlling factors are not explicit to be classified (Fig. 8.7a); whereas the singularity-based result can assist to infer the hydrothermal mineralization by interpreting interactions of three controlling factors (Fig. 8.7b). However, although the composite colors representing different combinations of the three controlling factors, current results are essentially dependent on geological interpretation to the composite color and quantitative and qualitative interpretation of mineral potentials may not be feasible to support of mineral exploration. Therefore, in addition to the RGB composite image, other integration methods are necessary to be attempted to improve the mineral exploration modeling process.

8.3.2 Principal component analysis

In former chapters, principal component analysis (PCA) as a classic multivariate analysis method were successfully applied to integrate geo-variables for characterizing controlling factors of the hydrothermal mineralization in southeastern Yunnan mineral district, China. In order to achieve an improved delineation of mineral potentials by RGB composite image, PCA is currently employed to integrate geo-information of the three controlling factors (i.e., granitic intrusions, the Gejiu formation and faults). Similar to the RGB composite image, the areas of outcrops of granitic intrusions identified from the geological map are masked off from the geo-information of granitic intrusions as well.

Therefore, the three sets of geo-information integrated by PCA in this section are spatial distributions of buried granitic intrusions, the Gejiu formation and faults, respectively.

Table 8. 3 Results of PCA of three controlling factors identified by traditional methods.

Principal Components (PCs)	PC1	PC2	PC3
Component variance (Eignvalues)	1.37	0.91	0.72
Standard Deviation	1.17	0.95	0.85
Relative Importance of Components	0.46	0.30	0.24
Cumulative Importance of Components	0.46	0.76	1.00

For the geo-information identified by traditional methods, high values of the Gejiu formation and faults indicate presences of their corresponding controlling factors, while low values of the granitic intrusions indicate the presence of their corresponding factor. Applying PCA to the geo-information identified by traditional methods, results in Table 8.3 indicate that the PC1 with an eignvalue greater than 1 can be retained for further analysis (Kaiser, 1960). The loadings of the three sets of geo-information in PC1 support that low scores of PC1 are qualified to describe interactions of the three controlling factors which illustrate the spatial distribution of mineral potentials of the study area (Fig. 8.8). From the patterns (Fig. 8.8b), mineral occurrences are well correlated with the areas with low scores.

Table 8. 4 Results of PCA of three controlling factors identified by singularity-based methods.

Principal Components (PCs)	PC1	PC2	PC3
Component variance (Eignvalues)	1.13	0.99	0.88
Standard Deviation	1.06	0.99	0.94
Relative Importance of Components	0.38	0.33	0.29
Cumulative Importance of Components	0.38	0.71	1.00

For the geo-information identified by singularity-based methods, low values of the Gejiu formation and faults indicate presences of their corresponding controlling factors, while high values of granitic intrusions indicate the presence of their corresponding controlling factor. Applying PCA to the three sets of geo-information, the results in Table 8.4 indicate that the PC1 with an eignvalue greater than 1 can be retained for further analysis. According to the loadings of the three factors in PC1, the low scores are accepted as indicators to the mineral potentials in the study areas (Fig. 8.9). From the patterns (Fig. 8.9b), mineral deposits are well correlated with areas with low scores.

Comparing two spatial distributions of mineral potentials (Figs. 8.8b and 8.9b), there are some improvements of the result by singularity-based methods. First of all, the currently achieved result is more remarkable. Some overestimated and underestimated mineral potentials by traditional methods are confined by singularity-based methods. It well demonstrates the advantages of singularity index mapping technique in separating geo-anomalies from both high and weak background. Secondly, the singularity-based result is more interpretable to the process of hydrothermal mineralization because singularity indices integrated by PCA characterize geochemical behaviors associated to various geo-processes. From the patterns (Fig. 8.9b), spatial distributions of mineral potentials (i.e., low scores) satisfy that the granitic intrusions provided heat and metal resources; ore-forming fluids migrated within the space produced by faults; and the hydrothermal mineralization occurred at the mineralization-favored locations within the contract zones of the granitic intrusions and the Gejiu formation. In contrary, such inference is not easy

to be clarified by the spatial distributions of mineral potentials from traditional methods identified geo-information (Fig, 8.8b).

If currently achieved PCA results are compared with RGB composite images demonstrated in the last section, some differences among these results are worth to be discussed. First, mineral potentials delineated by PCA results are more explicit. The results can be used independently, whereas RGB composite images were dependent on interpretation to various composite colors. Second, as introduced formerly, the hydrothermal mineralization in the study area was caused by the interactions of its controlling factors at the specific locations, whereas the PCA results cannot indicate these interactions properly. Mineralization favored areas supported by all sets of geo-information are integrated without ranking them in any orders to demonstrate the degrees that each controlling factor contributed to the hydrothermal mineralization. In other words, the PCA results can depict the comprehensive mineral potentials efficiently, but necessary interpretable geological meanings to the mineralization are not supported sufficiently. Therefore, in order to achieve a quantitatively, qualitatively and easily interpretable result, more integration methods need to be attempted.

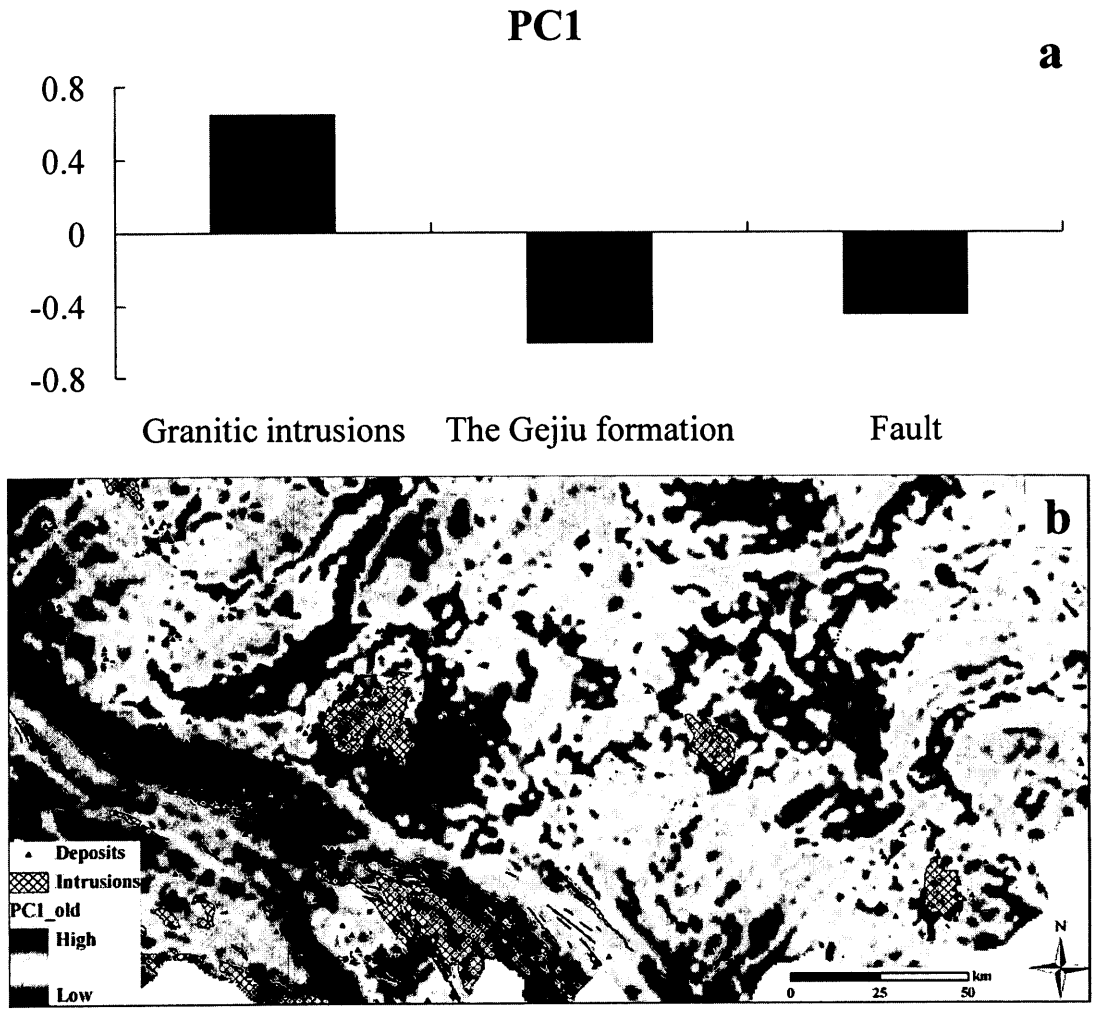

Fig. 8. 8. Applications of PCA to integrate geo-information identified by traditional methods. **a:** Loadings of each controlling factors in PC1 supporting that PC1 corresponding to mineral potentials. **b:** Scores of PC1 indication the mineral potentials.

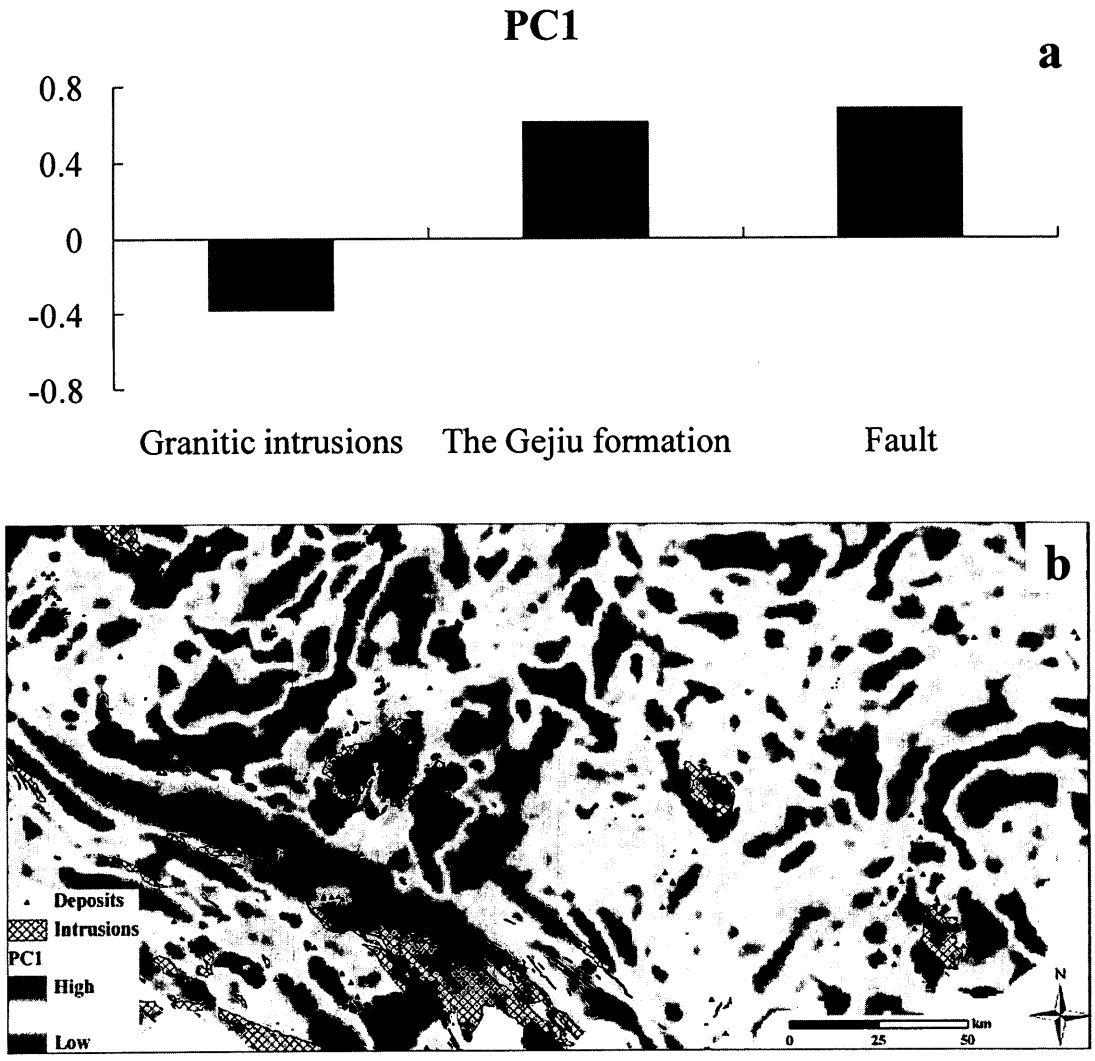

Fig. 8. 9. Applications of PCA to integrate geo-information identified by singularity-based methods. **a:** Loadings of each controlling factors in PC1 supporting that PC1 corresponding to mineral potentials. **b:** Scores of PC1 indicate mineral potentials.

8.3.3 Weights of evidence

Based on the Bayesian probability theory, weights of evidence (WofE) can map mineral potentials in areas where a number of occurrences were discovered. As introduced in former sections of this chapter, areas highly associated with the hydrothermal

mineralization had been identified by student's *t*-values from geo-information of the three controlling factors. As shown in the pre-defined binary maps (Figs. 5.7, 8.2, 8.3, 8.4, and 8.5), green patterns are the mineralization favored space supported by their corresponding controlling factors, respectively. By the WofE method, all of these binary patterns with explicit geological meanings are combined. Indications of integrated patterns to the hydrothermal mineralization can be interpreted according to the combinations of controlling factors (i.e., qualitatively and easily interpretable). Furthermore, the Bayesian theory-based WofE method can calculate the posterior probability of the hydrothermal mineralization for all patterns within the areas based on the prior probability of mineral occurrences in the study area (i.e., quantitatively interpretable).

For the integration of geo-information identified by traditional methods, three sets of geo-information are integrated and the specific interactions of certain controlling factors are easily to be interpreted (Table 8.5). Furthermore, applying the formulas introduced in the chapter of methodology to the parameters in Table 8.5, posterior probabilities of patterns of all combinations are calculated based on a prior probability of 0.017 for mineral deposit occurrence. The spatial distributions of posterior probabilities well demonstrate the hydrothermal mineralization-favored spaces, and can be interpreted either quantitatively or qualitatively (Fig. 8.10a). Similarly, three sets of geo-information identified by singularity-based methods are integrated and the posterior probabilities of patterns of all combinations are calculated as well (Table 8.6). Simultaneously, the spatial distributions of posterior probabilities indicate favorability of certain areas to hydrothermal mineralization in the study area (Fig. 8.10b).

When results from geo-information identified by both traditional methods and singularity-based methods are evaluated by the prior probability (i.e., 0.017) of the hydrothermal mineralization, patterns of three controlling factors are present (Fig. 8.10) where posterior probabilities of two results are nearly 18 and 25 times greater than the prior probability, respectively (Tables 8.5 and 8.6). It indicates that both results are meaningful and the three sets of singularity-based geo-information provide a more explicit result. Furthermore, comparing the spatial distributions of integrated patterns of two results, it can be noticed that mineral potentials by the singularity-based result (Fig. 8.10b) are more informative than the traditional methods-based result (Fig. 8.10a). Areas with mineral occurrences located which were indicated as low or non-favorable to mineralization by traditional methods (Fig. 8.10a) are now inferred as targets with high mineral potentials by singularity-based methods (Fig. 8.10b). All of these facts further demonstrate the efficiency of singularity index mapping technique in separating anomalies from both weak and strong background.

In comparison with the results of RGB composite image (Fig. 8.7) and PCA (Figs. 8.8 and 8.9), the newly achieved spatial distributions of posterior probabilities not only describe qualitatively interactions of controlling factors to mineralization but also indicate quantitatively probabilities of mineral deposit occurrence at different locations. Therefore, in addition to informative integration results by the RGB composite image and the PCA, the WofE provides improved results to indicate mineral potentials in a more straightforward and informative way. The following mineral exploration can be guided by geological meanings of integrated patterns and corresponding posterior probabilities.

Table 8. 5 Weights of evidence method (WofE) for integrating geo-information identified by traditional methods.

Patterns	Areas	Number of mineral occurrences	W^+	S^+	W^-	S^-	$C=W^+-W^-$	S(C)	T=C/S(C)
Gejiu	229	17	1.97	0.15	-0.23	0.08	2.2	0.17	12.73
Intrusions	576	21	0.77	0.22	-0.06	0.07	0.83	0.23	3.55
Fault	677	15	0.16	0.09	-0.22	0.11	0.38	0.14	2.63

Patterns	Posterior probability	Posterior/prior
Background	0.010	0.60
Granitic intrusions	0.023	1.38
Fault	0.015	0.88
Granitic intrusions and fault	0.034	2.01
Gejiu	0.092	5.42
Gejiu and granitic intrusions	0.211	12.43
Gejiu and Fault	0.135	7.92
Integration anomaly	0.309	18.17

Table 8. 6 Weights of evidence method (WofE) for integrating geo-information identified by singularity-based methods.

Patterns	Areas	Number of mineral occurrences	W^+	S^+	W^-	S^-	$C=W^+-W^-$	S(C)	T=C/S(C)
Gejiu	386	42	1.94	0.16	-0.2	0.08	2.14	0.18	11.81
Intrusions	258	10	1.2	0.14	-0.24	0.08	1.44	0.16	9.09
Fault	658	11	0.10	0.08	-0.23	0.13	0.34	0.16	2.14

Patterns	Posterior probability	Posterior/prior
Background	0.009	0.53
Granitic intrusions	0.037	2.18
Fault	0.012	0.71
Granitic intrusions and fault	0.051	3.00
Gejiu	0.074	4.35
Gejiu and granitic intrusions	0.312	18.35
Gejiu and Fault	0.114	6.71
Integration anomaly	0.434	25.53

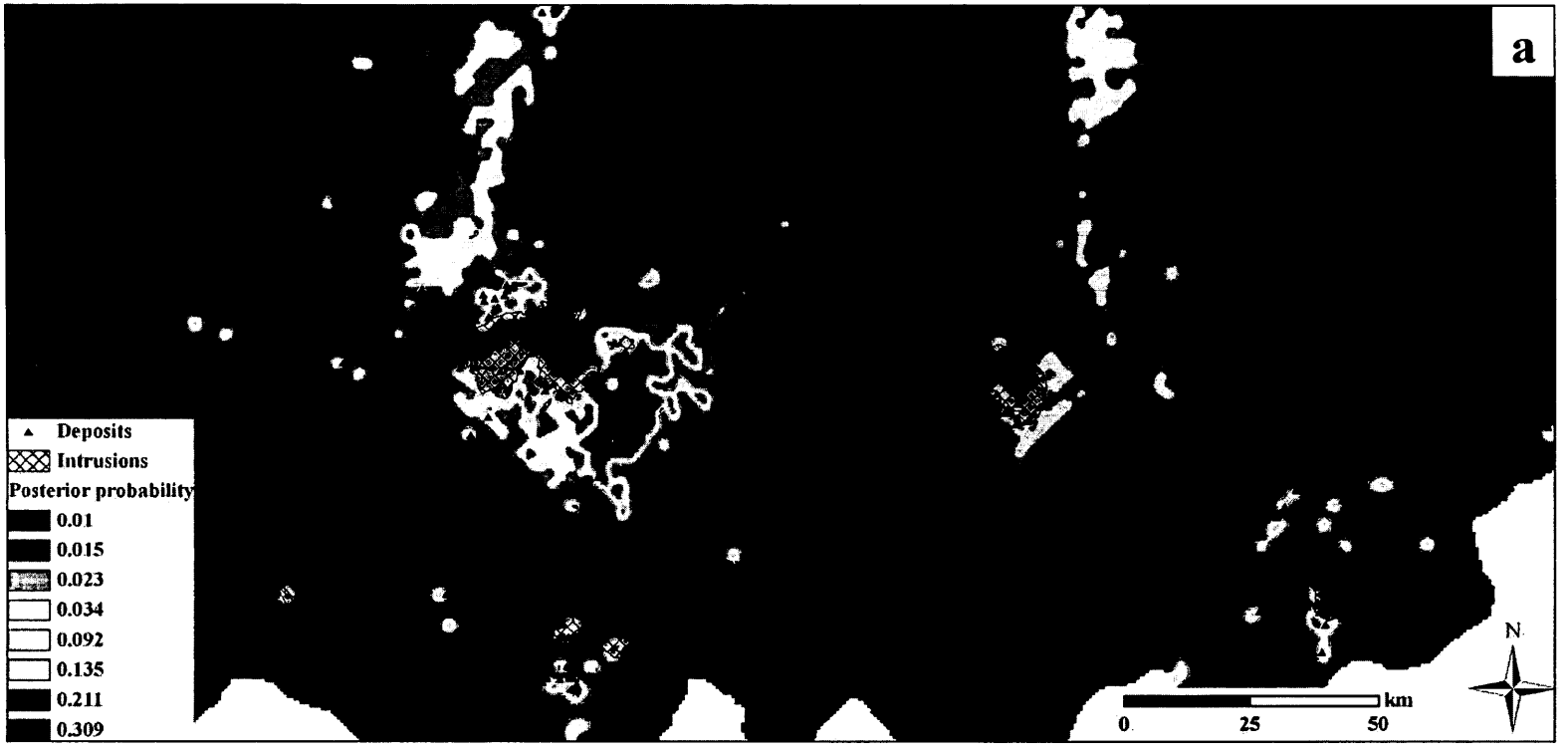
a
Deposits
Intrusions
Posterior probability
0.01
0.015
0.023
0.034
0.092
0.135
0.211
0.309
N
km
0
25
50

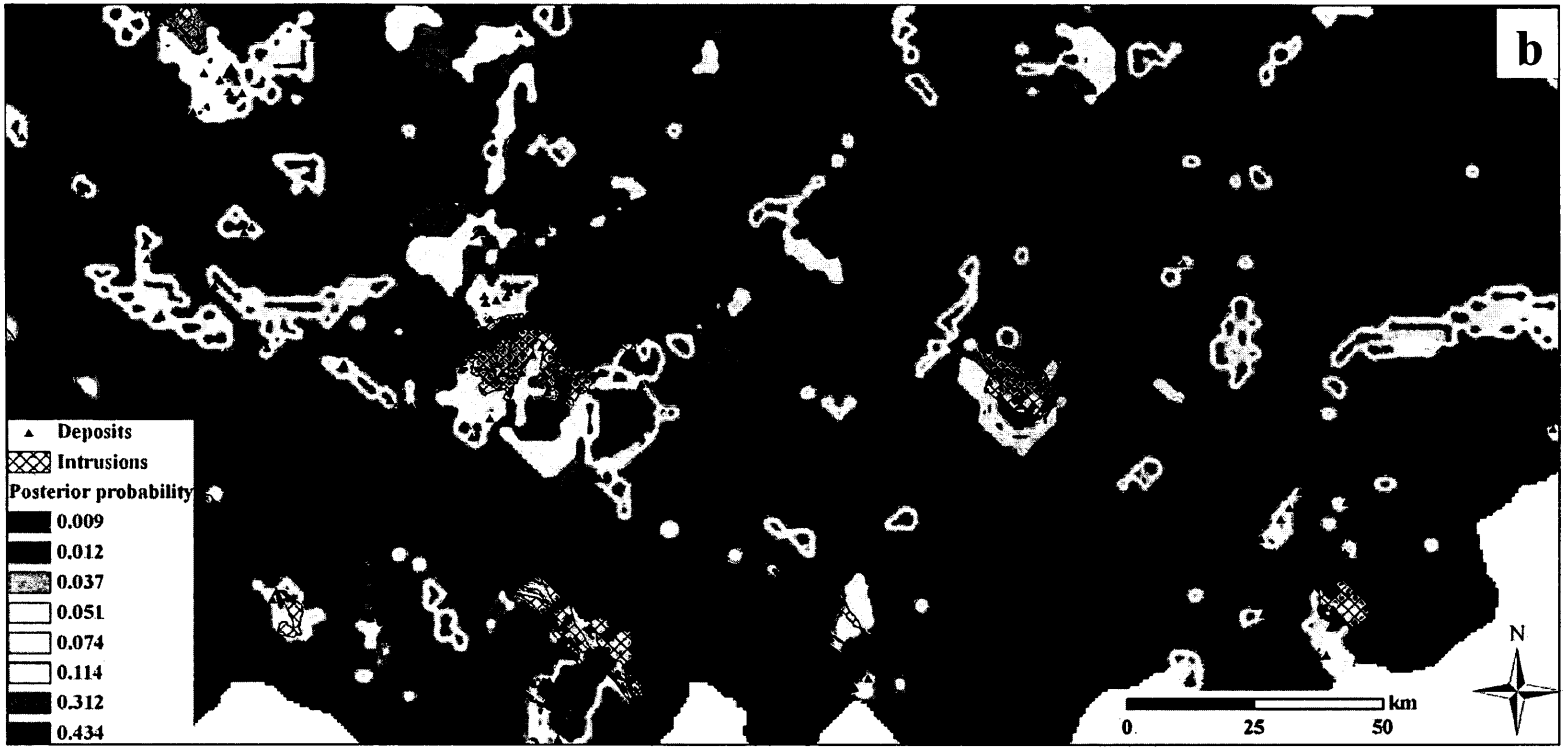

Fig. 8. 10. Applications of WofE to mapping mineral potentials. **a:** Posterior probability of mineralization by geo-information identified by traditional methods. **b:** Posterior probability of mineralization indicated by geo-information identified by singularity-based methods.

8.4. Discussions

In this chapter, the student's *t*-test is used to define binary patterns with highest spatial association with mineral occurrences. Normally, the *t*-test is applied only to evaluate if the spatial relationship between a point pattern and a map pattern is statistically significant at the 5% or 1% significance level. This is equivalent to test if the estimated *t*-value is greater than 2 or 3. However, there are some large student's *t*-values as obtained in current example (Table 8.5) which might be related to the selection of sample size. However, our previous experiments (Zhao et al, 2012) with multiple sample size demonstrated that the *t*-value decreases with increasing sample sizes while the threshold is relatively stable. Therefore, in this study, to delineate areas highly associated with mineralization supported by their corresponding controlling factors, these binary patterns are currently accepted, and more detailed investigations regarding the student's *t*-test will be implemented in future work.

Geo-information of three controlling factors of the hydrothermal mineralization identified by both traditional and singularity-based methods is integrated to delineate mineral potentials of southeastern Yunnan mineral district, China. Integration methods consisting of RGB composite image, PCA and WofE are employed. Among these results, the ones by integrating singularity-based geo-information well demonstrate the advantages of this technique in characterizing geo-anomalies.

For the results by RGB composite images, combinations of controlling factors indicating mineralization favored spaces can be interpreted from composite colors directly; however, due to the complicated patterns of secondary colors, mineralization caused by various interactions of the controlling factors cannot be clarified properly. Furthermore, the interpreted interactions of controlling factors cannot be further quantified to describe the mineral potentials. For the results by PCA, although mineral potentials can be indicated more explicitly and comprehensively than the RGB composite images, interactions of controlling factors contributed to the hydrothermal mineralization cannot be depicted and the delineation is not quantitative. As a further attempted integration method, the WofE provides the most significant results, by which delineations are both quantitatively and qualitatively interpretable to map the mineral potentials of the study area. Comparing results by three integration methods, the WofE possesses advantages of RGB (i.e., explicit geological meanings) and PCA (i.e., explicit delineation), simultaneously. Further, mineral potentials are described in forms of posterior probability of occurrence of hydrothermal mineralization that is a meaningful improvement in comparison with the other two methods. Therefore, the result of the WofE by integrating singularity-based geo-information is accepted as the final result by the mineral exploration modeling in support of the future mineral exploration in southeastern Yunnan mineral district, China.

As repeatedly introduced in former chapters, mineralization is a complex non-linear geo-process associated with various geological activities. Geological activities or controlling factors analyzed in current study are three general factors (i.e., faults, granitic intrusions and ore-bearing strata). Currently achieved mineral potentials are from a regional

prospective. More detailed controlling factors or geological activities which are not involved in this study will be considered in localized areas. Their associated geo-exploratory datasets will be collected and analyzed in future work.

Chapter 9. Discussions and conclusions

The three main objectives introduced in the chapter 1 to characterize the non-linear properties of singular geo-processes associated with the hydrothermal mineralization, to depict spatial distributions of ore controlling factors, and to map mineral potentials in Southeastern Yunnan Sn-Cu polymetallic mineral district, China had been achieved according to a series of geo-information extraction and integration methods, respectively. Furthermore, limitations regarding scale dependence in geophysical data analysis, less descriptive to spatial variations of geological signatures, insufficient concerns to geological features in geochemical data analysis are improved as well. In this dissertation, the general mineral exploration modeling process producing an improved indication to mineral potentials well demonstrates advantages of these spatial analysis methods in geological exploration.

In the aspect of geo-anomaly (i.e., geo-information) extraction, singularity index mapping technique are currently used to characterize spatial variations of physical and/or chemical signatures of mineralization associated geological bodies (i.e., controlling factors) which were traditionally identified simply based on the location information of geological occurrences. Limitations regarding to the scale dependence of band-pass filter for identifying the granitic intrusions are rectified by using the singularity method. Furthermore, extracted by the singularity method and integrated by PCA, recognized geochemical anomalies which were mainly used to delineate spatial distributions of

mineralization associated geochemical signatures are innovatively used to characterize the geochemical signatures of the Gejiu formation. The result well indicates the mineralization favored positions within the Gejiu formation. The application of advanced geochemical anomaly extraction methods which were mainly to investigate ore-forming elements is currently extended to analyze geological features associated with mineralization. In chapter 5, areas favorable to the hydrothermal mineralization are delineated by characterizing spatial variations of physical distributions of fault traces. The result is more beneficial to describe favorable spaces for mineralization produced by the non-linear fault activities. In conclusion, geo-information of the three controlling factors identified by singularity index mapping technique is more quantitatively and qualitatively interpretable to the spatial variations of physical or chemical properties. The quantification of the influence of the controlling factors on the hydrothermal mineralization will benefit further mineral exploration. In addition, geological features measured by different observations were expressed in various units. By singularity methods, characterized geological features can be described uniformly that greatly improves the interpretation of these geological features.

In the aspect of geo-anomaly integration, although RGB as an intuitive integration is not convenient to delineate mineral potentials, interactions of the controlling factors can still be interpreted from the composite map (i.e., geologically interpretable). It might be the first time to use the RGB composite image to map mineral potentials in the study area. In this dissertation, PCA commonly used to characterize ore-forming element associations is firstly applied to integrate the geo-information of controlling factors for mineral potential

mapping in southeastern Yunnan mineral district, China. Based on correlations of the three controlling factors, PCA is used to integrate the three sets of geo-information, result of which is evaluated to delineate spatial distributions of mineral potentials. However, although the result well demonstrates the mineralization favored areas supported by its associated geological activities, interactions of these factors cannot be interpreted or described through the integration, approximately. To solve the problems aroused by using both RGB and PCA methods, the WofE method is applied to map the mineral potentials, the result of which not only qualitatively describe the interactions of the controlling factors but also quantitatively describe the mineral potentials by providing posterior probabilities. Therefore, the WofE is chosen as the geo-information integration method of the mineral exploration modeling in this dissertation.

In addition to the extraction and integration involved in the mineral exploration modeling, this dissertation newly introduces a fault trace-oriented singularity index mapping method, and it is applied to characterize the controlling anisotropic effects of faults to the hydrothermal mineralization. Although the geo-information is not further used in mapping mineral potentials, the case study of the new method well demonstrates the application of the idea of geo-information integration, by which spatial information of faults and geochemical signatures are used jointly for characterizing interactions of tectonic activities and mineralization. According to the case study, a new attribute of fault traces is defined based on the identified anisotropic controlling effects of faults to the mineralization.

In comparison with the traditional method-based modeling process, the singularity-based mineral exploration modeling process using quantitatively and qualitatively characterized spatial variations of the controlling factors as main components provides more explicit mineral potentials to support future exploration in the study area. Since only three general controlling factors of the hydrothermal mineralization are selected, the result is accordingly to be regional. For more detailed spatial distributions of mineral potentials at local scale, additional localized controlling factors and geo-exploratory datasets with higher resolution are necessary to be analyzed.

Several issues (e.g., data quality, errors in modeling process, etc.) can cause spatial analysis results with uncertainties that should be kept in mind. In current study, there are several ways to investigate the uncertainty. In the aspect of geo-information extraction, spatial distributions of R^2 and standard deviation of estimated singularity indices of Bouguer anomalies, aeromagnetic and fault traces are supplied in Appendix to evaluate the uncertainties of geo-information extraction. In the aspect of geo-information integration, student's *t*-test is employed to define binary patterns: one for geological features and the other for background. The student's *t*-test defines an optimal threshold separating patterns highly associated with mineralization from the other patterns indicative to geological features with uncertainties. In addition to the treatments implemented in this study, the uncertainty can be investigated quantitatively as well. Therefore, evaluating uncertainty by means of mathematical approaches will be discussed in my future work.

Appendix


Deposits
Intrusions
High : 1
Low : 0.99


Deposits
Intrusions
High : 0.21
Low : 0


Deposits
Intrusions
High : 1
Low : 0.99

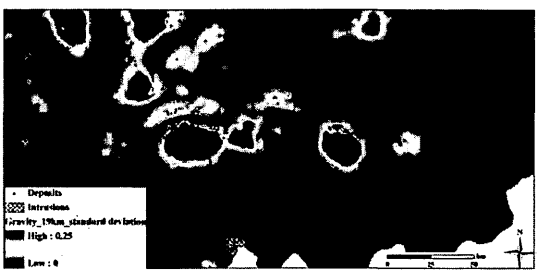
Deposits
Intrusions
High : 0.25
Low : 0


Deposits
Intrusions
High : 1
Low : 0.99

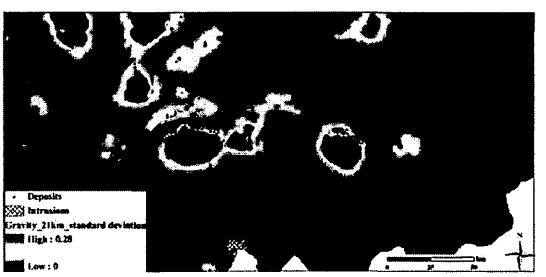
Deposits
Intrusions
High : 0.29
Low : 0


Deposits
Intrusions
High : 1
Low : 0.99


Deposits
Intrusions
High : 0.31
Low : 0

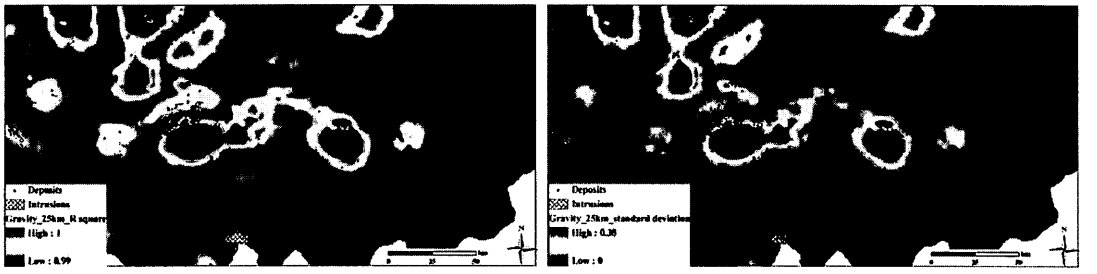

Fig. A. 1. Spatial distributions of *R* square and standard deviation of estimated singularity index of Bouguer anomalies.

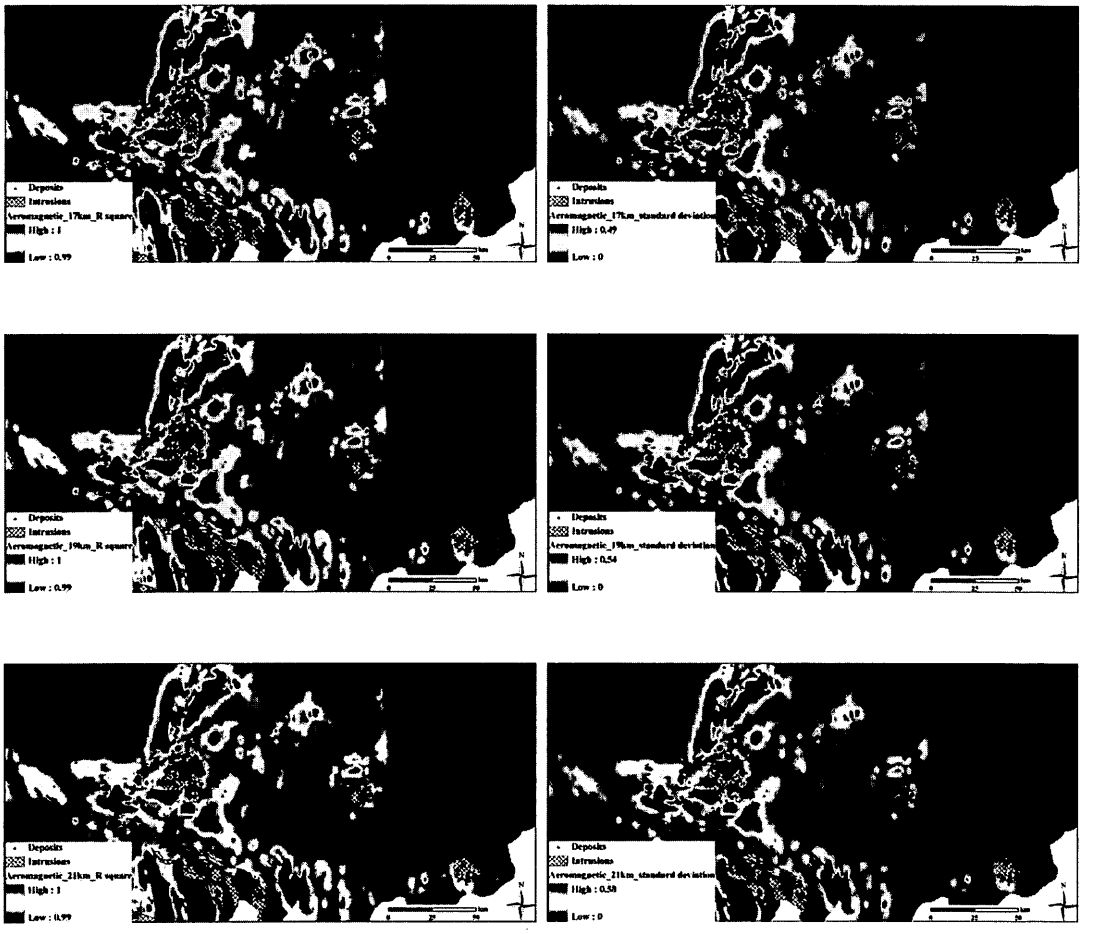

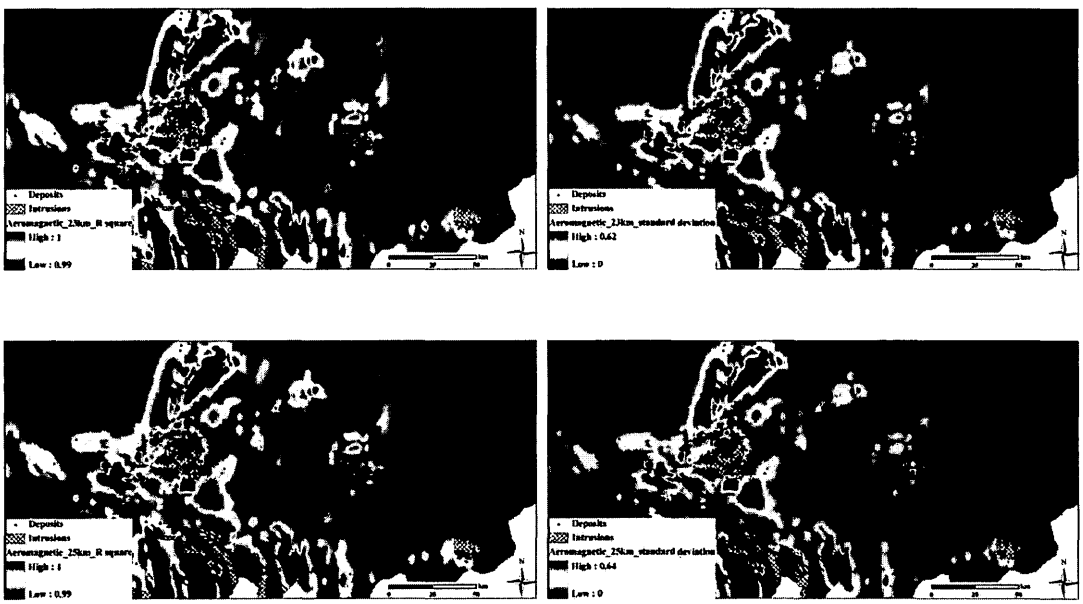

Fig. A. 2. Spatial distributions of *R* square and standard deviation of estimated singularity index of RTP transformed aeromagnetic data.

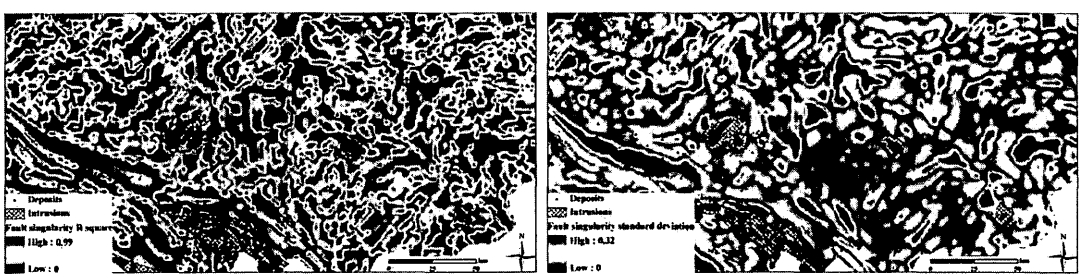

Fig. A. 3. Spatial distributions of *R* square and standard deviation of estimated singularity index of RTP transformed aeromagnetic data.

References

Agarwal, B. N. P., Sivaji, CH., 1992. Separation of regional and residual anomalies by least-squares orthogonal polynomial and relaxation techniques: a performance evaluation. Geophysical Prospecting 40, 143-156.

Agterberg, F.P., 1989. Computer programs for mineral exploration. Science 245, 76-81.

Agterberg, F.P., 1992. Combining indicator patterns in weights of evidence modeling for resource evaluation. Natural Resources Research 1, 39-50.

Agterberg, F.P., 1994. Fractals, multifractals and change of support. In: Dimitrakopoulos, R. (Ed.), Geostatistics for the Next Century, Kluwer, Dordrecht, pp. 223-234.

Agterberg, F.P., 1995. Multifractal modeling of the sizes and grades of giant and supergiant deposits. International Geology Review 37, 1-8.

Agterberg, F.P., 2012a. Sampling and analysis of chemical element concentration distribution in rock units and orebodies. Nonlinear Processes in Geophysics 19, 23-44.

Agterberg, F.P., 2012b. Multifractals and geostatistics. Journal of Geochemical Exploration 122, 113-122.

Agterberg, F.P., Bonham-Carter, G.F. and Wright, D.F., 1990. Statistical pattern integration for mineral exploration. In: Gaal, G. and Merriam, D.F. (Eds.), Computer applications in resource exploration, prediction and assessment for metals and petroleum. Pergamon Press, Oxford, pp. 1-21.

Agterberg, F.P., Cheng, Q., Brown, A., Good, D., 1996. Multifractal modeling of fractures in the Lac Du Bonnet Batholith, Manitoba. Computer & Geosciences 22, 497-507.

Ali, K., 2005. Application of GeoDAS and other advanced GIS technologies for modeling stream sediment geochemical distribution patterns to assess gold resources potential in Yunnan Province, South China. M.Sc. Thesis, York University, 166 pp.

Ali, K., Cheng, Q., Li, W. and Chen, Y., 2006. Multi-element association analysis of stream sediment geochemistry data for predicting gold deposits in south-central Yunnan Province, China. Geochemistry-Exploration Environment Analysis 6, 341-348.

An, P., Moon, W.M., Rencz, A.N., 1991. Application of fuzzy theory for integration of geological, geophysical and remotely sensed data. Canadian Journal of Exploration Geophysics 27, 1-11.

Bhattacharyya, B. K., 1965. Two-dimensional harmonic analysis as a tool for magnetic interpretation. Geophysics 30, 829-857.

Bonham-Carter, G.F., 1994. Geographic Information Systems for Geoscientists: Modelling with GIS. Computer Methods in the Geosciences, first ed. Pergamon, New York.

Bonham-Carter, G.F., Agterberg, F.P., Wright, D.F., 1989. Weights of evidence modelling: a new approach to mapping mineral potential. In: Agterberg, F.P. and Bonham-Carter, G.F. (Eds), Statistical Applications in the Earth Sciences. Geological Survey of Canada, pp. 171-183.

Carranza, E.J.M., 2004. Weights of evidence modeling of mineral potential: a case study using small number of prospects, Abra, Philippines. Nature Resources Research 13, 173-187.

Carranza, E.J.M., 2008. Geochemical Anomaly and Mineral Prospectivity Mapping in GIS. Handbook of Exploration and Environmental Geochemistry, vol. 11. Elsevier, Amsterdam.

Carranza, E.J.M., Hale, M., 2001. Geologically constrained fuzzy mapping of gold mineralization potential, Baguio district, Philippines. Natural Resources Research 10, 125-136.

Carranza, E.J.M., Owusu, E.A., Hale, M., 2009. Mapping of prospectivity and estimation of number of undiscovered prospects for lode gold, southwestern Ashanti Belt, Ghana. Mineralium Deposita 44, 915-938.

Carranza, E.J.M., Sadeghi, M., 2010. Predictive mapping of prospectivity and quantitative estimation of undiscovered VMS deposits in Skellefte district (Sweden). Ore Geology Reviews 38, 219-241.

Chen, X., Lin, Z., Xie, F., 1998. Geological and geochemical characteristics of the Bainiuchang superlarge silver polymetallic deposits of superimposed mineralization, Yunnan province. Scientia Geologica Sinica 33, 115-123. (in Chinese with English abstract)

Cheng, Q., 1999. Multifractality and spatial statistics. Computer&Geosciences 25, 949-961.

Cheng, Q., 2000. GeoData Analysis System (GeoDAS) for Mineral Exploration: User's Guide and Exercise Manual. Material for the Training Workshop on GeoDAS held at York University, Toronto, Canada. 204 p.

Cheng, Q., 2000. GeoData Analysis System (GeoDAS) for mineral exploration: user's guide and exercise manual. Material for the Training Workshop on GeoDAS held at York University, Toronto, Canada.

Cheng, Q., 2006. GIS based fractal/multifractal anomaly analysis for modeling and prediction of mineralization and mineral deposits. In: Harris, J.R. (Ed.), GIS for the Earth Sciences. Geological Association of Canada, St. John's, Newfoundland, pp. 285-296.

Cheng, Q., 2007a. Mapping singularities with stream sediment geochemical data for prediction of undiscovered mineral deposits in Gejiu, Yunnan Province, China. Ore Geology Reviews 32, 314-324.

Cheng, Q., 2007b. Multifractal imaging filtering and decomposition methods in space, Fourier frequency, and eigen domains. Nonlinear Process Geophysics 14, 293-303.

Cheng, Q., 2008. Non-Linear Theory and Power-Law Models for Information Integration and Mineral Resources Quantitative Assessments. Mathematical Geosciences 40, 503-532.

Cheng, Q., 2011. Singularity modeling of geo-anomalies and recognition of anomalies caused by buried sources. Earth Science-Journal of China University of Geosciences 39, 307-316. (in Chinese with English abstract)

Cheng, Q., 2012. Singularity theory and methods for mapping geochemical anomalies caused by buried sources and fore predicting undiscovered mineral deposits in covered areas. Journal of Geochemical Exploration 122, 55-70.

Cheng, Q., Agterberg, F.P., 1999. Fuzzy weights of evidence method and its application in mineral potential mapping. Natural Resources Research 8, 27-35.

Cheng, Q., Agterberg, F.P., 2009. Singularity analysis of ore-mineral and toxic trace elements in stream sediments. Computers & Geosciences 35, 234-244.

Cheng, Q., Agterberg, F.P., Ballantyne, S.B., 1994. The separation of geochemical anomalies from background by fractal methods. Journal of Geochemical Exploration 51, 109-130.

Cheng, Q., Bonham-Carter, G., Wang, W., Zhang, S., Li, W., Xia, Q., 2011. A spatially weighted principal component analysis for multi-element geochemical data for mapping locations of felsic intrusions in the Gejiu mineral district of Yunnan, China. Computer&Geosciences 37, 662-669.

Cheng, Q., Li, L., Wang, L., 2009. Characterization of peak flow events with local singularity method. Nonlinear Processes in Geophysics 16, 503-513.

Cheng, Q., Xia, Q., Li, W., Zhang, S., Chen, Z., Zuo, R., Wang, W., 2010. Density/area power-law models for separating multi-scale anomalies of ore and toxic elements in stream sediments in Gejiu mineral district, Yunnan Province, China. Biogeosciences 7, 3019-3025.

Chung, C.F., Agterberg, F.P., 1980. Regression-Models for estimating mineral-resources from geological map data. Journal of the International Association for Mathematical Geology 12, 473-488.

Cianciara, B., Marcak, H., 1979. Geophysical anomaly interpretation of the potential fields by means of singular points method and filtering. Geophysical Prospecting 27, 251-260.

Cooper, G. R. J., Cowan, D. R., 2005. Differential reduction to the pole. Computer&Geosciences 31, 989-999.

Cui, Y., 2000. Geological characteristics of No.18-2 tin-bearing granite of Kafang ,Yunxi, its ore-forming genesis and prospecting direction. Mineral Resources and Geology, 14, 175-177. (in Chinese)

Dai, F., 1990. Regional distribution pattern of Sn-bearing polymetal deposits in southeastern Yunnan. Geology and Prospecting 1990, 17-21. (in Chinese with English abstract)

Darnley, A.G., 1995. International geochemical mapping-a review. Journal of Geochemical Exploration 55, 5-10.

De Paor, D.G., 1996. Structural Geology and Personal Computers, first ed. Elsevier Science, Oxford.

Dimri, V. P., 2000. Crustal fractal magnetisation, In: Dimri, V. P. (Ed.), Application of fractals in earth sciences. Balkema, New York, pp. 89-95.

Dimri, V. P., Srivastava, R. P., 2005. Fractal modeling of complex subsurface geological structures, in: Dimri, V. P. (Ed.), Fractal behaviour of the Earth system. Springer, New York, pp. 23-37.

Edwards, R., Atkinson, K., 1986. Ore Deposit Geology and its influence on mineral exploration. first ed. Chapman and Hall, London.

Einaudi, M.T., Burt, D.M., 1982. Introduction, terminology, classification and composition of skarn deposits. Economic Geology 77, 745-754.

Ervin, 1997. Theory of bouguer anomaly. Geophysics 42, 1468.

Faulkner, D.R., Jackson, C.A.L, Lunn, R.J., Schlische, R.W., Shipton, Z.K., Wibberley, C.A.J., Withjack, M.O., 2010. A review of recent developments concerning the structure, mechanics and fluid flow properties of fault zones. Journal of Structural Geology 32, 1557-1575.

Ford, A., Blenkinsop, T.G., 2008. Evaluating geological complexity and complexity gradients as controls on copper mineralization, Mt Isa Inlier. Australian Journal of Earth Sciences 55, 13-23.

Gao, J., Nian, H., Chen, S., Li, X. and Guo, J., 2004a. Spatial distribution characteristic of mineralizated fracture zone and metallogenetic elements in the south of Gejiu ore district, Yunna Province---take Longshujiao fault as an example. Contributions to Geology and Mineral Resources Research 19, 238-242. (in Chinese with English abstract)

Gao, J., Nian, H., Li, X., Chen, S. and Guo, J., 2004b. Metallogenesis of Sn, Cu poly-metallic deposit in the south of Gejiu ore district Yunnan Province. Journal of Kunming University of Science and Technology (Science and Technology) 29, 79-84. (in Chinese with English abstract)

Gao, Z., 1996. On the genesis of the Bainiuchang Ag polymetallic deposit in Mengzi. Yunnan Geology 15, 40-58. (in Chinese with English abstract)

Grunsky, E.C., Smee, B.W., 1999. The differentiation of soil types and mineralization from multi-element geochemistry using multivariate methods and digital topography. Journal of Geochemical Exploration 67, 287-299.

Guan, R., 1991. An approach of mineralization of granite mass in the structure tectonicmagmatic belt in the Southeast of Yunnan. Mineralogy and Petrology 11, 92-101. (in Chinese with English abstract)

Guan, R., 1993. Basic characteristics and correlation of main granite bodies in southeast Yunnan. Yunnan Geology 12, 373-382. (in Chinese with English abstract)

Guilbert, J.M., Park, C.F., 1986. The geology of ore deposits. fouth ed. W. H. Freeman and Company, New York.

Haldar, S.K., 2012. Mineral Exploration: Principles and Applications. first ed. Elsevier. Oxford.

Harris, D., Zurcher, L., Stanley, M., Marlow, J., Pan, G., 2003. A comparative analysis of favorability mappings by weights of evidence, probabilistic neural networks, discriminant analysis, and logistic regression. Natural Resources Research 12, 241-255.

Harris, J.R., 1989. Data integration for gold exploration in eastern Nova Scotia using a GIS, Remote Sensing for Exploration Geology, Calgary, Alberta, pp. 233-249.

Harris, J.R., Bowie, C., Rencz, A.N. and Graham, D., 1994. Computer-enhancement techniques for the integration of remotely sensed, geophysical, and thematic data for the geosciences. Canadian journal of remote sensing 20, 210-221.

Harris, J.R., Rencz, A.N., Ballantyne, B., Sheridon, C., 1998. Mapping altered rocks using Landsat TM and lithogeochemical data: Sulphurets-Brucejack Lake district, British Columbia, Canada. Photogrammetric Engineering and Remote Sensing 64, 309-322.

Harris, J.R., Sanborn-Barrie, M., 2006. Mineral potential mapping: examples from the Red Lake Greenstone Belt, Northwest Ontario. In: Harris, J.R. (Ed.), GIS for the Earth Sciences. Geological Association of Canada, pp. 1-21.

Harris, J.R., Wilkinson, L., Grunsky, E.C., 2000. Effective use and interpretation of lithogeochemical data in regional mineral exploration programs: application of Geographic Information Systems (GIS) technology. Ore Geology Reviews 16, 107-143.

Hawkes, H.E. and Webb, J.S., 1962. Geochemistry in mineral exploration. first ed. Harper's Geo-science Series. Harper & Row, New York.

Heinrich, C.A., 1995. Geochemical evolution and hydrothermal mineral deposition in Sn (–W– base metal) and other granite-related ore systems: Some conclusions from Australian examples. In Magmas, Fluids, and Ore Deposits, Mineralogical Association of Canada Short Course Series 23, 203-220.

Hodgson, C.J., 1990. Uses (and Abuses) of ore deposit models in mineral exploration. Geoscience Canada 17, 79-89.

Hood, P. J., Teskey, D. J., 1989. Aeromagnetic gradiometer program of the Geological Survey of Canada. Geophysics 54, 1012-1022.

Hood, P., McClure, D. J., 1965. Gradient measurements in ground magnetic prospecting. Geophysics 30, 403-410.

Jolliffe, I.T., 2002. Principal Component Analysis, second ed. Springer, New York.

Kaiser, H.F., 1960. The application of electronic computers to factor analysis. Educational and Psychological Measurement 20, 141-151.

Kearey, P., Brooks, M., Hill, I., 2002. An Introduction to Geophysical Exploration. third ed. Blackwell, Oxford.

Kim, Y., Sanderson, D.J., 2005. The relationship between displacement and length of faults: a review. Earth-Science Reviews 68, 317-334.

Koch, G.S. and Link, R.F., 1980. Statistical Analysis of Geological Data, second ed. Dover Publications, New York.

Kowalik, W.S. and Glenn, W.E., 1987. Image-Processing of aeromagnetic data and integration with Landsat Images for improved structural interpretation. Geophysics, 52, 875-884.

Li, Q., Cheng, Q., 2006. VisualAnomaly: A GIS-based multifractal method for geochemical and geophysical anomaly separation in Walsh domain. Computer&Geosciences 32, 663-672.

Li, S., 1998. Metallogenic analysis of Sn-Cu rich orebodies in the Gejiu mining area, Yunnan. Geotectonica et Metallogenia 22, 148-155. (in Chinese with English abstract)

Li, Y., Oldenburg, D. W., 1998. Separation of regional and residual magnetic field data. Geophysics 63, 431-439.

Li, Y., Qin, D., Dang, Y. and Yang, J., 2005. Research on relation between tin ore deposit and (Ultra) ferromagnesian Rock. Engineering Science 7, 269-274. (in Chinese with English abstract)

Li, Y., Qin, D., Dang, Y., Xue, C., Tan, S., and Hong, T., 2006. Mineralizations in basalts of the Gejiu tin deposit in Yunnan Province. Journal of Jilin University (Earth Science Edition) 36, 326-335. (in Chinese with English abstract)

Liu, C., 2007. Metallogenic conditions comparison between the eastern area and the western, and assessment of mineral resources in the western, Gejiu Sn deposit. Ph.D Thesis, China University of Geosciences (Wuhan), Wuhan, 120 pp.

Lovejoy, S., Pecknold S., Schertzer, D., 2001. Stratified multifractal magnetization and surface geomagnetic fields-I: spectral analysis and modelling. Geophysical Journal International 145, 112-126.

Lue, B., 2005. Direction of new round of prospecting in Gejiu tin and copper polymetallic mine. Mineral Resources and Geology 19, 260-266. (in Chinese)

Luo, J., 1995. The metallogenic model of tin, lead, zinc and silver deposits in southeastern Yunnan, China. Yunnan Geology 14, 319-332. (in Chinese)

Luo, X., Dimitrakopoulos, R., 2003. Data-driven fuzzy analysis in quantitative mineral resource assessment. Computers & Geosciences 29, 3-13.

Malamud, B. D., Turcotte, D. L., Barton, C. C.. 1996. The 1993 Mississippi river flood: a one hundred or a one thousand year event? Environmental & Engineering Geoscience 2, 479-486.

Mandelbrot, B.B., 1972. Possible refinement of the lognormal hypothesis concerning the distribution of energy dissipation in intermittent turbulence. In: Rosenblatt, M., and Van Atta, C. (Eds.), Statistical Models and Turbulence, Lecture Notes in Physics, vol. 12. Springer, New York, pp. 333-351.

McCaffrey, K., Lonergan, L., Wilkinson, J., 1999. Fractures, Fluid Flow and Mineralization, first ed. Geological Society, London, Special Publications, 155.

Micklethwaite, S., Sheldon, H.A., Baker, T, 2010. Active fault and shear processes and their implications for mineral deposit formation and discovery. Journal of Structural Geology 32, 151-165.

Misra, K., 2000. Understanding mineral deposits. first ed. Kluwer Academic Publishers, Norwell.

Nabighian, M.N., Grauch, V.J.S., Hansen, R.O., LaFehr, T.R., Li, Y., Peirce, J.W., Phillips, J.D., and Ruder, M.E., 2005a. 75th Anniversary-the historical development of the magnetic method in exploration. Geophysics 70, 33-61.

Nabighian, M.N., Ander, M.E., Grauch, V.J.S., Hansen, R.O., LaFehr, T.R., Li, Y., Pearson, W.C., Peirce, J.W., Phillips, J.D., and Ruder, M.E., 2005b. 75th Anniversary-historical development of the gravity method in exploration. Geophysics, 70, 63-89.

Pan, G.C., Harris, D.P., 2000. Information Synthesis for Mineral Exploration. first ed. Oxford University Press, New York.

Pecknold, S., Lovejoy, S., Schertzer, D., 2001. Stratified multifractal magnetization and surface geomagnetic fields-II: multifractal analysis and simulation. Geophysiccal Journal International 145,127-144.

Pereira, H.G., Renca, S., Saraiva, J., 2003. A case study on geochemical anomaly identification through principal components analysis supplementary projection. Applied Geochemistry 18, 37-44.

Pirajno, F., 2009. Hydrothermal Processes and Mineral Systems. first ed., Springer, Berlin.

Porwal, A., Carranza, E.J.M., Hale, M., 2004. A hybrid neuro-fuzzy model for mineral potential mapping. Mathematical Geology 36, 803-826.

Qin, D., Li, Y., 2008. Researches of Gejiu Tin-Copper Polymetallic Deposits, first ed. Science Press, Beijing, China. 173 p. (in Chinese)

Qin, D., Li, Y., Fan, Z., Hong, T., Li, L., and Lin, X., 2006a. The geochemistry and mineralization evolvement of Gejiu tin ore deposits. Engineering Science 8, 19-27. (in Chinese with English abstract)

Qin, D., Li, Y., Tan, S., Chen, A., Xue, C., Fan, Z., Dang, Y., Tong, X., Wu, J., Li, Y., and Wang, H., 2006b. Metallogenic ages of Gejiu tin ore deposit in Yunnan Province. Chinese Journal Of Geology 41, 122-132. (in Chinese with English abstract)

Rencz, A.N., Harris, J.R., Watson, G.P., Murphy, B., 1994. Data integration for mineral exploration in the Antigonish Highlands, Nova Scotia. Canadian Journal of Remote Sensing 20, 258-267.

Rivard, B., Kellet, R.L., Saint-Jean, R., Singhroy, V.H., 1994. Characterization of faulting and dyke intrusion in the Benny deformation zone, north range of Sudbury, from airborne magnetics and SAR. Canadian Journal of Remote Sensing 20, 324-328.

Schertzer, D., Lovejoy, S., 1987. Physical modeling and analysis of rain and clouds by anisotropic scaling of multiplicative processes. Journal of Geophysical Research 92, 9693-9714.

Smith, L.I., 2002. A tutorial on Principal Components Analysis. Cornell University, USA.

Tan, S., Qin, D., Chen, A., Fan, Z., Xue, C., Li, J., Xia, J., and Pu, C., 2004. Regional crust evolution and metallogenesis of Gejiu tin deposit-A discussion. Acta Mineralogica Sinica 24, 157-163. (in Chinese with English abstract)

Tang, C., Nie, Q., Liu, C., Gao, J., Wang, R., and Yang, S., 2004. Synthetic analysis of remote sensing and geologic information on prediction of perspective ore districts in Kafang ore field of Gejiu mining district in Yunan Province. Acta Mineralogica Sinica 24, 164-170. (in Chinese with English abstract)

Tao, Y., Ma, D. and Gao, Z., 2002. An insight into hydrothermal process of involved in the formation of Gejiu tin deposits as indicated by trace element geochemistry. Geology-Geochemistry 30, 34-39. (in Chinese with English abstract)

Thorarinsson F., Magnusson, S. G., 1990. Bouguer density determination by fractal analysis. Geophysics 55, 932-935.

Torabi, A., Berg, S.S., 2011. Scaling of fault attributes: a review. Marine and Petroleum Geology 28, 1444-1460.

Turcotte, D.L., 1997. Fractals and Chaos in Geology and Geophysics, second ed. Cambridge University Press, Cambridge.

Veneziano, D., 2002. Multifractality of rainfall and scaling of intensity-duration-frequency curves. Water Resources Research 38, 1-12.

Veneziano, D., Furcolo, P., 2002. Multifractality of rainfall and scaling of intensity-duration-frequency curves. Water Resources Research 38, 42-1-42-12.

Wang, L., 2004. Researches on metallogenic Series, metallogenic evolution and metallogenic prognosis in the Gejiu tin-copper polymetallic ore-concentrating district. Ph.D. Thesis, Central South University, 132 pp.

Wang, W., Zhang, G., Liang, J., 2010. Spatial variation law of vertical derivative zero points for potential field data. Applied Geophysics 7, 197-209.

Wang, W., Zhao, J., Cheng, Q., 2011. Analysis and integration of geo-information to identify granitic intrusions as exploration targets in southeastern Yunnan district, China. Computer & Geosciences 37, 1946-1957.

Wang, W., Zhao, J., Cheng, Q., Liu, J., 2012. Tectonic-geochemical exploration modeling for characterizing geo-anomalies in southeastern Yunnan district, China. Journal Geochemical Exploration 122, 71-80.

Wang, W., Zhao, J., Cheng, Q., 2013a. Application of singularity index mapping technique to gravity/magnetic data analysis in southeastern Yunnan mineral district, China. Journal of Applied Geophysics 92, 39-49.

Wang, W., Zhao, J., Cheng, Q., 2013b. Fault trace-oriented singularity mapping technique to characterize anisotropic geochemical signatures in the Gejiu mineral district, China. Journal of Geochemical Exploration (2013), doi: 10.1016/j.gexplo.2013.07.009.

Woodall, 1994. Empiricism and concept in successful mineral exploration. Australian Journal of Earth Sciences 41, 1-10.

Xie, X., Mu, X., Ren, T., 1997. Geochemical mapping in China. Journal of Geochemical Exploration 60, 99-113.

Xiong, G. and Shi, S., 1994. Physical-geological model of the Gejiu tin district and its application. Geological Review 40, 19-27. (in Chinese with English abstract)

Xu, Y., Cheng, Q., 2001. A fractal filtering technique for processing regional geochemical maps for mineral exploration. Geochemistry: Exploration, Environment, Analysis 1, 147-156.

Xypolias, P., Koukouvelas, I. K., 2004. Fault trace parameters as a tool for analysing remotely sensed fault arrays: An example from the eastern Gulf of Corinth, Greece. International Journal of Remote Sensing 25, 4685-4699.

Yang, S., 1990. Types and associations of ore deposits along the Southeastern Yunnan tin ore belt. Mineral Deposits 9, 37-48. (in Chinese with English abstract)

Yu, C., 2002. Complexity of earth systems-fundamental issues of earth sciences (I). Earth Sciences-China University of Geosciences 27, 509-519 (in Chinese with English abstract).

Yuan, J., Zhu, S., Zhai, Y., 1979. Mineral Deposits, first ed. Geological Publishing House, Beijing. (in Chinese)

Zhai, Y., 2003. Regional structure and regional geochemistry and metallogeny. Geological survey and research 26, 1-7. (in Chinese with English abstract)

Zhai, Y., Deng, J., Li, X., 1999. Essentials of Metallogeny, first ed. Geological publishing house, Beijing, China. (in Chinese with English abstract)

Zhang, H., Liu, J., Li, X., Zhang, X., 2006. Relationship of granites to tin, silver, copper, lead, zinc, polymetallic deposits in southeastern Yunnan, China. Contributions to Geology and Mineral Resources Research 21, 87-90. (in Chinese with English abstract)

Zhao, J., Chen, S., Zuo, R., Carranza, E.J.M., 2011. Mapping complexity of spatial distribution of faults using fractal and multifractal models: vectoring towards exploration targets. Computer & Geosciences 37, 1958-1966.

Zhao, J., Wang, W., Dong, L., Yang, W., Cheng, Q., 2012. Application of geochemical anomaly identification methods in mapping of intermediate and felsic igneous rocks in eastern Tianshan, China. Journal of Geochemical Exploration 122, 81-89.

Zhao, P., 1999. Theory and Practice of Geoanomaly in Mineral Exploration. first ed. China University of Geosciences Press, Wuhan, China. (in Chinese with English abstract)

Zhao, W., Chellappa, R., Phillips, P.J. and Rosenfeld, A., 2003. Face recognition: A literature survey. Acm Computing Surveys 35, 399-459.

Zheng, Q., Yang, D., 1997. The mineralization evolution and metallogenic model of the Gejiu tin-polymetallic deposit in Yunnan Province. Geological Exploration for Non-Ferrous Metals 6, 82-87. (in Chinese with English abstract)

Zhou, J., Xu, K., Hua, R., Zhao, Y., 1997. A Discussion on genesis of the tin polymetallic sulfide deposits of Southeastern Yunnan. Yunnan Geology 16, 40-58. (in Chinese with English abstract)

Zhuang, Y., Wang, R., Yang, S. and Yi, J., 1996. Geology of Gejiu tin-copper polymetallic deposit. Earthquake publishing house, Beijing, China. (in Chinese with English abstract)

Zuo, R., Cheng, Q., Xia, Q., Agterberg, F.P., 2009. Application of singularity mapping technique to identify local anomalies using stream sediment geochemical data, a case study from Gangdese, Tibet, western China. Journal of Geochemical Exploration 101, 225-235.

Zuo, R., Xia, Q., 2009. Application fractal and multifractal methods to mapping prospectivity for metamorphosed sedimentary iron deposits using stream sediment geochemical data in eastern Hebei province, China. Geochimica et Cosmochimica Acta 73, A1540-A1540.